

The relationship between the molecular structure and ion adsorption on goethite

Promotor: dr. W. H. van Riemsdijk
Hoogleraar in de Bodemscheikunde en chemische bodemkwaliteit

promotiecommissie
prof. L. Charlet,
dr. C.A.J. Appelo
prof. dr. ir. N. van Breemen
dr. ir L.K. Koopal

Univeriteit Grenoble-I.
Consultant, Amsterdam.
Wageningen Universiteit
Wageningen Universiteit

1100201.0001

The relationship between the molecular structure and ion adsorption on goethite

R.P.J.J. Rietra

Proefschrift
ter verkrijging van de graad van doctor
op gezag van de rector magnificus
van Wageningen Universiteit,
prof. dr. ir. L. Speelman,
in het openbaar te verdedigen
op woensdag 14 november 2001
des namiddags te vier uur in de Aula.

CIP gegevens Koninklijke bibliotheek, Den Haag

Rietra, R.P.J.J.

The relationship between molecular structure and the ion adsorption on goethite
Thesis Wageningen University - with ref.-with summary in Dutch -128 p.

ISBN 90-5808-503-1

Subject headings: adsorption / goethite

Abstract

Rietra, R. P. J. J. 2001, **The relation between the molecular structure and ion adsorption on goethite**. Doctoral Thesis, Wageningen University, Wageningen, The Netherlands. ISBN ISBN 90-5808-503-1; 130 pages

A study is presented on the adsorption of inorganic ions on goethite with emphasis on the adsorption of oxyanions. Experimental results for a range of oxyanions (PO_4 , AsO_4 , VO_4 , WO_4 , MoO_4 , CrO_4 , SeO_3 , SeO_4 , SO_4 , Cl , NO_3 , ClO_4) and Ca are presented and interpreted using the CD-MUSIC model. For some of these ions the coordination and structure of the adsorbed ions on goethite are known from spectroscopy (SO_4 , SeO_4 , PO_4 , AsO_4 , SeO_3). Ideally, surface complexes derived from spectroscopy correspond with those resulting from the modeling of macroscopic adsorption data. This would assure that the mechanistic description of ion binding scales from the microscopic molecular structure to the macroscopic adsorption behavior. In the CD-MUSIC model it is assumed that the charge of the adsorbed ions is distributed at the interface as a function of the coordination and structure of the adsorbed ions and that this distribution of charge can be estimated using the bond valence concept of Pauling. In this study it is found that the macroscopic proton-ion adsorption stoichiometry is almost solely determined by the interfacial charge distribution of adsorbed complexes. It is shown that the experimentally determined proton-ion adsorption stoichiometry can be predicted on the basis of the spectroscopically identified structures of sulfate, selenite, phosphate and arsenate on goethite. By doing so a direct relationship is demonstrated between the molecular structure of adsorbed ions and macroscopic adsorption phenomena. By using this knowledge it is in principle possible to identify the structure and coordination of adsorbed complexes from the macroscopic adsorption data and vice versa. It is found that the spectroscopically suggested differentiation between inner- and outersphere complexes of sulfate and selenate, and the differentiation between bidentate and monodentate phosphate can be modeled satisfactory with the CD-MUSIC approach although the differentiation cannot be established solely from the available adsorption data. It is also found that the proton adsorption on goethite decreases in electrolyte solutions of NaCl , NaNO_3 and NaClO_4 (below the PZC) in the order $\text{Cl} > \text{NO}_3 > \text{ClO}_4$ while sulfate and phosphate adsorption is lower in the order $\text{Cl} < \text{NO}_3 < \text{ClO}_4$. These results can be explained well by assuming outersphere complexes of the electrolyte anions on the goethite surface with different intrinsic affinities.

Additional index words:

Ion adsorption modeling, goethite, iron oxide, CD-MUSIC, phosphate, arsenate, vanadate, molybdate, tungstate, sulfate, selenate.

The space is just a few kilometers from us (Lovelock)

NOV 201, 3080

Stellingen

1. Het pH afhankelijke adsorptiegedrag van ionen is onafhankelijk van de chemische bindingsaffiniteit indien er maar één type adsorptie-evenwicht is.

Dit proefschrift

2. De proton-ion stoichiometrie is een functie van de structuur en de coordinatie van de geadsorbeerde complexen. De conclusie van Fokkink (1987) dat de proton-ion stoichiometrie in het algemeen niet ion-specifiek is, is niet correct.

L.G.J Fokkink, Ion adsorption on oxides, Phd Thesis WAU, 1987

3. De incorporatie van electrostatica in oppervlaktecomplexerings modellen is de belangrijkste factor welke de modellen naast een beschrijvend ook een voorspellend karakter geeft.
4. De gemeenschappelijke genetische code van al het leven wijst erop dat het leven waarschijnlijk maar één keer is ontstaan. Dit bemoeilijkt een natuurwetenschappelijke onderbouwing van het ontstaan van het leven.
5. Milieunormstellingen zijn nog te vaak gebaseerd op detectiegrenzen en achtergrondwaarden. Dit leidt tot te strenge normen voor selenium in het Bouwstoffenbesluit.

Aalbers et al. Bouwstoffen nader bekeken, Eburon, 1998.

6. Een duurzaam energiegebruik wordt het snelst bereikt door zoveel mogelijk energie te verbruiken.
7. Heilige grond is vruchtbare bodem voor oorlog

Stellingen behorende bij het proefschrift "The relationship between the molecular structure and ion adsorption on goethite" te verdedigen door R.P.J.J. Rietra op 14 november 2001 te Wageningen.

Voorwoord

De mensen die belangrijk waren bij het maken dit boekje wil ik hier bedanken. Zo zijn daar Lianne, Erik en Gerdine, die heel veel ICP analyses hebben uitgevoerd op een voor mij plezierige manier, en Rein die mij en de studenten bij elk wissewasje hielp, en Arie en Egbert, die goed gezelschap geven op een lab. Zoals zo veel anderen heb ik het dagelijkse gezelschap van aajoes als heel fijn ervaren, daarvoor mijn dank en complimenten. Plezier beleefde ik aan de samenwerking met Chiel Cuypers, Susanne de Rooij, Ahmad Kurnain en Marit Tamminga, tijdens hun afstudeervakken. Speciaal dank aan Jeanine Geelhoed, Jeroen Filius en Paul Verburg voor het aanhoren van mijn geklets, en Peter Venema voor zijn hulp bij de "automatische" titrator. *Also I gratefully acknowledge Mike Machesky, David Kinniburgh, Hotze Wijnja and Rob Comans for their comments on some of the manuscripts, and I thank Stephan Hug, Per Persson, and especially Johannes Lützenkirchen for many discussions.* Dank aan Dr. Verduin voor het gebruik van het isotopenlab bij Virologie.

Naast mede auteurs van de verhalen in dit boekje zijn Tjisse Hiemstra en Willem van Riemsdijk mijn begeleiders geweest zonder wie ik het onderzoek veel minder relevant had gevonden. Speciaal dank aan Tjisse voor zijn vertrouwen en Willem voor zijn interesse. Ik kan het niet nalaten om te zeggen dat ik aan een mooi onderwerp heb mogen werken: adsorptie, het lijkt ingewikkeld, en voor berekeningen is vaak een computer nodig, maar het gevoel dat het misschien relatief eenvoudig te begrijpen is maakt het heel aantrekkelijk. Janet wordt nergens in de verhaaltjes genoemd maar heeft ook vaak meegezwommen tussen de ionen en gezocht naar de bindingsplekjes. Ik heb me goed gevoeld aan dat goethietoppervlak.

Contents

1	General Introduction	1
2	Effects of electrolyte ions on adsorption of anions on goethite Outersphere adsorption	15
3	The relation between the molecular structure and ion adsorption on variable charge minerals Innersphere adsorption	31
4	Sulfate adsorption on goethite Extended study of one anion	49
5	Comparison between selenate and sulfate adsorption on goethite Inner- and outersphere adsorption	71
6	Interaction between calcium and phosphate adsorption on goethite Interaction between ions	87
7	Miscellaneous data and future challenges	103
	Summary	109
	Samenvatting	112
	Levensloop	115

General Introduction

General problem

Soils have a large variety of important functions for humans such as plant growth for food production and purification of water to be used as drinking water. The functioning of a soil can be influenced by human activity in a relatively simple way by adjustment of the chemical characteristics of a soil. This is of interest as it enables one to increase food production by addition of nutrients but it is also of interest as the functioning of a soil can be seriously hampered by addition of pollutants. The effect that nutrients and pollutants have on organisms is often strongly dependent on the concentration in the soil solution and therefore dependent on the binding of these components by the soil and its chemical characteristics. The distribution of chemical components between the soil solution and solid matter varies strongly between soils and this is related to the fact that the chemical composition of soils can differ strongly and that soils are composed of very complex assemblages of minerals and humic materials. In soils the fate of especially the oxyanions is often determined by the binding to variable charge minerals of iron, aluminum and manganese, due to the reactivity and high surface areas of these minerals. The binding behavior of ions on variable charge minerals is also of importance in aquatic systems, in the production of catalysts, in waste materials such as ashes from burning fuel, and in water treatment when iron and manganese are oxidized. It is the aim in this thesis to improve the possibilities for prediction of the binding behavior of ions on variable charge minerals.

To enable the prediction of the behavior of environmentally important nutrients and pollutants the so-called surface complexation models have been developed. The surface complexation models developed for ion adsorption on variable charged minerals are based on the description of chemical equilibrium equations in which activity corrections are calculated on the basis of the an electrostatic double layer model of the surface. Different versions of the surface complexation model have been developed due to uncertainties in the molecular picture of the surface reactions and accessory thermodynamic equilibria. The advantage of the surface complexation model is that it offers a molecular description of the surface reactions in relation to the macroscopic adsorption behavior. It also enables predictions to be made for conditions outside the range where data are available.

An important problem of the surface complexation models for variable charge minerals is that often a good description of a limited range of data can be obtained when using fundamentally different molecular equations. This has hampered the development of a unified model for variable charge minerals. However in recent years huge progress has been made in determining the coordination and speciation of adsorbed complexes on variable charge minerals using spectroscopy. Also in other fields innovations have been made, such as characterization of the crystallographic planes using AFM, determining the

electromobility using photo-acoustic electromobility, and calculation of the relative acidities of surface groups using quantum mechanical calculations. Knowledge of the surface coordination and speciation of ions ideally can be used to give information about the distribution of these ions over the aqueous and solid phases. It is the challenge now to translate the microscopic knowledge of adsorbed ions in model parameters that enable the prediction of macroscopic behavior of ions between the solution and variable charge minerals. In this thesis the adsorption model for variable charge minerals will be further developed by studying the adsorption behavior in relation to spectroscopically determined coordination and speciation in terms of the surface complexation model for variable charge minerals.

Objectives

The problem in short is that an increase of knowledge, from molecular techniques such as spectroscopy, about the coordination and speciation of adsorbed ions on environmentally important minerals can hardly be used today to give better predictions of the fate of nutrients and pollutants in soil and aquatic systems. An approach to incorporate structural detail in a surface complexation model is the CD-MUSIC model. One problem is the correct parameterization of this model. The objectives of the present study are therefore to study ion adsorption on goethite and to describe the results in terms of the CD-MUSIC model in order to further develop the model for variable charge minerals. The current model assumptions and model parameter values are tested by studying the ion adsorption on goethite for a range of ions, across a broad range of conditions, and by comparing the model results with spectroscopically derived coordination and speciation. In this way also the significance of molecular knowledge to predict the distribution of ions over the solid/aqueous interface can be enhanced.

Present approach

Studied is the modeling of ion adsorption on goethite. Goethite is chosen as it has been used previously in many laboratory studies, the coordination and speciation of a range of ions has been investigated on goethite, and it is ubiquitous in environmental systems. The colloidal particles of goethite consist of different surface planes and surface groups. To be able to model ion-adsorption on goethite account has to be made for the reactivity of the different surface groups. The Charge Distribution Multisite Complexation model (CD-MUSIC) is a model (1) that defines different surface groups on the basis of the coordination of surface oxygen's to its underlying metal ions using a bond valence analysis. The CD-MUSIC model will be used in this thesis, as it is so far the only model that enables the incorporation of knowledge about coordination and speciation from spectroscopy in a surface complexation model. A short introduction to modeling surface equilibria and the CD-MUSIC approach is given to elucidate the objectives of this thesis.

A chemical equilibrium reaction is usually written as the product of two species, such as: $(AB) = K (A)(B)$, where K is the equilibrium constant, which is related to the total Gibbs free energy (ΔG_{tot}) as $\Delta G_{tot} = -RT \ln K$. The product and

the species are written between () to emphasize that the activity of the species is to be used in the equation. The concentration and activity are related by the activity coefficient, which in aqueous chemistry is a function of ionic strength and the charge of the ion, and is usually calculated with the Davies or the Debye-Hückel equation. This approach cannot be applied for chemical equilibria on large polyelectrolytes or mineral surfaces because the species influence each other by the formation of surface charge, which is a consequence of the specific binding of charged ions.

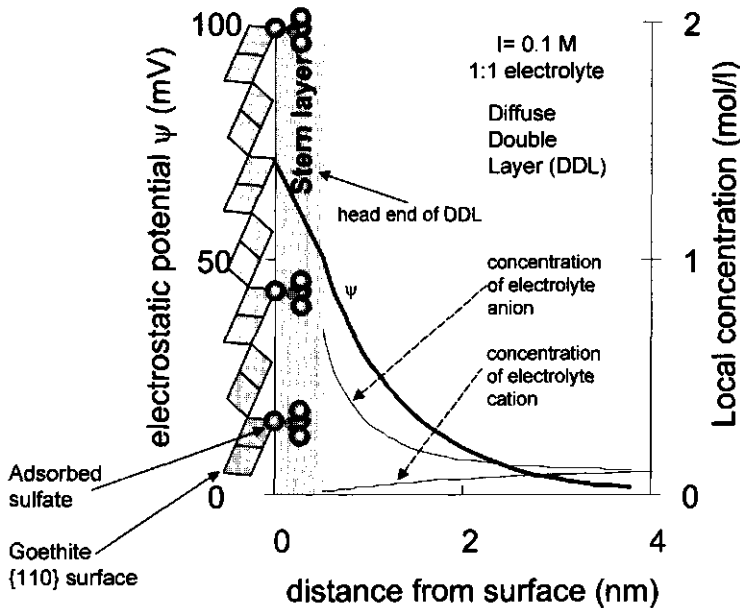


Figure 1. Schematic presentation of the dimensions of the electric double layer model, Stern layer model, and the {110} surface plane of goethite (1). At low pH values the goethite surface can have a high adsorption of protons, which causes a positive charge and potential that attracts anions such as sulfate. The surface charge is neutralized by the ions in the diffuse double layer. Therefore the local concentration of the counterions increases near the surface. The charge can also be compensated, or can be caused, by adsorption of ions at the surface. Shown here are sulfate ions (SO_4^{2-}) adsorbed on the surface of goethite.

Surface charge can develop on mineral surfaces due to the chemical adsorption of protons and other charged ions. Due to electroneutrality the charge must be neutralized by the adsorption of other charged ions. At the mineral/water interface charge can be located at the surface and the counter ions can be located in the solution. Due to the diffuse distribution of counter ions near the surface also an electrostatic potential profile will develop. The picture with one part of the charge at the mineral surface, and the counter charge in solution is called a diffuse double layer because the density of the counter charge varies in the solution as a function of the distance to the surface. The variation of the electric potential with distance from the charged plane has been dealt with in the Gouy-Chapman theory. The

problem in this theory of the unrealistically high counter ion concentrations at high surface potentials close to the surface can be overcome by accounting for the finite size of the counterions. This concept implies a finite minimum distance of approach of the counter and co-ions to the surface, and is called the Stern model. This approach implies extra parameters, the dielectric constant in the Stern layer and the layer thickness of the Stern layer, which have to be estimated (2, 3).

Surface reactions can be described as mass law equations, if the effect of surface charge on the surface equilibria is taken into account. Such models are called surface complexation models. The total Gibbs free adsorption energy (ΔG_{ads}) is operationally broken down in a chemical and a coulombic part: $\Delta G_{\text{ads}} = \Delta G_{\text{chem}} + \Delta G_{\text{coul}}$ where $\Delta G_{\text{coul}} = \Delta zF\psi$. The basic problem using the double layer model in surface reactions is the uncertainty about the location of adsorbed charge in the picture of the double layer model, as drawn in Figure 1, and therefore the uncertainty of the electrostatic contribution to the overall adsorption energy. In the last 30 years this has resulted in different versions of the surface complexation model for variable charge minerals (1, 4-8).

Mechanisms for surface equilibria

The development of the surface complexation models has also resulted in different definitions of the protonation reactions on surface groups. A model that is well known and that is incorporated in many computer codes (9-11) is the so-called 1site-2pK approach where the protonation of 1 site is described by two equilibrium reactions: $\text{MOH}^0 \rightleftharpoons \text{MO}^- + \text{H}^+$ and $\text{MOH}_2^+ \rightleftharpoons \text{MOH}^0 + \text{H}^+$, in which MO represents a surface oxygen coordinated to a metal ion. A more simple reaction for the surface protonation of iron- and aluminum (hydr)oxides is the 1 pK approach: $\text{MOH}_2^{+0.5} \rightleftharpoons \text{MOH}^{-0.5} + \text{H}^+$. There is no consensus on the type of model to be used (12) but in the recent literature the 1pK approach is getting more appraisal due to its easy parameterization and interpretation (13-17).

To describe the surface chemical equations and the charges involved use is made of the Pauling bond valence concept (18). A central parameter in the concept is the distribution of charge. For stable oxide structures this concept implies that the charge of a central ion is distributed over its surrounding ligands. This leads to the definition of the bond valence (v) as the charge of a cation divided by its coordination number (CN): $v = z/\text{CN}$. Application of this approach gives an estimation of the charge on surface oxygen groups and adsorbed complexes. At the mineral surface of goethite the oxygen's can be coordinated to one, two and three metal ions leading to singly, doubly and triply coordinated groups. These groups are denoted for goethite as: $\text{FeO}^{-1.5}$, Fe_2O^{-1} , $\text{Fe}_3\text{O}^{-0.5}$, since the charge attribution of a single Fe^{3+} to the surface oxygen is $v = z/\text{CN} = 3/6 = 0.5$. For a singly coordinated surface group on goethite, protonation can lead to the following charges: $\text{FeO}^{-1.5} + 2\text{H}^+ \rightleftharpoons \text{FeOH}^{-0.5} + \text{H}^+ \rightleftharpoons \text{FeOH}^{+0.5}$.

Ions that are adsorbed via ligand-exchange with surface oxygen's attribute a part of their charge to the oxygen(s) which are coordinated with the surface and the remaining part to ligands at a certain distance from the mineral surface. For innersphere adsorbed sulfate the application of the bond valence for an S-O bond,

with $v = 6/4 = 1.5$, leads to a neutral surface oxygen: $\text{Fe-O}^0\text{-S}$ as the sum of bond valence contributions completely neutralizes the charge of the surface oxygen, which forms the bond between the mineral and sulfate. However also hydrogen bonds can contribute charge to the surface oxygen.

Very accurate models are available to calculate actual bond valences for mineral structures on the basis of bond lengths in the interior of minerals (19). The bond lengths at the mineral surfaces are however not exactly known. It has been shown that the same bond lengths as in the interior of the mineral can be used to calculate realistic proton affinities in a relatively simple manner (20, 21). This approach is based on a relation between proton affinities and the degree of charge saturation of the oxygen valence (20). However there is some uncertainty with respect to the number and the contribution of hydrogen bonds, and it is difficult to test if the necessary assumptions are correct because only the combined effect of different proton affinities can be determined experimentally. Attempts have also been made to predict proton affinities based on molecular mechanics calculations (17, 22). However, also in a molecular mechanics approach simplifying assumptions have to be made.

Bond valence analyses has also been used to identify stable surface complex configurations, as it is expected that only neutral or near neutral sum of bond valences lead to stable configurations (23, 24). A factor that complicates the use of the Pauling bond valence concept or the use of more accurate bond-valence calculations is that the bond length at surfaces may be different from a similar bond in the interior of the mineral. Determination of bond-lengths is possible for some bonds with EXAFS, which enables accurate bond-valence calculations (23, 28, 34). Another factor that complicates simple calculations using the Pauling bond valence concept or more accurate bond-valence calculation is that the number of hydrogen bonds and the charge attribution of hydrogen bonds to surface oxygen's is not well known. The Pauling bond valence concept is nevertheless a very helpful tool for understanding the coordination of surface complexes.

It has been suggested that only the singly coordinated surface groups (Fe-O) are reactive for innersphere complexation of anions such as phosphate, arsenate and sulphate. It can be simply deduced that this is very plausible using the Pauling bond valence concept to calculate the sum bond valence contribution for singly, doubly and triply coordinated oxygen's with for instance sulphate (Fe-O-S , $\text{Fe}_2\text{-O-S}$, $\text{Fe}_3\text{-O-S}$). Assuming a bond valence of 1.5 valence units (v.u.) for a S-O bond and 0.5 v.u. for a Fe-O bond, the sum of bond valences on the surface oxygen are 0, +0.5, and +1 v.u., respectively for the singly, doubly and triply coordinated surface groups. As only neutral or almost neutral sum of bond valences seem plausible this leads to the conclusion that only singly coordinated oxygen will react with sulphate to form an innersphere complex.

For bonds of selenate, tungstate, chromate and molybdate (Se-O , W-O , Cr-O , Mo-O) also a bond valence of 1.5 v.u. may be used, and therefore also for these anions only singly coordinated oxygen's are expected to be reactive. For bonds of phosphate, arsenate, and vanadate (P-O , As(V)-O , V-O) bond valences of 1.25 v.u. may be used, leading to a sum of bond valences on the surface oxygen of -0.25, +0.25, and +0.75 v.u. respectively, for the singly, doubly and triply coordinated

surface groups. Although the absolute difference from zero is the same for singly and doubly coordinated oxygen's, the singly coordinated group is still considered to be the most reactive if spectroscopic data are taken into account. Hydrogen bonding and/or distortion of the structure of the surface complex may further reduce the net calculated charge on the surface oxygen. Distorted bonds, or in other words, unequal lengths of the O(H) ligands of the oxyanion, have been determined by EXAFS for Pb, Np(V), Th, U (25-28), and it is the basis for determining the coordination with FTIR for carbonate, sulfate and phosphate (29-33).

For other anions such as silicate, arsenite, but especially for cations, it is less simple to deduce if stable innersphere bonds can be formed with singly, doubly, and triply coordinated surface groups. On the basis of bond valences analysis for surface groups of Fe-oxides and bonds with Pb(II) it was concluded that in principle singly and triply coordinated surface groups, and possibly also doubly coordinated surface groups can form stable surface complexes with Pb (34). This leads to a model for which the verification of the model parameters can be rather complicated.

Detail of modeling

The easiest way to further develop the model for variable charge minerals is to restrict the amount of adjustable model parameters to the minimum. It is therefore that the degree of detail of the model to be used is discussed here. The CD-MUSIC model is developed to describe all important ion adsorption data, taking into account the chemical composition of the surface planes, and the coordination and speciation of the adsorbed ions. On the basis of the two dominant surface planes of goethite, the 110 and 021 plane (37-39) and the surface composition of these planes, it is possible to establish a model to describe ion adsorption on goethite (20,21,40,41). This approach is called the full-site approach, or multisite model, as it incorporates the different site densities and proton affinities of the surface planes. Using this model for variable charged minerals might result in databases for different ions and different minerals if there is a straightforward procedure to obtain all the parameter values. A multisite model will give a rather large number of model variables. This may seem unreasonably problematic for the application of such a model (42). However different reactive sites have been verified experimentally: complexes with different surface groups have been found for F (43) and Cd (44, 45), and these support a multisite approach (46,47).

A more simple model than the full-site approach can be used, and has been used (1,17,35,36,47-54), without losing the structural detail of the adsorbed complexes by assuming only the major surface equilibria, which in case of goethite are the proton affinity for the singly and the triply coordinated surface groups, resulting in a so-called 2site approach. The two types of sites are both proton reactive, and for a range of anions it can be assumed that only the singly coordinated surface groups are reactive, as has been outlined earlier. The proton affinity for both groups can be different as used in the multisite approach, resulting in a 2site-2pK model, but for simplicity one can also assume that the proton affinities for both surface groups are equal, resulting in a 2site-1pK model. A special case is the 1site-2pK, or *delta* pK, approach as it is used in the Triple Layer

model (4), Constant Capacitance model (5) and in the Generalized double layer model (6).

It is important to know what the effect is of using different model approaches (a 2site-1pK, 2site-2 pK, or multisite approach) to describe ion adsorption. In the Appendix a comparison of the models is given. It can be concluded that for ions that only form complexes with singly coordinated surface groups it is possible to derive approximately the same model parameters values with the simple 2site-1pK model as with the multisite approach. The relative simplicity of the 2site-1pK model is ideal to test the current model for variable charged minerals. This is therefore the model that is used in this thesis along with ions for which this model is appropriate. The 2site-1pK model has been described in detail in reference 1.

Methods to be used

Ion adsorption is usually determined in batch experiments with a solid adsorbent (e.g. goethite), an ion of interest (e.g. sulfate), and a large quantity of so-called indifferent electrolyte (e.g. NaNO_3). This high concentration of NaNO_3 is to keep the amount of adsorption in the diffuse part of the electrical double layer of the specific ion of interest insignificant. This can result in graphs such as given for demonstration in Fig. 2a. They give the adsorption or equilibrium concentration as a function of the pH. From a series of adsorption edges (e.g. Fig. 2a) one can create a series of adsorption isotherms (eg. Fig. 2b). The advantage of adsorption isotherms (e.g. Fig. 2b) is that the data can be given independent of the experimental conditions used (amount of solid relative to adsorbate). Characterization of adsorption by adsorption edges or isotherms is of course limited to the range where the concentrations can be detected by analytic means. These types of experiments will be performed for most ions in this thesis except for the adsorption of electrolyte ions.

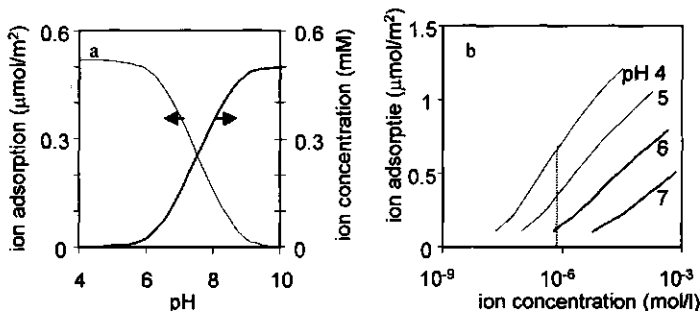


Fig. 2a&b. Examples of adsorption data presentation. (2a) A so-called adsorption edge gives the adsorption, or concentration, as a function of pH at a constant concentration of solid, adsorbate and salt strength. (2b) adsorption isotherms give adsorption as a function of the equilibrium concentration in solution at a constant pH and salt strength. Adsorption isotherms can be determined for equilibrium concentrations that are above the detection limit (dotted line)

Other techniques to determine ion adsorption characteristics are pH stat ion titrations or acid-base titrations. Examples of presentations of data are given in Fig.

2c&d. An advantage of these experiments (e.g. Fig. 2c) is that they can easily be performed in an automated set-up and in a CO_2 free atmosphere. Acid-base titrations (e.g. Fig. 2c) will be used to characterize the adsorption on goethite when the adsorbed amount cannot be determined accurately from the difference between the total concentration and the concentration in solution: the adsorption of electrolyte ions, and sulfate and selenate at high concentrations. A disadvantage of the acid-base titrations is that most ions do not have fast adsorption kinetics. This is less of a problem in pH stat titrations (e.g. Fig. 2d). Another advantage of the pH stat titration is the simplicity of the determination of the proton-ion adsorption stoichiometry at low adsorption levels and for equilibrium concentrations below the detection limit.

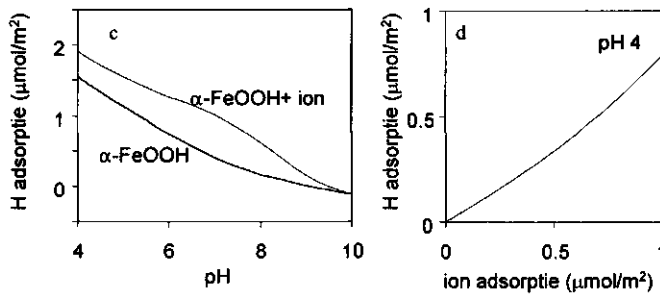


Fig. 2c&d. Examples of adsorption data presentations.(2c). Acid-base titrations at a constant concentration of solid and salt strength, with or without adsorbate.(2d) pH stat titration, proton/base consumption as a function of ion addition at a constant pH and salt strength.

The different techniques to characterize ion adsorption will be used in this thesis. Other techniques, such as spectroscopy, microscopy etc. have not been employed and information will be used from literature. The spectroscopic information of the coordination of the adsorbed complexes is translated in terms of a charge distribution in the Stern layer by using the Pauling bond valence approach (1). This is illustrated in Fig. 3 for sulfate and selenite. The charge distributions across both planes (z_0 and z_1) at both sides of the Stern layer are calculated with the Pauling bond valence concept. The charge attribution to the surface (z_0) for the given examples can be calculated from the overall charge (-2) and the number of ligands (n) that form a bond with the surface ($z_0 = z_{\text{ion}} n/\text{CN}$), (where CN is the coordination number). The coefficients z_0 and z_1 are used in the calculation of the electrostatic contribution to the overall affinity for the ion adsorption equilibrium.

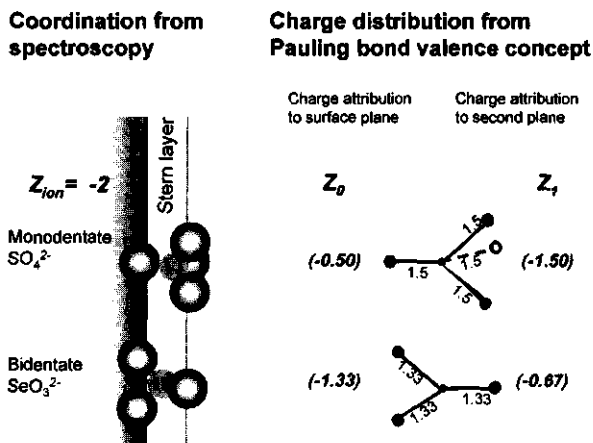


Fig. 3. Schematic representation of the monodentate surface-coordination of sulfate and bidentate surface-coordination of selenite, and the allocation of the charge (see text) over the two electrostatic planes in the Stern model as shown in Fig. 1.

Outline

In **chapter 2** of this thesis outersphere complexes of electrolyte anions on goethite are characterized because the modeling of outersphere complexes has hardly been tested. Experimental determination of the adsorbed amount of these ions is however very difficult and possibly not feasible. The adsorption can be characterized by determining the differences between the primary charging behavior of goethite in solutions of different sodium salts: NaCl, NaNO₃ and NaClO₄. In general, adsorption in multicomponent systems is used as an independent test for the model, or the model parameters, that have been derived for more simple systems. In this case the different ion pair formation constants of the monovalent electrolyte anions on the goethite surface are derived from proton adsorption data, and are tested by predicting the effect of the different electrolyte anions on the adsorption of sulfate and phosphate.

In **chapter 3** the relation between the microscopic structure of adsorbed complexes on goethite is studied in relation to the macroscopic ion adsorption behavior. The influence of the different model parameters on the model description of the proton co-adsorption is studied. The adsorption of several anions is compared by studying one specific adsorption characteristic: the proton co-adsorption as a function of the ion adsorption at constant pH. The anions studied are: sulfate, selenate, chromate, molybdate, tungstate, phosphate, arsenate and vanadate. The differences and similarities between the anions are determined and discussed on the basis of the possible structures of the adsorbed species.

In **chapter 4** an extended data set of sulfate adsorption on goethite is determined. Sulfate is chosen as spectroscopic work has revealed that it is a very suitable model system to study anion adsorption on iron oxides because only one surface species of sulfate was initially found. The influence of the model parameters

for the description of the data is studied and the possibility of finding unique model parameters values is determined.

In **chapter 5** the adsorption of sulfate and selenate is studied because very recent spectroscopic studies have given a more detailed knowledge of the adsorption of sulfate and selenate as was available for the analysis in chapter 4. On the one hand it is studied if the structural knowledge can be incorporated in the CD-MUSIC model. On the other hand it is studied if one can derive the same structural knowledge from the macroscopic adsorption data as compared to spectroscopy.

In **chapter 6** the interaction of phosphate and calcium is studied because previous studies have shown that calcium has a large influence on the phosphate adsorption although the interpretation of the results was unclear due to the formation of precipitates. Calibration of model parameters for the adsorption of calcium and phosphate on goethite for conditions without precipitation will enable a prediction of the phosphate adsorption for environmentally relevant conditions.

As has been mentioned previously, adsorption in the multicomponent system ($\text{PO}_4\text{-Ca-NaNO}_3\text{-FeOOH}$) will be used as an independent test for the model parameters that have been derived for the more simple systems ($\text{Ca-NaNO}_3\text{-FeOOH}$ and $\text{PO}_4\text{-NaNO}_3\text{-FeOOH}$). Especially phosphate data at high pH values are determined to test if mono- and bidentate surface species can be distinguished on the basis of the macroscopic adsorption behavior as both complexes have been suggested using spectroscopy

In **chapter 7** some miscellaneous data are given, model parameters for all studied ions are summarized, and future challenges are presented.

References

1. Hiemstra, T. and Van Riemsdijk, W.H. (1996) A surface structural approach to ion adsorption: The charge distribution (CD) model *J. Colloid Inter. Sci.* **179**, 488-508.
2. Hiemenz, P.C. Principles of colloid and surface chemistry, Marcel Dekker, NY, 1986.
3. Lyklema, J. Fundamentals of Interface and Colloid Science Vol. II Solid-Liquid Interfaces, Academic Press, 1995.
4. Yates, D.E., Levine, S., and Healy, T.W. (1974) Site-binding model of the electrical double layer at the oxide/water interface. *J. Chem. Soc. Faraday Trans. I*, **70**, 1807-1818.
5. Davis, J.A., James, R.O., Leckie, J.O. (1978) Surface ionization and complexation at the oxide/water interface. I. Computation of double layer properties in simple electrolytes *J. Colloid Inter. Sci.* **63**, 480-499.
6. Schindler, P.W. and Stumm, W. "The Surface Chemistry of oxides, hydroxides, and oxide Minerals", in W. Stumm, Ed., Aquatic Surface Chemistry, J. Wiley & Sons, NY, 1987.
7. Dzombak, D.A. and Morel, F.M.M. Surface complexation modelling, Hydrous Ferric Oxide, J. Wiley & Sons, NY, 1990.
8. Davis, J.A. and Kent, D.B., in "Mineral-Water Interface Geochemistry, Reviews in Mineralogy" (M.F. Hochella and A.F. White eds.), Vol. 23, 177-260, Mineralogical Society of America, Washington D.C., 1990.
9. Keizer, M. G. and van Riemsdijk, W. H. "ECOSAT: technical report of the department soil science and plant nutrition" Wageningen Agricultural University, Wageningen, 1998.
10. Allison, J. D.; Brown, D. S; Novo-Gradac, K. J. MINTEQA2/PRODEFA2 A Geochemical Assessment model for environmental systems: version 3.11 databases and version 3.0 user's manual. Environmental Research Laboratory, U.S., EPA, Athens, G.A.
11. Apello, C.A.J. and Postma, D. Geochemistry, groundwater and pollution, Balkema, Rotterdam, 1996.

12. Westall J. and Hohl H. (1980) A comparison of electrostatic models for the oxide/solution interface. *Adv. Colloid Interface Sci.* **12**, 265-294.
13. Borkovec M. (1997) Origin of 1-pK and 2-pK models for ionizable water-solid interfaces. *Langmuir* **13**, 2608-2613.
14. Lützenkirchen J. (1998) Comparison of 1-pK and 2-pK versions of surface complexation theory by the goodness of fit in describing surface charge data of (hydr)oxides. *Environ. Sci. Technol.* **32**, 3149-3154.
15. Machesky M. L., Wesolowski D. J., Palmer D. A., and Ichiro-Hayashi K. (1998) Potentiometric titrations of rutile suspensions to 250°C. *J. Colloid Interface Sci.* **200**, 298-309.
16. Felmy A. R. and Rustad J. R. (1998) Molecular statics calculations of proton binding to goethite surfaces: thermodynamic modeling of surface charging and protonation of goethite in aqueous solution. *Geochim. Cosmochim. Acta* **62**, 25-31.
17. Boilly, J.F., Person, P., Sjöberg, S. (2000) Benzenecarboxylate surface complexation at the goethite (FeOOH)/water interface: II. Linking IR spectroscopic observations to mechanistic surface complexation models for phthalate, trimellitate, and pyromellitate. *Geochim. Cosmochim. Acta* **64**, 3453-3470.
18. Pauling L. (1929) The principles determining the structure of complex ionic crystals. *J. Am. Chem. Soc.* **51**, 1010-1026.
19. Brown I. D. (1978) Bond valences-Simple structural model for inorganic chemistry. *Chem. Soc. Rev.* **7**, 359-376.
20. Hiemstra T., Venema P., and Van Riemsdijk W. H. (1996) Intrinsic proton affinity of reactive surface groups of metal (hydr)oxides: The bond valence principle. *J. Colloid Interface Sci.* **184**, 680-692.
21. Venema P., Hiemstra T., Weidler, P.G., and van Riemsdijk W. H. (1998) Intrinsic proton affinity of reactive surface groups of metal(hydr)oxides *J. Colloid Interface Sci.* **198**, 282-295.
22. Rustad, J.R., Dixon, D.A., Felmy, A.R. (2000) Intrinsic acidity of aluminium, chromium (III) and iron (III) μ_3 -hydroxo functional groups from ab initio electronic structure calculations. *Geochim. Cosmochim. Acta* **64**, 1675-1680.
23. Bargar, J.R., Brown, G.E. Jr. and Parks, G.A. (1997) Surface complexation of Pb(II) at the oxide-water interfaces: I. XAFS and bond-valence determination of mononuclear and polynuclear Pb(II) sorption products on aluminium oxides. *Geochim. Cosmochim. Acta* **61**, 2617-2637.
24. Brown, G.E. Jr., Henrich, V.E., Casey, W.H., Clark, D.L., Eggleston, C., Felmy, A., Goodman, D.W., Gratzel, M., Maciel, G., McCarthy, M.I., Neilson, K.H., Sverejenski, D.A., Toney, M.F., Zachara, J.M. (1999) Metal oxide surfaces and their interactions with aqueous solutions and microbial organisms. *Chem. Rev.* **99**, 77-174.
25. Combes J. M., Chrisholm, C. J., Brown, G. E., Jr, Parks, G. A., Conradson, S. D., Eller, P. G., Triay, I. R., Hobart, D. E., Meijer, A. (1992) EXAFS spectroscopy study of neptunium(V) sorption at the α -FeOOH/water interface. *Environ. Sci. Tech.* **26**, 376-382.
26. Waite, T.C., Davis, J.A., Payne, T.E., Waychunas, G.A. and Xu, N. (1994) Uranium (VI) adsorption to ferrihydrite : application of a surface complexation model. *Geochim. Cosmochim. Acta* **58**, 5465-5478.
27. Östholms, E., Manceau, A., Farges, F., Charlet, L. (1997) Adsorption of Thorium on amorphous silica: an EXAFS study. *J. Colloid Interface Sci.* **194**, 10-21.
28. Bargar, J. R., Towle, S. N., Brown, G. E., Jr., Parks, G. A. (1997) Structure, composition, and reactivity of Pb(II) and Co(II) sorption products and surface functional groups on single-crystal α -Al₂O₃. *J. Colloid Interface Sci.* **85** 473-493.
29. Hug S. J. (1997) In situ Fourier Transform Infrared Measurements of sulfate Adsorption on hematite in aqueous solutions *J. Colloid Interface Sci.* **188**, 415-422.
30. Wijnja, H. and Schulthess, C. P. (2000) Vibrational spectroscopic study of selenate and sulfate adsorption mechanisms on Fe and Al (hydr)oxide surfaces. *J. Colloid Interface Sci.* **229**, 289-297.
31. Peak, D., Ford, R. G., and Sparks, D. L. (1999) An in-situ ATR-FTIR investigation of sulfate bonding mechanisms on goethite *J. Colloid Interface Sci.* **218**, 289-299.

32. Tejedor-Tejedor M. I. and Anderson M. A. (1990) Protonation of phosphate on the surface of goethite as studied by CIR-FTIR and electrophoretic mobility. *Langmuir* **6**, 602-611.
33. Wijnja, H. and Schultess, C. P. (1999) ATR-FTIR and DRIFT spectroscopy of carbonate species at the aged γ - Al_2O_3 /water interface. *Spectrochim. Acta A* **55**, 861-872.
34. Bargar, J.R., Brown, G.E. Jr. and Parks, G.A. (1997) Surface complexation of Pb(II) at the oxide-water interfaces: II. XAFS and bond-valence determination of mononuclear and polynuclear Pb(II) sorption products on iron oxides. *Geochim. Cosmochim. Acta* **61**, 2639-2652.
35. Venema P., Hiemstra T., and Van Riemsdijk W. H. (1996) Comparison of different site binding models for cation sorption; description of pH dependency, salt dependency and cation-proton exchange. *J. Colloid Interface Sci.* **181**, 45-59.
36. Boilly, J.F. The surface complexation of ions at the goethite (α -FeOOH)/water interface: a multisite complexation approach, Ph.D. thesis. Umeå University, Sweden, 1999.
37. Schwertmann, U. The influence of aluminium on iron hydroxides: IX. Dissolution of Al-goethites in 6 M HCl. *Clays Clay Minerals* **19**, 9-19.
38. Weidler, P.G., Schwin, T., and Gau, H.E.(1996) Vicinal faces on synthetic goethite observed by atomic force microscopy. *Clays Clay Minerals* **44**, 437-442.
39. Weidler, P.G., Hug, S. J., Wetche, T. P., and Hiemstra, T.(1998) Determination of growth rates of (100) and (110) faces of synthetic goethite by scanning force microscopy. *Geochim. Cosmochim. Acta* **62**, 3407-3412.
40. Hiemstra T., Van Riemsdijk W. H., and Bolt G. H. (1989). Multisite proton adsorption modelling at the solid/solution interface of (hydr)oxides: a new approach. I model description and evaluation of intrinsic reaction constants. *J. Colloid Interface Sci.* **133**, 91-104.
41. Hiemstra T., De Wit J. C. M., and Van Riemsdijk W. H. (1989). Multisite proton adsorption modelling at the solid/solution interface of (hydr)oxides: a new approach. II application to various important (hydr)oxides. *J. Colloid Interface Sci.* **133**, 105-117.
42. Goldberg, S. in: "Structure and surface reactions of soil particles", Ed. Huang, P.M., Senesi, N., Buffle, J. p. 378-412, J. Wiley & Sons, 1998.
43. Nordin, J.P., Sullivan, D.J., Phillips, B.L., and Casey, W. H. Mechanisms for fluoride-promoted dissolution of bayerite [β - $\text{Al}(\text{OH})_3(\text{s})$] and boehmite [γ - AlOOH]: ^{19}F -NMR spectroscopy and aqueous surface chemistry. *Geochim. Cosmochim. Acta* **63**, 3513-3524.
44. Spadini, L. Manceau, A., Schindler, P.W., and Charlet, L. (1994) Structure and stability of Cd^{2+} surface complexes on ferric oxides. *J. Colloid Interface Sci.* **168**, 73-86.
45. Manceau, A., Nagy, K.L., Spadini, L., Ragnarsdottir, K.V. (2000) Influence of anionic layer structure of Cd surface complexes. *J. Colloid Interface Sci.* **228**, 306-316.
46. Venema P., Hiemstra T., and Van Riemsdijk W. H. (1996) Multi site adsorption of cadmium on goethite. *J. Colloid Interface Sci.* **183**, 515-527.
47. Hiemstra, T. and Van Riemsdijk, W.H. Fluoride adsorption on goethite in relation to different types of surface sites *J. Colloid Interface Sci.* **225**, 94-104.
48. Filius J. D., Hiemstra T., and Van Riemsdijk W. H. (1998) Adsorption of small weak organic acids on goethite: modeling of mechanisms *J. Colloid Interface Sci.* **195**, 368-380.
49. Geelhoed, J. S.; Hiemstra T.; van Riemsdijk W. H. (1997) Phosphate and sulfate adsorption on goethite: single anion and competitive adsorption. *Geochim. Cosmochim. Acta* **61**, 2389-2396.
50. Geelhoed, J. S.; Hiemstra, T.; van Riemsdijk, W. H. (1998) Competitive interaction between phosphate and citrate on goethite *Environ. Sci. Tech.* **32**, 2119-2123.
51. Hiemstra, T. and Van Riemsdijk, W.H. (1999) Surface structural ion adsorption modeling of competitive binding of oxyanions by metal (hydr)oxides. *J. Colloid Interface Sci.* **210**, 182-193.
52. Hiemstra, T., Yong, H., and Van Riemsdijk, W.H. (1999) Interfacial charging phenomena of aluminium (hydr)oxides. *Langmuir*. **15**, 5942-5955.
53. Hiemstra, T., and Van Riemsdijk, W.H. (1999) Effect of different crystal faces on experimental interaction force and aggregation of hematite. *Langmuir*. **15**, 8045-8051.
54. Venema, P., Hiemstra, T. and Van Riemsdijk, W.H. (1996) Interaction of cadmium with phosphate on goethite *J. Colloid Interface Sci.* **192**, 94-103.

Appendix

It is shown here that approximately the same model parameter values for ion adsorption can be found using the general 2site-1pK model or the more detailed multisite model.

The CD approach works mathematically also in combination with the classical 1 site- δ pK approach in situations where the electrostatics effects dominate the pH dependent binding. Such a situation is likely to be the case at low adsorption densities. However, since this approach is not based on insight on the molecular level, it can not be used to link the results in a sensible way to molecular detail on the binding mechanism as can be inferred from spectroscopy, like a mono- or bidentate binding mechanism. The interpretation of the sum bondvalence which is to be expected to be close to 2 for a bridging oxygen in a molecular sound picture also does not work for such a case.

In Fig. A1a the basic acid-base behaviour of goethite is shown for four different model approaches, using published model parameters: the 2site-1pK, 2sites-2pK., multisite approach, and the 1site- δ pK (δ pK=4) approach. In Fig. A1b and A4c the description is given of sulphate adsorption using the parameter values from Chapter 3 (the 2site-1pK model was used in Chapter 3). Also given are the modelled points using the other models by fitting the charge distribution for the adsorbed complex and the intrinsic affinity constant for sulphate ($\log K_{int}$). The same model curves are established by using model parameter values that are rather similar in very different models, see Table A1. This shows that the dependence of the type of model for the parameter assessment of the sulphate adsorption-complex is small.

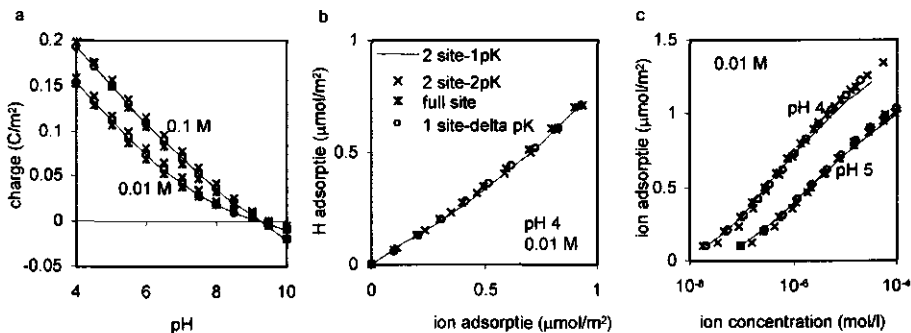


Fig. A1. Four rather different formulations of the surface acid-base equilibria can give almost exactly the same description of (a) acid-base behaviour of goethite, (b) the proton-sulphate adsorption stoichiometry, and (c) sulfate adsorption, using approximately the same model parameter values for the adsorbed complex (see Table 1).

CHAPTER 1

Table A1 Model parameter values for the complexation of sulfate on singly coordinated surface groups in four rather different models of the acid-base equilibria on the goethite surface. The differences between the charge distributions, and the $\log K_{int}$ are small: the dependence of the type of model used is small.

	Reference	Model approach	Charge distribution		Log K_{int}
			(z_0, z_1)	f	
1	Chapter3	2 site-1 pK	(-0.35,-1.65)	0.48	10.35
2	36	2 site-2 pK	(-0.40,-1.60)	0.47	10.2
3	20	multisite (full site)	(-0.25,-1.75)	0.45	10.0
4	35	1 site-2 pK (ΔpK)	(-0.45,-1.55)	0.42	10.2

Electrolyte anion affinity and its effect on oxyanion adsorption on goethite

Abstract

The influence of various types of background electrolytes (NaCl, NaNO₃, and NaClO₄) on the proton adsorption, and on the adsorption of sulphate and phosphate on goethite have been studied. Below the PZC the proton adsorption on goethite decreases in the order Cl⁻>NO₃⁻>ClO₄⁻. The decreasing proton adsorption affects the adsorption of oxyanions on goethite. Anion adsorption of strongly binding polyvalent anions is lower in the studied electrolytes in the order Cl⁻<NO₃⁻<ClO₄⁻. The ion pair formation constants of monovalent electrolyte anions on the goethite surface are derived from proton adsorption data. It is shown that the derived ion pair formation constants enable the prediction of the effect of different electrolyte anions on adsorption of polyvalent anions. Especially at low oxyanion and high electrolyte concentrations the differences between the electrolytes influence the anion adsorption considerably. The effect is in principle not different for anions with a higher affinity for goethite such as phosphate in comparison with sulphate but the effect is only there if the particles are positively charged, which in case of phosphate is only the case at relatively low P concentration and sufficiently low pH values.

CHAPTER 2

This chapter has been published in:
Rietra, R. P. J. J., T. Hiemstra, W. H. van Riemsdijk
Journal of Colloid and Interface Science 229,199-206 (2000)

Introduction

The main goal of the development of surface complexation models is the description and prediction of ion adsorption in multicomponent systems such as soils, sediments, and aquifers. Mechanistically oriented models should ideally account for the structural characteristics of the mineral-water interface like the type of binding sites, the electrostatic profile near the surface, and the location of the adsorbed ions in it (1, 2). Many ions form innersphere surface complexes as observed in a growing number of spectroscopic studies. Monovalent electrolyte ions are normally assumed to be adsorbed as outersphere complexes. Such outersphere complexes have previously been used in surface complexation models to explain the relatively high surface charge on metaloxides in combination with relatively low zeta potentials (9-11). The existence of surface complexes of monovalent electrolyte ions has been demonstrated by determining the simultaneous adsorption of the electrolyte cations and anions in the PZC of an adsorbent (4-8).

The adsorption of sulphate on goethite is strongly influenced by the concentration of the electrolyte, as was shown recently by Persson and Lövgren (12). These experiments were done using NaCl as electrolyte. However using NaNO₃ much less influence of the electrolyte concentration is found (13, 20). A preliminary study (14) showed that these differences might be understood from differences in the affinity of nitrate and chloride for the goethite surface. It is supported by specific effects of the type of electrolyte on sulphate adsorption in soils, where the highest sulphate adsorption is in sodium-perchlorate and the lowest adsorption in sodium chloride (15). Differences between the adsorption of varying electrolyte ions have been determined directly by Sprycha (7, 8) and were derived indirectly from the differences between the proton adsorption in different salts (e.g. 17), and from critical coagulation concentrations (18).

Here we study the adsorption of the electrolyte anions chloride, nitrate and perchlorate, and their effect on ion adsorption of stronger bound polyvalent anions like sulphate and phosphate. The adsorption of a monovalent electrolyte ion such as nitrate provides a typical example of outersphere adsorption on a metal(hydr)oxide (16). Outersphere complexes have been incorporated in electrostatic surface complexation models by locating the charge of these ions in an electrostatic plane at a distance from the surface plane. In this study the affinity of these complexes will be derived by modeling the acid-base behavior of goethite in the presence of the different electrolytes. The results will then be used to predict the effect of the various monovalent anions on the adsorption of sulphate and phosphate, and will be compared with experimental results. Sulphate was chosen since an extended data set exists which has been described well using only one surface complex (20), in line with the spectroscopic results of Hug (19). Phosphate is chosen since it has also been characterized by spectroscopy (37) and has been modelled previously (26).

Materials and Methods

Synthesis and Characterization

All chemicals (Merck p.a.) were stored in plastic bottles and all experiments have been performed in plastic vessels to avoid silica contamination. The water used throughout the experiments was always ultrapure ($\approx 18 \mu\text{S}/\text{cm}$). A goethite suspension was prepared according to Hiemstra et al. (22): a freshly prepared 0.5 M $\text{Fe}(\text{NO}_3)_3$ was slowly titrated with 2.5 M NaOH to pH 12, after which the suspension was aged for 3 days at 60°C and subsequently dialyzed in water. The BET(N_2) specific surface area of the goethite is 96.4 m^2/g . Goethite of the same batch was used previously by Geelhoed et al. (13) and Rietra et al. (20).

Acid-base titrations

For acid-base titrations, a suspension of goethite was made from a sample of the dialyzed goethite suspension. With addition of HNO_3 the suspension was kept at a pH value of 5.5, and was continuously purged with N_2 to remove CO_2 . From this salt-free suspension, sub-samples of approximately 60 ml were prepared for titrations. After addition of salt to the suspensions in the vessels, a N_2 atmosphere was maintained by flushing clean moistened N_2 -gas through the vessel during a night previous to performing the titrations. The goethite concentration used in various titrations was between 12 to 15 g/l goethite. Acid-base titrations have been performed in an automated set up (23) at two or three electrolyte concentrations with NaOH and HNO_3 . The electrolyte concentrations used in the various experiments were 0.005-0.02-0.1 M NaNO_3 , 0.02-0.5 M NaNO_3 , 0.02-0.1 M NaClO_4 , or 0.02-0.1 M NaCl. Venema et al. (24) previously discussed the details about the experimental method used for the titrations. The total amount of NO_3 resulting from the acid HNO_3 addition is of small significance in 0.02 M NaClO_4 or NaCl ($< 10\%$ NaNO_3) and of no significance in 0.1 M ($< 3\%$ NaNO_3) NaClO_4 or NaCl.

The proton adsorption in the different electrolytes has been determined relatively to each other using the charge of a salt-free goethite suspension as a reference point. The initial differences in pH between samples in NaCl, NaNO_3 or NaClO_4 characterize the difference of the proton adsorption between the samples because the total amount of protons ($\text{H}_T\text{-OH}_T$) is identical.

Adsorption isotherms

Adsorption experiments were performed in individual centrifuge tubes with fixed amounts of salt, goethite, and sulphate, and differing pH values to give adsorption-edges. The tubes were equilibrated for 20 hours in end-over-end rotation. They were centrifuged, and samples of the supernatant were taken for analysis with ICP-AES. The pH was measured in the remaining supernatant. The amount of adsorbed ions was calculated from the difference between the total initial ion concentration and the final ion concentration of the suspension.

Proton-phosphate titrations at constant pH

Samples of 60 ml of goethite suspension with an electrolyte concentration of 0.01 M or of 0.05 M NaCl, NaNO₃, or NaClO₄ were titrated to pH≤5.5 and left overnight in N₂ atmosphere to remove CO₂. For the pH-STAT titration a standardized 0.01 M HNO₃ solution was used. Phosphate was added in steps of 0.3 ml solution of 0.01 M NaHPO₄ + 0.006 M HNO₃ (36). After each addition of phosphate solution, the pH was corrected to the initial pH with the acid. A reaction time of at least 20 minutes and a maximum drift criterion of 0.002 pH units per minute was used between each titration of anion in order to obtain equilibrium. The total amount of added phosphate was sufficiently small compared with the amount of goethite to give practically 100% adsorption. In this case the proton balance can be calculated easily from the amount of added acid and protons in the phosphate solution since correction for changes in solution are negligible. The details of the calculation of the proton adsorption are given in Rietra et al. (20).

Electrophoretic mobility

Measurements of the electrophoretic mobility have been carried out using a laser Doppler velocimetry setup (ZetaSizer 3, Malvern) according to the method of Minor et al. (25). Electrophoretic mobilities have been measured of goethite suspensions of 0.05 g/l for a series of electrolyte concentrations in NaClO₄, NaNO₃ and NaCl at pH 4.

Model calculations

Model calculations have been done using the CD-MUSIC model. This model has previously been applied to describe the adsorption of the oxyanions used in this study, phosphate (26), and sulphate (20). The Basic Stern model (26, 27) is used as a description for the electrostatic double layer. The CD-MUSIC model is an extension of the MUSIC model (21, 26). An important feature of the model is the notion that innersphere surface complexes should not be treated as point charges. Innersphere complexes of ions are assumed to have a spatial distribution of charge. A fraction of the charge is attributed to the surface since only a fraction of the ligands of the adsorbing polyvalent ions are involved in ligand exchange with the surface. The remaining part of the charge is located at a certain distance of the surface. The charge attribution (z_i) to the electrostatic planes can be estimated for known surface structures of adsorbed ions by using the Pauling bond valence concept (26). The estimated charge attribution is calculated according to: $z_i = n_i (v-2)$, where n_i is the number of ligands per electrostatic plane i , and v is the Pauling bond valence (valence of central "ion" divided by the coordination number). The site densities for the goethite are taken from Hiemstra and van Riemsdijk (26).

Calculations were carried out with Ecosat, a computer code for the calculation of chemical equilibria (28). The Davies equation (constant is 0.2) is used to calculate the ion activity coefficients at 25°C (the equilibria used are as in ref. 13).

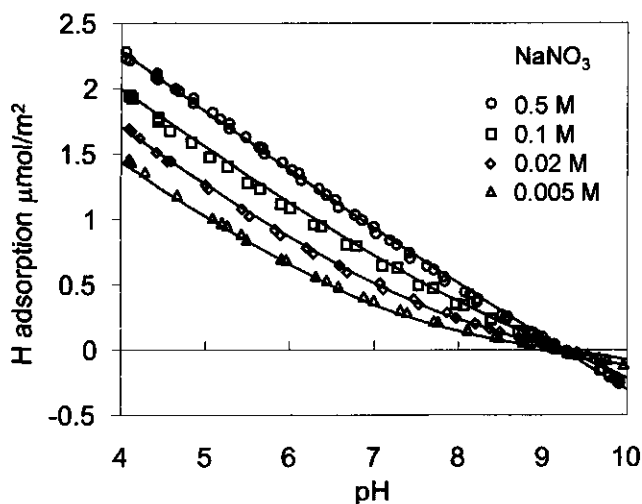


Fig 1. Proton adsorption of goethite as a function of pH and ionic strength in NaNO_3 . The PZC is assigned to the common intersection point in NaNO_3 , assuming identical ion pair formation constants for Na^+ and NO_3^- on goethite. The lines are calculated using the CD-MUSIC model.

Results and Discussion

Affinity of Cl^- , NO_3^- , ClO_4^- for goethite

The proton adsorption at the goethite surface as a function of pH and NaNO_3 is shown in Fig. 1. The results are similar to the results of Venema et al. (24) and Hiemstra and van Riemsdijk (26). The PZC is assigned to the common intersection point (c.i.p.) at pH 9.25. The capacitance of the Stern layer (C) and the surface ion pair formation constants were calculated by least squares fitting resulting in $C=0.905 \text{ F/m}^2$ and $\log K = -1.0$, assuming the same ion pair formation constants for the sodium and nitrate ions (20). Options for using other model parameter values for the ion pair formation constants and capacitance are very limited. Higher values for the Stern capacity have to be compensated by lower ion pair formation constants, and vice versa. A combination of a lower capacitance and higher ion pair formation constants gives more linear curves than those shown in Fig. 1, while a combination of a higher capacitance and lower ion pair formation constants will lead to more bent curves. This behavior enables the calculation of the ion pair formation constants from the proton adsorption curves using an electrostatic model. The same model has also been used (29) to describe simultaneously the zeta potentials, proton adsorption, and the adsorption data of Na and Cl ions on Al hydroxides. It is noted that due to the high PZC little detailed information can be obtained on the behavior of the monovalent cation, sodium. An often-used simplifying assumption is that the affinities of the monovalent cation and anion are the same. In this case this assumption can not be made, since the experiments of this study show that the affinities of the surface for the various monovalent anions are clearly different. We have made the somewhat arbitrary assumption that the affinity of the surface for nitrate and sodium is the same. This is in line with our earlier work on ion

adsorption in NaNO_3 . New experimental techniques (29, 41, 42), like the novel acoustic electrophoreses, may in future lead to additional information at the high electrolyte levels (shift of isoelectric point) enabling a full differentiation of individual ion pair formation constants.

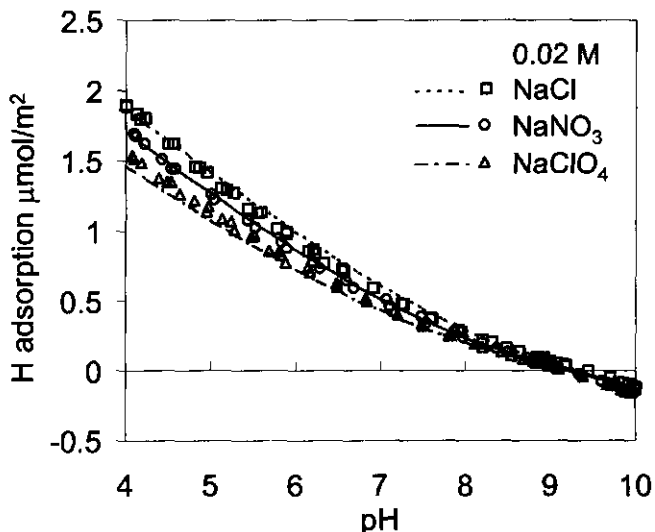


Fig. 2. Proton adsorption of goethite as a function of pH at an ionic strength of 0.02 M NaClO_4 , NaNO_3 or NaCl . The lines are calculated using the CD-MUSIC model.

In Fig. 2 and 3 the proton adsorption in electrolytes with different anions is shown relative to that in NaNO_3 for resp. 0.02 M and 0.1 M. The influence of the type of anion of the electrolyte is most evident at low pH values. These results can be interpreted in terms of different affinities of goethite for different monovalent electrolyte anions. The proton adsorption as a function of pH enables the calculation of the ion pair formation constants for perchlorate ($\log K = -1.7$) and chloride ($\log K = -0.5$). The value of the ion pair formation constant of perchlorate is low ($\log K = -1.7$).

It can be rationalized that there is no significant non-electrostatic contribution to the ion pair formation for perchlorate. This follows when one uses an equal affinity for the surface site (S) for perchlorate as for water: $\text{S}-\text{H}_2\text{O} + \text{ClO}_4^- = \text{S}-\text{ClO}_4^- + \text{H}_2\text{O}$, and H_2O is defined as a concentration (note $[\text{H}_2\text{O}] = 55.5 \text{ mol/l}$). Defining the equilibrium on the basis of an activity of water of one yields a $\log K$ value of $\log(1/55.5) = -1.7$.

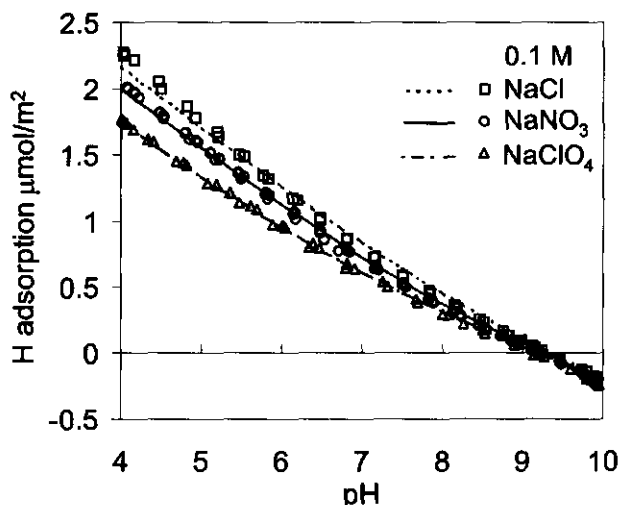


Fig. 3. Proton adsorption of goethite as a function of pH at an ionic strength of 0.1 M NaClO₄, NaNO₃ or NaCl. The lines are calculated using the CD-MUSIC model.

Instead of using different surface ion pair formation constants the differences between the proton adsorption in the different electrolytes can also be rationalized by assuming different distances between the surface and the adsorbing ions. This option is not considered because it will lead to a high complexity of the model for multicomponent systems such as found in nature.

Our data show that the chloride ion has a higher affinity for the surface. An even stronger preference of chloride has been found for RuO₂ (30). The proton adsorption on RuO₂ in 0.05 M KCl (1.0 μmol/m²) was found to be 2.5 times higher compared to the proton adsorption in 0.05 M KNO₃ (0.4 μmol/m²). In our studies only a factor of approximately 1.2 between NaCl and NaNO₃ at pH 4.5 is found.

The effect that different types of electrolyte anions have on the acid-base behavior of goethite is not commonly known although some authors pointed to it (31, 32). Zeltner and Anderson (31) noticed that the proton adsorption on goethite in NaNO₃ was slightly higher compared to NaClO₄. Gunneriusson et al. (32) found a higher proton adsorption on goethite in NaCl compared to NaNO₃, in contrast to an earlier observation of the same authors, reporting no significant difference (33). The specific order of the proton adsorption as function of the anions (Cl > NO₃ > ClO₄) is not a general one. For instance, almost no differences were found for proton adsorption in these different electrolytes for rutile (34). Differences were found in NaCl, NaBr or NaI for Al₂O₃ (8) and anatase (7). The proton adsorption on anatase and Al₂O₃ in NaCl, NaBr and NaI had the order Cl ≅ Br > I, which is in line with the lower adsorption of I compared to Cl on anatase.

We have tried to use electromobility to test whether the zeta potential is influenced by the difference between electrolytes by determining the electromobility as function of salt and salt concentration at pH 4. Like others we have found that the electromobility did not vary systematically as a function of the salt concentration (31, 35) and conclude that the electromobility is not related to the zeta potential with a simple relation. The effect of different monovalent electrolytes

on polyvalent ion adsorption is probably a better tool to study the usefulness of model predictions.

Effect of electrolyte binding on oxyanion adsorption

On the basis of the model parameters derived we have analyzed the conditions (e.g. pH, salt- and oxyanion concentration) for which a possible effect of varying the monovalent anion of the electrolyte on sulphate and phosphate adsorption can be expected. Sulphate and phosphate are chosen since the model parameters for both ions are well established and sulphate and phosphate are respectively examples for low and high affinity polyvalent anions. Using the parameter set of Rietra et al. (20) for sulphate, and of Hiemstra and van Riemsdijk (26) for phosphate, we predict that in case of sulphate and phosphate an effect of varying the anion of the electrolyte is only important for conditions where the goethite is positively charged.

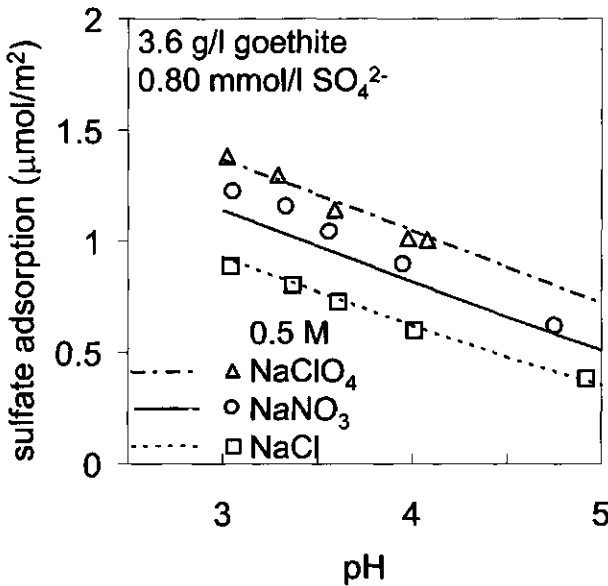


Fig. 4. Effect of pH and outer-sphere ions on sulphate adsorption in 0.5 M in NaClO₄, NaNO₃ or NaCl. The lines are model calculations.

The sulphate-goethite system remains positively charged in most conditions, as was shown by Rietra et al. (20). The effect of varying the electrolyte on the adsorption of sulphate on goethite is shown in Fig. 4 for the 0.5 M electrolyte concentration. Especially the difference between adsorption in perchlorate and chloride is considerable. The curves are modeled by using the same model parameters for sulphate as used previously (20) and the ion pair formation constants derived from the acid-base curves in Fig. 1-3. There is a very good agreement between the model predictions and the measurements. The effect of using an electrolyte concentration of 0.1 M is shown in Fig. 5. The difference between the different electrolyte anions is smaller and in agreement with the model predictions.

Calculations show that an effect of the type of electrolyte in 0.01 M electrolyte is only predicted at low sulphate concentrations and low pH values.

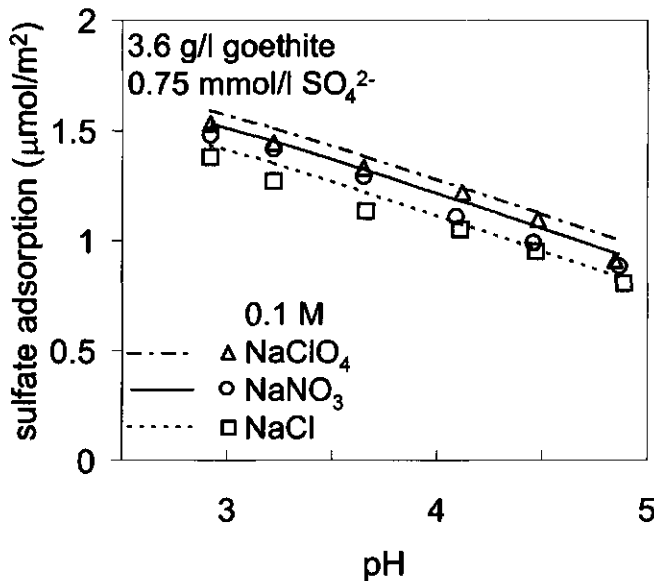


Fig. 5. Effect of pH and outer-sphere ions on sulphate adsorption in 0.1 M in NaClO₄, NaNO₃ or NaCl. The lines are model calculations.

In case of phosphate, the goethite is only positively charged at relatively low pH values and low phosphate loadings. The phosphate concentrations are in these conditions near or below detection limit (app. 1 μmol/l). Figure 6 shows that the calculated phosphate adsorption is only affected by the type of electrolyte anion at phosphate concentrations below the detection limit. This limits the evaluation as done for sulphate adsorption. We have therefore looked for an alternative.

It is in principle relatively easy to determine effects of electrolyte from the co-adsorption of protons for the conditions where almost 100 % of the phosphate is adsorbed (36). The results are shown in Fig. 7. The proton adsorption is given relative to the proton adsorption of goethite in 0.05 M NaClO₄. The effect of using NaCl or NaNO₃ instead of NaClO₄ is that the initial proton adsorption is higher. The data show a decreasing effect of the electrolyte anion on the proton co-adsorption with increasing phosphate adsorption. This is due to the decrease in the positive surface charge with increasing adsorption (26, 37). As the charge of the goethite becomes closer to neutral the effect of the different electrolyte anions on the proton adsorption disappears. The curves are predicted well by using the model for phosphate as given by Hiemstra and van Riemsdijk (26) in combination with the ion pair formation constants determined from the acid-base titrations. The effect of the different electrolytes is modeled using the previously determined (Fig. 2 and 3) ion pair formation constants ($\log K_{\text{Cl}} = -0.5$, $\log K_{\text{NO}_3} = -1.0$, $\log K_{\text{ClO}_4} = -1.7$, $\log K_{\text{Na}} = -1.0$). The proton-phosphate adsorption stoichiometry, which is the slope of the curves in Fig. 7, is different in the three electrolytes. As will be outlined, this can be

directly interpreted in terms of an effect of the different electrolytes on the pH dependence of the phosphate adsorption.

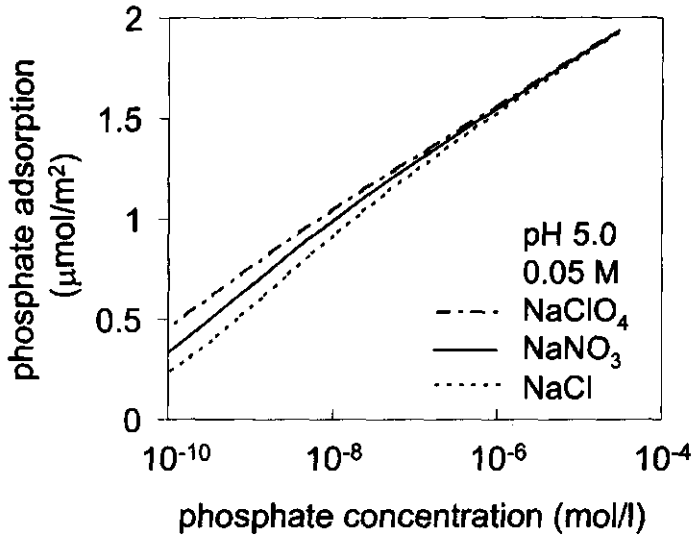


Fig. 6. Predicted effect of different electrolytes on phosphate adsorption at pH 5 and an electrolyte concentration of 0.05 M.

Thermodynamic consistency between proton-ion adsorption stoichiometry and adsorption isotherms

The slope of the proton-ion adsorption curve at a given pH (Fig. 7) is related to the pH dependency of the adsorption as shown by Perona and Leckie (38). The general thermodynamic relation is:

$$\chi = (\partial \Gamma_H / \partial \Gamma_i)_{pH} = -(\partial \log(a_i) / \partial \log H)_{\Gamma_i} \quad [1]$$

,where Γ_H , Γ_i , and a_i are respectively the proton adsorption, ion adsorption and the ion activity. Given in words, the equation shows that the slope of the proton-ion titration curve is equal to the shift of an adsorption isotherm with pH. In case of, for instance sulphate, the slope of the proton-sulphate titration curve is directly related to the shift of the adsorption isotherm with pH. In case of phosphate the situation is less straightforward since this ion protonates in solution, which also changes the activity of PO_4^{3-} with pH.

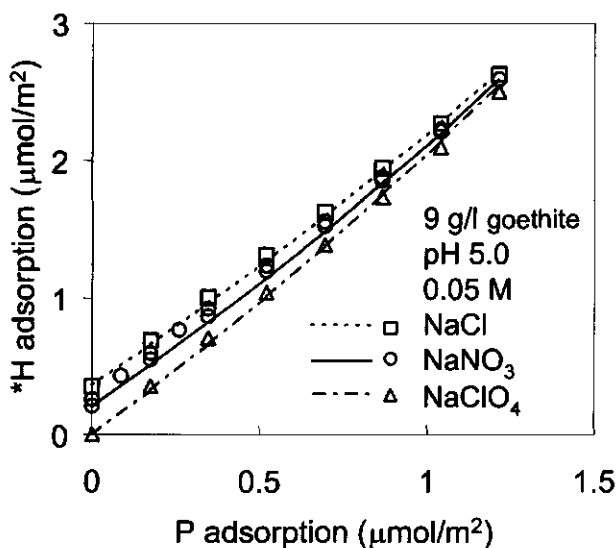


Fig. 7. Proton adsorption of goethite as a function of phosphate adsorption at pH 5.0 in 0.05 M in NaClO₄, NaNO₃ or NaCl. Note (*) that the proton adsorption in the different salts is relative to the proton adsorption at pH 5.0 in 0.05 M NaClO₄ and is determined by addition of the salts to identical salt-free goethite samples and titrating acid down to pH 5.0. The lines are model predictions.

We have extended the thermodynamic consistency relationship for ions that change their speciation in solution. To do so we have defined the ratio of proton co-adsorption and oxyanion adsorption using the unprotonated oxyanion as the reference situation (36). This reference situation was chosen because of structural considerations, since the oxyanions that were considered in this study are believed to form unprotonated surface complexes at low surface coverages. The choice of this reference state was also quite useful in the context of understanding the relationship between the structure of the adsorbed complex and the measured adsorption behavior (36). In the appendix we derive the thermodynamic consistency relationship between the experimental proton co-adsorption and oxyanion adsorption (χ), with the unprotonated ion as reference, and the pH dependency of ion equilibrium concentration at a constant ion adsorption level. For phosphate as an example, the result is:

$$(\chi - [H_P]/[P_{diss}])_{pH} = - \{ \partial \log [P_{diss}] / \partial \log (H) \}_{\Gamma_P} \quad [2]$$

where χ is the proton-ion adsorption stoichiometry (slope of proton-ion titration curve in Fig. 7) as defined above and H_P is the number of protons present on the dissolved phosphate (P_{diss}), i.e. the average degree of protonation of phosphate in solution at a certain pH. Equation 2 can be applied to the data of Fig. 7 for the prediction of the pH dependency of the adsorption isotherms in the three different electrolytes. The left hand side of equation 2 equals the proton-ion adsorption stoichiometry at a certain pH, corrected for the average degree of protonation in

solution. Equation 2 is illustrated in Fig. 8. The slope of the curve of the proton-ion titration curve in NaNO_3 in Fig. 7 and 8 is $\chi = \partial\Gamma_{\text{H}}/\partial\Gamma_{\text{P}} = 2.13$, as measured in the phosphate adsorption interval $0.7\text{--}1.0 \mu\text{mol}/\text{m}^2$. The average degree of protonation in solution at pH 5 ($H_{\text{P}}/P_{\text{diss}}$) equals 1.99. It implies a shift of $-\Delta\log P_{\text{diss}}/\Delta\log H = \Delta\log P_{\text{diss}}/\Delta\text{pH} = 0.12$ in the phosphate adsorption isotherm going from pH 4.5 to 5.5. Experimentally one finds in NaCl and NaClO_4 a value for χ of respectively 1.98 and 2.23. It implies that in NaCl almost no effect of pH is found and that in NaClO_4 the $\Delta\log P_{\text{diss}}$ is about 0.24 going from pH 4.5 to pH 5.5. It is interesting to notice that there is no pH dependency in our example in Fig 8 (NaNO_3) at $P_{\text{diss}} = 10^{-9} \text{ mol/l}$. Here the slope of the proton-ion titration is equal to 1.99, which is also the mean degree of protonation of phosphate in solution ($H_{1.99}\text{PO}_4$).

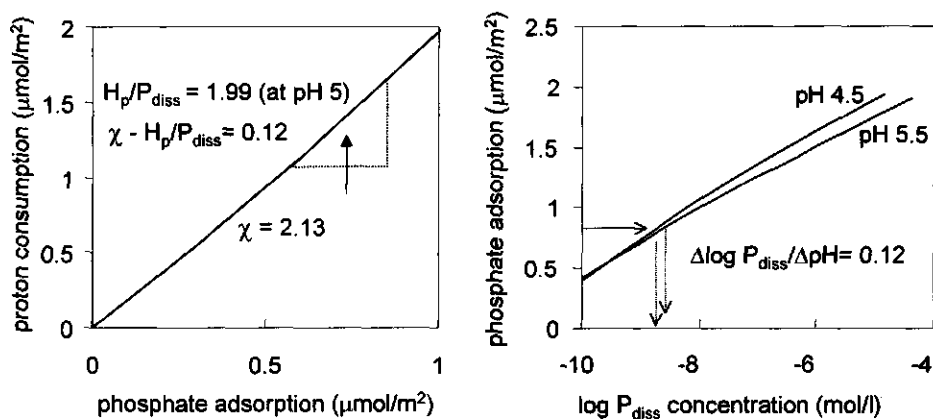


Fig. 8. Thermodynamic consistency between proton-ion adsorption curve and the pH dependency of ion adsorption exemplified for phosphate. The thermodynamic consistency says how the proton consumption as a function of ion adsorption at constant pH is related to the pH dependency of the ion adsorption. It is illustrated here for an ion that has a variable protonation/hydrolysis in solution (see text).

Conclusions

The acid-base behaviour of oxides changes as a function of the type of electrolyte anion. Chloride seems more able to screen the positive charge of the goethite particles than nitrate, and perchlorate is a rather inert anion. Variation in proton adsorption on goethite in different types of electrolytes can be modeled, assuming a difference in affinity for the interaction of outersphere complexes with surface sites. Differences between acid-base behavior in these electrolytes are hardly mentioned in literature and often ignored. The different ion pair formation constants for the interaction with the goethite surface, as derived from the description of the proton adsorption data in different electrolytes, predict the effect of different electrolytes on polyvalent ion adsorption when the CD-MUSIC model is used.

Acknowledgements

The authors thank Th. A. Vens for producing the goethite. We also thank A. J. Korteweg and A. J. Van der Linde from the Department of Biomolecular Sciences (Laboratory of Physical Chemistry and Colloid Science) respectively for the BET analysis and for assistance during use of the Zetasizer.

References

1. Brown, G. E., Henrich, V. E., Casey, W. H., Clark, D. L., Eggleston, C., Felmy, A., Goodman, D. W., Gratzel, M., Maciel, G., McCarthy, M. I., Nealon, K. H., Sverjenski, D. A., Toney, M. F., and Zachara, J. M., *Chem. Rev.* **99**, 77 (1999).
2. Van Riemsdijk, W. H., and Hiemstra, T., From molecular structure to ion adsorption modeling, in: *Mineral-water interfacial reactions: kinetics and mechanisms*. Sparks, D. L. and Grundl, T. J., Eds.; American Chemical Society: Washington DC, 1998, symposium series 715.
3. Bargar, J. R., Towle, S. N., Brown, G. E., Jr., and Parks, G. A., (1996) Outer-sphere Pb(II) adsorbed at specific surface sites on single crystal α -alumina. *Geochim. Cosmochim. Acta* **60**, 3541-3547.
4. Smit, W., and Holten, C. L. M., (1980) Zeta-potential and radiotracer adsorption measurements on EFG Al_2O_3 single crystals in NaBr solutions *J. Colloid Interface. Sci.* **78**, 1-14.
5. Shiao, S. Y., and Meyer R. E., *J. Inorg. Nucl. Chem.* **43**, 3301 (1981).
6. Foissy, A., MPandou, A., Lamarche, J. M. (1982) Surface and diffuse-layer charge at the TiO_2 -electrolyte interface. *Colloids and Surf.* **5**, 363-368.
7. Sprycha, R., (1984) Surface charge and adsorption of background electrolyte ions at anatase/electrolyte interface *J. Colloid Interface Sci.* **102**, 173-185.
8. Sprycha, R. (1989) Electrical double layer at alumina/electrolyte interface. II Adsorption of supporting electrolyte ions *J. Colloid Interface Sci.* **127**, 12-25.
9. Yates, D. E., Levine, S., and Healy, T. W. (1974) Site-binding model of the electrical double layer at the oxide/water interface. *J. Chem. Soc. Faraday Trans. 1* **70** 1807-1818.
10. Davis, J. A., James, R., Leckie, J. O. (1978) Surface ionization and complexation at the oxide/water interface. *J. Colloid Interface Sci.* **63**, 480-499.
11. Schudel M., Behrens S. H., Holthoff H., Kretzschmar R., and Borkovec M. (1997) Absolute aggregation rate constants of hematite particles in aqueous suspensions: a comparison of two different surface morphologies. *J. Colloid Interface Sci.* **196**, 241-253.
12. Persson, P., and Lövgren, L. (1996) Potentiometric and spectroscopic studies of sulfate complexation at the goethite-water interface. *Geochim. Cosmochim. Acta.* **60**, 2789-2799.
13. Geelhoed, J. S., Hiemstra, T., and van Riemsdijk, W. H., (1997) Phosphate and sulfate adsorption on goethite: Single anion and competitive adsorption *Geochim. Cosmochim. Acta* **61**, 2389-2396.
14. Rietra, R. P. J. J., Hiemstra, T., and van Riemsdijk, W. H., (1998) Characterization of ion adsorption with proton-ion titrations. *Mineralogical Magazine.* **62A**, 1269-1270.
15. Zhang, G. Y., Brümmer, G. M., and Zhang, Z. N., (1996) Effect of perchlorate, nitrate, chloride and pH on sulfate adsorption by variable-charge soils *Geoderma* **73**, 217-229.
16. Wijnja, H. and Schultess, C. P., (1999) ATR-FTIR and DRIFT spectroscopy of carbonate species at the aged $\text{g-Al}_2\text{O}_3$ /water interface. *Spectrochim. Acta A.* **55**, 861-872.
17. Breeuwisma, A. and Lyklema, J. J. (1973) Physical and chemical adsorption of ions in the electrical double layer on hematite ($\alpha\text{-Fe}_2\text{O}_3$) *J. Colloid Interface Sci.* **43**, 437.
18. Dumont, F., Warlus, J., and Watillon, A. (1990) Influence of the point of zero charge of titanium dioxide hydrosols on the ionic adsorption sequences. *J. Colloid Interface Sci.* **138** (2) 543-554.
19. Hug, S. J., (1997) In Situ Fourier Transform Infrared Measurements of sulfate Adsorption on hematite in aqueous solutions *J. Colloid Interface Sci.* **188**, 415-422.

20. Rietra R. P. J. J., Hiemstra, T. and van Riemsdijk W. H. (1999) Sulfate adsorption on goethite. *J. Colloid Interface Sci.* **218**, 511-521.
21. Hiemstra T., Van Riemsdijk W. H., and Bolt G. H. (1989). Multisite proton adsorption modelling at the solid/solution interface of (hydr)oxides: a new approach. I model description and evaluation of intrinsic reaction constants. *J. Colloid Interface Sci.* **133**, 91-104.
22. Hiemstra T., De Wit J. C. M., and Van Riemsdijk W. H. (1989). Multisite proton adsorption modelling at the solid/solution interface of (hydr)oxides: a new approach. II application to various important (hydr)oxides. *J. Colloid Interface Sci.* **133**, 105-117.
23. Kinniburgh D. G., Milne C. J., and Venema P. (1995) Design and construction of a personal-computer-based automatic titrator. *Soil Sci. Soc. Am. J.* **59**, (2) 417-422.
24. Venema P., Hiemstra T., and Van Riemsdijk W. H. (1996) Multi site adsorption of cadmium on goethite. *J. Colloid Interface Sci.* **183**, 515-527.
25. Minor, M., van der Linde A. J., van Leeuwen, H. P., and Lyklema, J. (1997) Dynamic aspects of electrophoresis and electroosmosis: A new fast method for measuring particle mobilities *J. Colloid Interface Sci* **189**, 370-375.
26. Hiemstra T. and Van Riemsdijk W. H. (1996) A surface structural approach to ion adsorption: the charge distribution (CD) model. *J. Colloid Interface Sci.* **179**, 488-508.
27. Westall J. and Hohl H. (1980) A comparison of electrostatic models for the oxide/solution interface. *Adv. Colloid Interface Sci.* **12**, 265-294.
28. Keizer, M. G. and van Riemsdijk, W. H. "ECOSAT: technical report of the department soil science and plant nutrition" Wageningen Agricultural University, Wageningen (1998).
29. Hiemstra, T., and Van Riemsdijk, W.H. (1999) Effect of different crystal faces on experimental interaction force and aggregation of hematite. *Langmuir*. **15**, 8045-8051.
30. Kleijn, J. M. and Lyklema, J. (1987) The electrical double layer on oxides: specific adsorption of chloride and methylviologen on ruthenium dioxide. *J. Colloid Interface Sci.* **120** (2) 511-522.
31. Zeltner, W. A., and Anderson, M. A. (1988) Surface charge development at the goethite/aqueous solution interface: effects of CO₂ adsorption. *Langmuir* **4**, 469-474.
32. Gunneriusson, L., Lövgren, L., and Sjöberg, S. (1994) Complexation of Pb(II) at the goethite (α -FeOOH)/water interface: the influence of chloride. *Geochim. Cosmochim. Acta* **58** (22) 4973-4983.
33. Gunneriusson, L., and Sjöberg, S. (1993) Surface complexation in the H⁺-goethite (α -FeOOH)-Hg(II)-chloride system. *J. Colloid Interface Sci.* **156**, 121-128.
34. Bérubé, Y. G., and Bruyn, de, P. L. (1968) Adsorption at the rutile-solution interface II Model of the electrochemical double layer. *J. Colloid Interface Sci.* **28** (1) 92-105.
35. Fernández-Nieves, A., and de las Nieves, F. J. (1999) The role of ξ -potential in the colloidal stability of different TiO₂/electrolyte solution interfaces. *Colloids Surf. A* **148**, 231-243.
36. Rietra, R. P. J. J., Hiemstra, T., and van Riemsdijk, W. H., (1999) The relation between molecular structure and ion adsorption behavior on variable charged minerals *Geochim. Cosmochim. Acta.* **63**, 3009-3015.
37. Tejedor-Tejedor M. I. and Anderson M. A. (1990) Protonation of phosphate on the surface of goethite as studied by CIR-FTIR and electrophoretic mobility. *Langmuir* **6**, 602-611.
38. Perona M. J. and Leckie J. O. (1985) Proton stoichiometry for the adsorption of cations on oxide surfaces. *J. Colloid Interface Sci.* **106**, 65-69.
39. Černik, M., Borkovec, M., and Westall, J. C., (1996) Affinity distribution description of competitive ion binding to heterogeneous materials *Langmuir* **12**, 6127-6137.
40. Stumm, W. and Morgan, J. J., Aquatic Chemistry. Wiley (1996).
41. Rowlands, W. N., O'Brien, R. W., Hunter, R. J., and Patrick, V., *J. Colloid Interface Sci.* **188**, 325 (1997).
42. Johnson, S. B., Franks, G. V., Scales, P. J., Healy, T. W., (1999) The binding of monovalent electrolyte ions on α -alumina. II The shear yield stress of concentrated suspensions. *Langmuir* **15**, 2844-2853.

Appendix

The proton-ion stoichiometry (χ) has been given previously (38) for unhydrolyzed/unprotonated ions (i) in which Γ_H is defined as the total amount of consumed protons in a ion titration at constant pH at a certain amount of adsorbed ion Γ_i . It is related to the change of the ion activity of the unhydrolyzed/unprotonated ion and the change of pH at a constant adsorbed amount of i, which is given as $(\partial \log(a_i)/\partial \log(H))_{\Gamma_i}$, according to:

$$\chi = (\partial \Gamma_H / \partial \Gamma_i)_{pH} = -(\partial \log(a_i) / \partial \log(H))_{\Gamma_i} \quad [A1]$$

Eq. [A1] says that the slope of the proton-ion adsorption curve for a given adsorption level (Γ_i) and at a constant pH is equal to the pH dependency of the equilibrium activity of an unhydrolyzed or unprotonated ion i at the given adsorption level Γ_i . The right hand side of eq. [A1] can be rewritten for the pH dependency of the total concentration of ion i in solution. The derivation is exemplified here for phosphate.

The total concentration of phosphate (P_{diss}) in solution can be written as the sum of species (with concentrations [i], activity (i) and activity coefficients γ_i):

$$[P_{diss}] = [PO_4^{3-}] + [HPO_4^{2-}] + [H_2PO_4^-] + [H_3PO_4] \quad [A2]$$

The number of protons (H_p) bound to these species equals:

$$[H_p] = 1[HPO_4^{2-}] + 2[H_2PO_4^-] + 3[H_3PO_4] \quad [A3]$$

Introduction of the different protonation steps leads to:

$$[P_{diss}] = (PO_4^{3-})/\gamma_{PO_4} + K_1(H)(PO_4^{3-})/\gamma + \dots \quad [A4]$$

or

$$(PO_4^{3-}) = [P_{diss}] \{ 1/\gamma_{PO_4} + k_1(H) + k_2(H)^2 + k_3(H)^3 \}^{-1} = [P_{diss}] A = [P_{diss}] B^{-1} \quad [A5]$$

with k_1, k_2 , and k_3 being the effective protonation constants ($k_i = K_i/\gamma_i$) for the successive protonation steps (40).

Introduction of this in the right hand side of eq. [A1] yields:

$$\chi = - \{ \partial \log(PO_4^{3-}) / \partial \log(H) \}_{\Gamma_p} = - \{ \partial \log[P_{diss}] / \partial \log(H) \}_{\Gamma_p} - (\partial \log A / \partial \log(H)) \quad [A6]$$

Using eq. [A5], the second term on the right hand of eq. [A6] is differentiated easily using $A=B^{-1}$:

$$\partial \log A / \partial \log(H) = (H)/A \quad \partial A / \delta(H) = -(H)/A B^{-2} \quad \partial B / \partial(H) = -(H)A \quad \partial B / \partial(H) \quad [A7]$$

$$\partial B / \partial(H) = k_1 + 2k_2(H) + 3k_3(H)^2 \quad [A8]$$

eq. [A6] can be written as:

$$\chi = - \partial \log [P_{diss}] / \partial \log(H) + (k_1(H) + 2k_2(H)^2 + 3k_3(H)^3) \{ 1/\gamma_{PO_4} + k_1(H) + k_2(H)^2 + k_3(H)^3 \}^{-1} \quad [A9]$$

It can be seen that eq. [A9] can be reduced to a simple relation using eq. [A1] and [A2]:

$$\chi = - (\partial \log[P_{diss}] / \partial \log(H))_{\Gamma_p} + ([H_p] / [P_{diss}]) = (\partial \Gamma_H / \partial \Gamma_i)_{pH} \quad [A10]$$

The final equation shows that the proton-ion adsorption stoichiometry (χ) can be related to the pH dependency of the total dissolved equilibrium concentration by correcting for the degree of protonation in solution ($[H_p]/[P_{diss}]$). This simple thermodynamic relation is very valuable to extrapolate the pH dependency of the equilibrium concentration to concentrations below the detection limit.

The relationship between molecular structure and ion adsorption on variable charge minerals

Abstract

Ion adsorption modelling is influenced by the presumed binding structure of surface complexes. Ideally, surface complexes resulting from modelling should correspond with those derived from spectroscopy, thereby assuring that the mechanistic description of ion binding scales from the microscopic molecular structure to the macroscopic adsorption behaviour. Here we show that the structure of adsorbed species is a major factor ruling the pH dependency of adsorption. An important aspect of the pH dependency is the macroscopic proton-ion adsorption stoichiometry. A simple and accurate experimental method was developed to determine this stoichiometry. With this method, proton-ion stoichiometry ratios for vanadate, phosphate, arsenate, chromate, molybdate, tungstate, selenate and sulphate have been characterised at one or two pH values. Modelling of these data shows that the macroscopic proton-ion adsorption stoichiometry is almost solely determined by the interfacial charge distribution of adsorbed complexes. The bond valence concept of Pauling can be used to estimate this charge distribution from spectroscopic data. Conversely, the experimentally determined proton-ion adsorption stoichiometry allows us to successfully predict the spectroscopically identified structures of, for example, selenite and arsenate on goethite. Consequently, we have demonstrated a direct relationship between molecular surface structure and macroscopic adsorption phenomena.

CHAPTER 3

This chapter has been published:

René P. J. J. Rietra, Tjisse Hiemstra & Willem H. van Riemsdijk
Geochimica et Cosmochimica Acta, Vol. 63, No. 19/20, pp.3009-3015,
1999.

Introduction

Geochemists are challenged to translate the knowledge of surface species coordination gained from in-situ spectroscopic techniques such as EXAFS, ATR-FTIR and CIR-FTIR into models for the calculation of chemical equilibria in soils, sediments and natural waters (1, 2). Ideally, a mechanistic ion adsorption model can describe adsorption data using physically realistic surface structures. In other words, the model should properly scale from the microscopic molecular level to the macroscopic level of an adsorption experiment (3).

The structure of minerals can be interpreted with great accuracy using bond valence theory (4), which is a refinement of the classical Pauling bond valence concept. This concept can also be applied to interfaces. The MUSIC (MultiSite Ion Complexation) model is a framework that illustrates how one can use the bond valence concept to develop and parameterise models that describe the basic charging of minerals (5-9).

Ion adsorption models should not only account for surface structure, but also for the structure of adsorbed ions. Extending the bond valence concept to describe inner- and outersphere surface complexes immediately leads to the notion that the charge of the adsorbing species is partly effective at the surface plane, and partly resides at a greater distance from the surface. This concept led to the development of the CD-MUSIC model (10), where CD stands for Charge Distribution.

In this contribution we will study the relation between the microscopic distribution of adsorbed charge and an important macroscopic property of ion adsorption, i.e. the pH dependency. The pH dependence of adsorption is classically studied either by measuring a series of adsorption isotherms at different, but constant pH values, or by measuring the change in adsorption with pH for various total solid and ion concentrations. This last procedure is commonly known as the 'adsorption edge' method. Here we follow another procedure to characterise the pH dependency of adsorption, i.e. the determination of the proton-ion adsorption stoichiometry. It has been shown by Perona and Leckie (11) and Āernik et al. (12) that the macroscopic proton-ion adsorption stoichiometry is related to the pH dependence of ion adsorption via the thermodynamic consistency relationship. The ratio between the proton co-adsorption/desorption and the amount of ion adsorbed is generally non-stoichiometric, and varies with pH, ionic strength and surface coverage (10, 11, 13-16).

We have studied the co-adsorption of protons as a function of the oxyanion adsorption on goethite at constant pH, for conditions where almost 100% of the anion of interest was adsorbed. This condition has the advantage that the adsorbed amount directly follows from the added amount of ions. It also has the advantage that the added amount of protons will yield the co-adsorption of protons since almost no protons are consumed by the solution. We define the macroscopic proton-ion adsorption stoichiometry as the amount of acid consumed upon addition of an oxyanion in the unprotonated form, divided by the amount of oxyanion adsorbed at constant pH. Note that this stoichiometry is not necessarily expressing the ion binding pH dependence directly because the degree of protonation in solution must also be accounted for.

The relation between the macroscopic proton-ion adsorption stoichiometry and the structure of surface complexes can be studied for ions with a known surface structure. For goethite, the surface complexes of sulphate, arsenate and selenite seem to be best known from spectroscopy (17-19). In the present study the macroscopic proton-ion adsorption stoichiometry for the above species has been determined for pH conditions that have also been used in the spectroscopic studies mentioned above. We will also present and evaluate data for phosphate, vanadate, chromate, tungstate, molybdate and selenate.

In the data analysis we assume that only one surface species per adsorbed ion is dominant. This seems reasonable given the spectroscopic results for sulphate (17), selenite (18, 20), and phosphate (21) for experimental conditions similar to those of this study (pH 4 to 6, ion adsorption below $1.5 \mu\text{mol}/\text{m}^2$). Under the experimental conditions used, the surface will remain positively charged, which prevents protonation of the adsorbed oxyanion. The positive repulsive electrostatic potential will strongly diminish the affinity of the adsorbed oxyanion for proton binding. This assumption is reasonable for most oxyanions. For example, phosphate ions exhibit very high affinity for proton binding in solution. However, protonation of the adsorbed complex on goethite occurs at low pH only at relatively high surface coverage's because under these conditions the particle charge (surface plus adsorbed phosphate) is near neutral or negative (10, 21).

The proton-ion stoichiometry has not been determined at high solution concentrations because the analysis of this in relation to surface species is more complicated as more than one surface species can exist (10, 21, 25). Also the experimental determination is more complicated as will be explained.

Materials and methods

Preparation of Goethite

Goethite was prepared by slow neutralisation of $\text{Fe}(\text{NO}_3)_3$ (Merck) with NaOH. The resulting precipitate was aged at 60°C for three days and subsequently dialysed (6). The suspension has been stored in the dark at 4°C for four years. The BET specific surface area ($96.4 \text{ m}^2/\text{g}$) and acid-base characteristics were similar to other goethite preparations from our laboratory (10, 22).

Proton-Ion Titration Experiments

Vessels containing approximately 60 ml of 10 g/l (i.e. $1000 \text{ m}^2/\text{l}$) goethite in 0.01 M NaNO_3 were kept under a N_2 atmosphere at pH 5.5 for at least two days to desorb and remove (bi)carbonate. Goethite was titrated by an automated titration system (23) with sodium salt solutions of vanadate, phosphate, arsenate, selenite, chromate, molybdate, tungstate, sulphate and selenate (Table 1). Under the experimental conditions the solution concentrations remained negligible compared to adsorbed amounts because of the high reactive surface area. The pH was kept constant by titration with standardised 0.01 M HNO_3 (Merck). The duration of each titration was

four to twelve hours. Electrode drift was negligible as was monitored in suspensions that were not titrated. Stock solution concentrations (Table 1) were calibrated against known standards with ICP-AES or ICP-MS. Differences between replicates were negligible.

Table 1. Sodium solutions of anions in this study. The solutions without additional acid were kept under N₂ atmosphere to prevent lowering of the pH, which might otherwise result in polymerisation.

1	Vanadate	0.007 M Na ₃ VO ₄
2	Phosphate	0.01 M Na ₂ HPO ₄ + 0.006 M HNO ₃
3	Arsenate	0.01 M Na ₂ HAsO ₄ + 0.006 M HNO ₃
4	Selenite	0.01 M Na ₂ SeO ₃
5	Chromate	0.01 M Na ₂ CrO ₄
6	Molybdate	0.01 M Na ₂ MoO ₄
7	Tungstate	0.01 M Na ₂ WO ₄
8	Sulphate	0.01 M Na ₂ SO ₄
9	Selenate	0.01 M Na ₂ SeO ₄

The experimental proton co-adsorption (Γ_H) is found from the difference between the number of protons added to the suspension (H_{added}) and the change in the number of protons in solution (ΔH_{sol}): $\Gamma_H = H_{\text{added}} - \Delta H_{\text{sol}}$ (10). In our experiments protons are added using only a 0.01 M HNO₃ titrant solution, or via a 0.01 M HNO₃ titrant solution in combination with partly acidified oxyanion stock solutions. H_{added} can then be calculated with $H_{\text{added}} = 0.01 \text{ M } V_{\text{acid}}$ and, in case of phosphate and arsenate, with $H_{\text{added}} = 0.01 \text{ M } V_{\text{acid}} + 0.016 V_{\text{ion}}$. In principle the amount of added protons left in solution can be calculated with for instance $\Delta H_{\text{sol}} = V_i(3[\text{H}_3\text{AO}_x] + 2[\text{H}_2\text{AO}_x] + 1[\text{HAO}_x]) + \Delta V(\text{H}^+ - \text{OH}^-)$, but these terms are negligible in our experiments since nearly 100% of the anion of interest is adsorbed and since ΔV is small (V_i is the total volume after addition of a volume (ΔV) of acid and ion solution). The value of ΔH_{sol} has to be taken into account, as was done by Hiemstra and van Riemsdijk (10), if the ion concentration in solution is not negligible.

CD-MUSIC Model Approach

A description of the most relevant characteristics of the CD-MUSIC model of Hiemstra and van Riemsdijk (10) is given here. The concept of charge distribution is based on the bond valence concept of Pauling (24). The Pauling bond valence (v) expresses the charge per bond and equals the valence (z) of the ion-centre divided by its coordination number (CN): $v = z/\text{CN}$. Application of Pauling's bond valence concept to the protonation reaction of a singly coordinated surface hydroxyl at the surface of goethite leads to the formulation, $\text{FeOH}^{-0.5} + \text{H}^+ \equiv \text{FeOH}_2^{+0.5}$, because Fe contributes 0.5 valence units per Fe-O bond. The bond valence concept can also be applied to the formation of an innersphere ion like selenite. The charges of the oxygen ligands of selenite (SeO_3^{2-}) are estimated from the Se-O bond valence $z/\text{CN} = 4/3 = 1.33$. EXAFS shows (18) that adsorbed selenite shares two of its ligands with the surface and one ligand is directed to the solution. This causes a spatial charge distribution at the mineral-solution interface (25).

The simplest way to incorporate the spatial charge distribution of adsorbed species in surface-chemical equilibria is the partitioning of the charges over two electrostatic planes, i.e. the use of an electrostatic double layer model with at least two electrostatic planes. One electrostatic plane contains the surface groups together with the oxygen's shared between the surface and the chemisorbed ion. The second plane contains the solution-oriented oxygen's of the adsorbed ions. Outersphere electrolyte ions are located at the outer-most electrostatic plane. If the outer-most electrostatic plane and the second plane are the same, it is a Basic Stern (BS) model (26). Otherwise it is a Three Plane (TP) model (10). The choice between these models is studied in the chapter on sulphate adsorption (27). The capacity (C) of the compact part of the double layer in the TP model is related to the capacitance's of the individual layers by, $C^{-1} = C_1^{-1} + C_2^{-1}$. Both the BS model and the TP model include a Gouy-Chapman layer to account for the potential profile of the diffuse part of the electrostatic double layer. The Basic Stern model is the simplest model that is able to incorporate information from a variety of experimental and theoretical approaches (7, 9, 10, 28-31). Our experiments were performed under conditions where the total particle was always positively charged. The total charge follows from the initial charge (at pH 4.2, $\Gamma_H \approx 2 \mu\text{mol}/\text{m}^2$, at pH 6.1, $\Gamma_H \approx 1 \mu\text{mol}/\text{m}^2$ in 0.01 M NaNO_3), the adsorbed ion charge (ion charge times ion adsorption: $z_{\text{ion}}\Gamma_{\text{ion}}$) and the co-adsorbed protons ($\Delta\Gamma_H$). Thus the total particle charge, $\Gamma_H + z_{\text{ion}}\Gamma_{\text{ion}} + \Delta\Gamma_H$, is always positive.

In this paper we have used monodentate and bidentate complex formation. The corresponding affinity constants can be defined as:

$$K_{\text{mono}} = \{ \text{FeO}^{+0.5+z_0} \text{AO}_{y-1}^{z_1} \} / [\{ \text{FeOH}_2^{+0.5} \} (\text{AO}_y^{z_{\text{ion}}})] \text{ and}$$

$$K_{\text{bi}} = \{ \text{Fe}_2\text{O}_2^{+1+z_0} \text{AO}_{y-2}^{z_1} \} / [\{ \text{FeOH}_2^{+0.5} \}^2 (\text{AO}_y^{z_{\text{ion}}})],$$

in which z_0 and z_1 are respectively the charge allocated to the 0-plane and the 1-plane ($z_0 + z_1 = z_{\text{ion}}$). The charge attributions to the planes are calculated with the Pauling bond valence concept: $z_i = n_i (v - 2)$, n_i is the number of ligands per electrostatic plane, and v is the Pauling bond valence (valence of the central ion divided by coordination number). The value -2 is the charge of the oxygen. Note that the charge attribution to the surface (z_0) for the given examples can also be calculated from the overall charge ($-2, -3$) and the number of ligands that form a bond with the surface ($z_0 = z_{\text{ion}} n/\text{CN}$). The coefficients z_0 and z_1 are used in the calculation of the electrostatic contribution to the overall affinity for the ion adsorption equilibrium according to $\ln K_i = \ln K_{\text{intrinsic}} - (z_0\psi_0 + z_1\psi_1)F/(RT)$, in which $K_{\text{intrinsic}}$ is the chemical component of the affinity.

Model Parameters

The CD-MUSIC model distinguishes between the different types of surface groups. The site density of proton reactive groups ($6.15 \text{ sites nm}^{-2}$) was estimated previously on the basis of the goethite structure (10). The acid-base behavior of the goethite used in this study could be described well with a capacitance of $0.91 \text{ (C/m}^2\text{)}$, which is similar to that used in previous studies (0.90 C/m^2 (10); 0.85 C/m^2 , (32)). The log K for ion pair complexation is set to -1 as in the previous studies. The acid-base behaviour can only be modelled within a small range of different log

K values for the ion pairs (approximately $-1.5 < \log K < -0.5$), different capacitance's and site densities.

As will be discussed later, the modelling of our proton-ion adsorption data is almost independent of the site density (if site density of proton reactive sites > 4 sites/nm²), as well as the chosen ion pair complexation constant and the capacitance if the combination of parameters leads to a reasonable description of the experimental acid-base behaviour. The maximum experimental ion adsorption used in this study is 1 $\mu\text{mol}/\text{m}^2$. This is much lower than the estimated amount of singly coordinated surface groups, which are the most reactive (10). Therefore, the protonation and adsorption equilibria are rather independent of the chosen site densities of 3.45 site/nm² for singly coordinated and 2.7 sites/nm² for triply coordinated surface groups (10).

Results and discussion

The macroscopic proton-ion adsorption stoichiometry

The measured co-adsorption of protons as a function of the amount of oxyanion adsorbed on goethite is given in Fig. 1 for conditions where the total particle charge is still positive. The data for chromate, molybdate and tungstate follow almost exactly the same trajectory (Fig. 1). Vanadate, phosphate, and arsenate form another group of oxyanions, which are almost indistinguishable from each other with respect to the relationship between proton co-adsorption and oxyanion adsorption. The data show that the group of trivalent anions (VO_4 , PO_4 and AsO_4) results in a considerably higher number of protons co-adsorbed per oxyanion than the group of bivalent anions.

The differences in co-adsorption of protons can be understood by considering the electrostatic interaction between the anionic charge and the surface. Maximum interaction will occur if the charge of an oxyanion is located at the surface plane where the protons are bound. If the relationship between surface potential and the pH is Nernstian, it can be shown that this will result in a stoichiometric co-adsorption of protons. Stoichiometric co-adsorption implies the adsorption of two protons per adsorbed bivalent anion, and the adsorption of three protons per trivalent anion. The macroscopic proton-ion adsorption ratio is less than stoichiometric. This might be rationalised by placing the adsorbed charge at a finite distance from the surface, leading to a smaller interaction (14, 32). Although the macroscopic proton-ion adsorption is non-stoichiometric for all ions, it is interesting that the quotient of the stoichiometries for the group of trivalent ions and the group of bivalent ions (chromate, molybdate and tungstate) is nearly equal to the quotient of the ionic charge of these ions (3/2). We will show later that this occurs if both groups of ions have the same coordination with the surface.

Not all oxyanions with a -2 charge show the same behaviour. Selenite (SeO_3) has a higher number of co-adsorbed protons per oxyanion than chromate, molybdate and tungstate. This suggests a stronger interaction between the anion charge and surface protons, which can be due to the lower coordination number of selenite compared to chromate, molybdate and tungstate (CN=3 versus 4). In case of

selenite, 2/3 of the ligands interact with the surface in forming a bidentate surface complex. This contrasts with chromate, molybdate and tungstate, where we expect a maximum of 2/4 of the ligands (in case of bidentate complexes) to be directly involved in complexation with the surface. The relatively higher interaction of selenite with the surface leads to a higher macroscopic proton-ion adsorption stoichiometry.

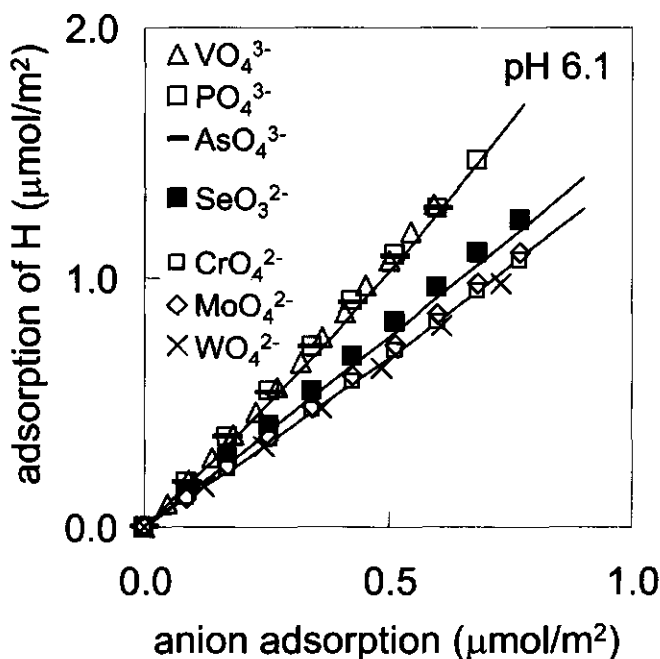


Fig. 1. Proton consumption as a function of ion adsorption at constant pH: pH 6.1 (0.01 M NaNO_3). The curves show the CD-MUSIC predictions based on the charge distributions from the surface complex structures of Fig. 3, which are calculated by applying the Pauling bond valence concept assuming bidentate complexes. Note that these predicted curves are not linear because the macroscopic proton-ion adsorption stoichiometry is not constant.

We have also measured the macroscopic proton-ion adsorption stoichiometry of two other divalent ions, sulphate and selenate (Fig. 2). The stoichiometry is determined at a lower pH (pH 4.2) to ensure sufficient ion adsorption. For comparative purposes the macroscopic proton-ion adsorption stoichiometry of selenite, chromate, tungstate, molybdate have also been measured at this lower pH. Trivalent anion adsorption was not studied at this lower pH because protonation of the adsorbed species might occur. Sulphate and selenate have a much lower co-adsorption of protons compared with chromate, molybdate and tungstate, pointing to a considerably lower interaction with the surface. A lower interaction can be due to a lower number of ligands being involved in ligand exchange with the surface

(monodentate versus bidentate binding). A low charge attribution to the surface is also expected for outersphere adsorption (to be discussed below).

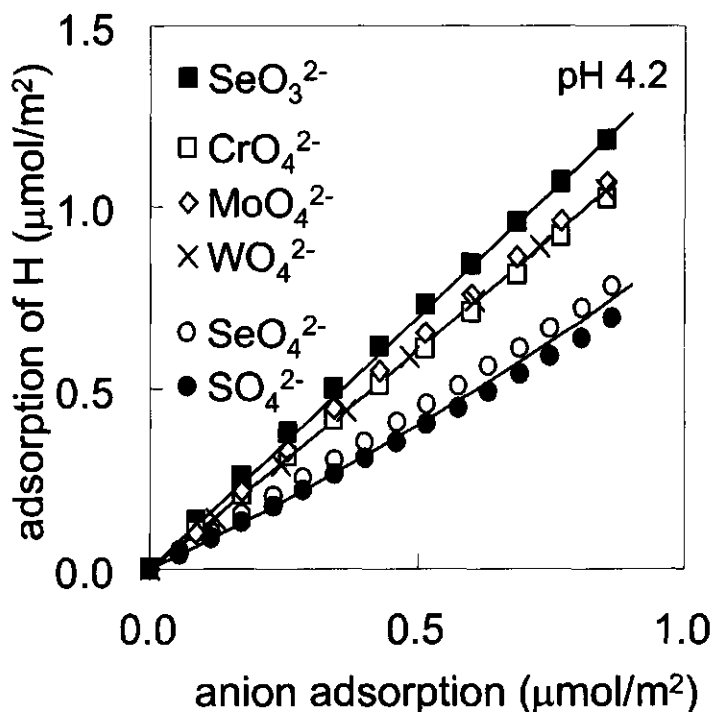
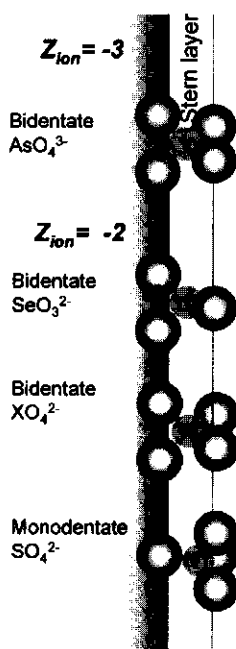


Fig. 2. Proton consumption as a function of ion adsorption at constant pH: pH 4.2 (0.01 M NaNO₃). The curves show the CD-MUSIC predictions based on the charge distributions from the surface complex structures of Fig. 3, which are calculated by applying the Pauling bond valence concept assuming bidentate complexes except for the lowest curve (monodentate).

Modelling

The co-adsorption of protons can be quantified by using the CD-MUSIC approach that relates the interfacial charge distribution to the structure of the adsorbed complex. The charge distribution concept is illustrated in Fig. 3, for relevant innersphere structures of various ions. The charge distribution in the interface (expressed in z_0 , z_1) is calculated using the Pauling bond valence concept (24), in which the central "cationic" charge is equally distributed over the surrounding oxygen ligands. The details of the calculations are given in the Figure caption. It follows from Fig. 3 that the portion of the charge attributed to the surface (z_0) depends on the structure and can vary from -0.50 to -1.33 for bivalent oxyanions. The co-adsorption of protons is higher if the negative charge attribution to the surface plane is higher.

Coordination from spectroscopy



Charge distribution from Pauling bond valence concept

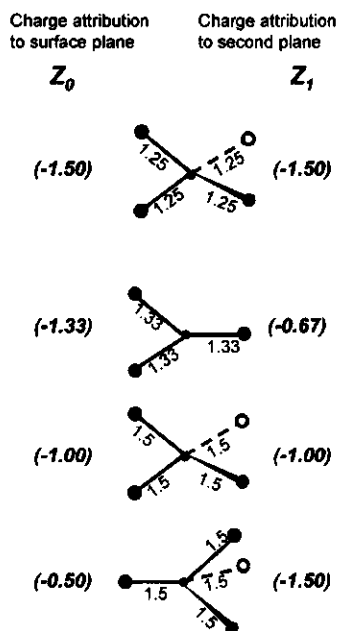


Fig. 3. Schematic representation of the surface-coordinations of ions and the allocation of the charge of the ion ($z_0+z_1=z_{ion}$) over the two electrostatic planes. The charge attributions to the planes are calculated with the Pauling bond valence concept: $z_i = n_i (v - 2)$, n_i is the number of ligands, and v is the Pauling bond valence (valence of the central ion divided by coordination number). The value -2 is the charge of the oxygen. Note that the charge attribution to the surface (z_0) for the given examples can also be calculated from the overall charge ($-2, -3$) and the number of ligands that form a bond with the surface ($z_0 = z_{ion} n/CN$). The coefficients z_0 and z_1 are used in the calculation of the electrostatic contribution to the overall affinity for the ion adsorption equilibrium. XO_4^{2-} is used to represent ions like CrO_4^{2-} , MoO_4^{2-} , and WO_4^{2-} .

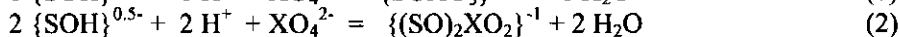
The structures given in Fig. 3 for arsenate (19, 33-35) and selenite (18) correspond with the spectroscopically found structures for pH values and surface coverage's comparable to the ones used in our experiments. The structure of sulphate adsorbed onto hematite was studied recently by Hug (17) with in-situ ATR-FTIR. Only one type of adsorbed sulphate complex is found to be dominant over a wide range of pH and surface coverage. Hug (17, 36) interpreted the spectrum as being the result of a monodentate innersphere complex. Similar spectra have also been observed for sulphate on goethite (Hug, personal communication). There is disagreement between spectroscopic studies concerning the coordination of phosphate by goethite (21, 37, 38). Tejedor-Tejedor and Anderson (21) assert that phosphate is adsorbed as a non-protonated bidentate surface complex at low

coverage and $\text{pH} > 5$, whereas Persson et al. (38) advocate the formation of a monodentate complex. We found very similar macroscopic proton-ion adsorption stoichiometries for phosphate and arsenate, which points towards a common bonding mechanism for both anions (see also ref. 25). Consequently, if arsenate is adsorbed as a bidentate complex under the conditions used (as suggested by EXAFS), the same is true for phosphate.

Modelling results

Systematic study of the macroscopic proton-ion adsorption stoichiometry has resulted in several new insights. We have found that the macroscopic proton-ion adsorption stoichiometry, which can be calculated with a given model, is independent of the intrinsic binding constant of the adsorbing species provided there is only one kind of adsorbed species. For a given variable charge model, the number of co-adsorbed protons at constant pH and ionic strength is only determined by the amount of the adsorbed oxyanion. The solution concentration and speciation corresponding to a certain oxyanion adsorption loading has no influence. Thus, we are clearly looking at surface properties. This observation has not been noted before as far as we know, and it has important implications for the characterisation of ion adsorption (as discussed below). Of course, the intrinsic affinity is a very important parameter for determining the relationship between the concentration in solution and the adsorbed amount, but not for the resulting macroscopic proton-ion adsorption stoichiometry (for the conditions of our experiments).

One may argue that the macroscopic proton-ion adsorption stoichiometry is not only determined by the charge distribution over the interface, but also by the formulation of the adsorption reaction and the protons that are involved in the reaction equation, i.e. the microscopic reaction stoichiometry. Consider the following reactions for the formation of a monodentate or a bidentate surface complex:



These equations suggest a strong difference between monodentate formation and bidentate formation with respect to the macroscopic proton-ion adsorption stoichiometry. This difference would be crucial if electrostatics would not be important. However calculations show that for the model we have used, there is almost no difference between the calculated macroscopic proton-ion adsorption stoichiometry applicable to monodentate or bidentate surface complexation if one uses the same charge distribution. In other words, the macroscopic proton-ion adsorption stoichiometry is determined dominantly by the charge distribution and not by the formulation of the reaction equation.

To illustrate this more clearly, we have calculated the proton co-adsorption for an oxyanion adsorption density of $0.5 \mu\text{mol}/\text{m}^2$ while varying the charge attribution to the surface, for an oxyanion with a -2 charge at pH 4.2, and a -3 charge at pH 6.1. The results are shown as lines in Fig. 4. The calculations were done using the Basic Stern model for both monodentate and bidentate coordination. The lines for both the monodentate and bidentate coordination coincide within the

scale of the graph. We have found that the calculated lines are also not affected if we change the site density, the ion pair complexation constants or the Stern layer capacitance, provided that we use a combination of parameters that still describes the acid-base characteristics of goethite in the presence of a simple electrolyte at different electrolyte concentrations. These parameters will influence the shape of the adsorption isotherms, but not the macroscopic proton-ion adsorption stoichiometry for the conditions of the experiments. From this we conclude that the experimental proton-ion adsorption stoichiometry can be directly interpreted in terms of the charge distribution.

In Fig. 4 we have also plotted the location of data points (black symbols) for the oxyanions whose bonding structure is known from spectroscopy (sulphate, selenite and arsenate). The values on the vertical axis follow from our experiments (Fig. 1 & 2), and the positions of the points on the horizontal axis are based on the calculated charge distribution using the structure of the adsorbed complex and the Pauling concept as shown in Fig. 3.

A shaded area is drawn in Fig. 4 to indicate the estimated conditions where the charge distribution can potentially result from charge transfer of hydrogen bridges in outersphere complexes (39). The maximum effect of this charge distribution from changes in hydrogen bonding is estimated to be 0.2 charge units per hydrogen bond in case of strong hydrogen bond formation. If we assume that at maximum, three of the oxygens of an oxyanion can be involved in hydrogen bonding with the surface in forming an outersphere complex, the maximum charge attribution to the surface is about 0.6 charge unit. In the shaded area a similar charge distribution can result either from innersphere (monodentate) or outersphere complexes. Although macroscopic proton-ion adsorption stoichiometries for sulphate and selenate are similar (Fig. 2), sulphate was interpreted to be a monodentate innersphere complex (17, 36), and selenate was interpreted to be either outersphere (18) or a bidentate innersphere complex (20). Our results for sulphate and selenate can be interpreted as either monodentate innersphere or as outersphere complexes, but a bidentate innersphere complex is in conflict with our results. Because of the uncertain contribution of hydrogen bridges to the charge distribution, we cannot distinguish between monodentate innersphere and outersphere complexes from macroscopic measurements. The results for arsenate and selenite are close to the calculated lines, indicating that the CD-MUSIC concept for these ions indeed scales from microscopic to macroscopic levels.

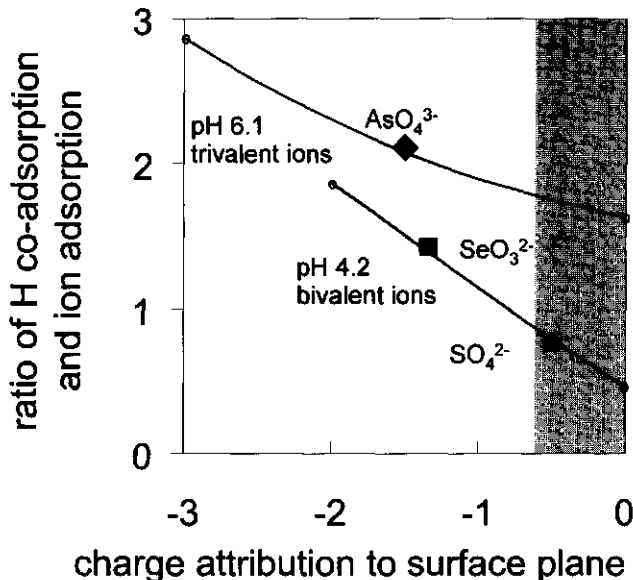


Fig. 4. The co-adsorption of H^+ , at $0.5 \mu\text{mol}/\text{m}^2$ ion adsorbed, as a function of the adsorbed ion charge attributed to the surface plane. The lines show the calculated relation for bivalent (pH 4.2) and trivalent ions (pH 6.1). Differences between monodentate and bidentate adsorption complexes are negligible. The points give the experimental proton-ion adsorption stoichiometry for arsenate, selenite and sulphate from Figs. 1 and 2 for a calculated charge distribution (Fig. 3). The charge distribution is calculated by applying the Pauling bond valence concept to the structure of an adsorbed complex (see Fig. 3). The small open circles refer to the predicted proton co-adsorption by treating the adsorbed charge as a point charge: the minimum and maximum H co-adsorption are calculated for placing the charge at the surface and outer-most electrostatic plane, respectively.

Application

Since the new method in combination with the CD-MUSIC model seems to give the correct results for adsorbed species of a presumed surface structure, we can use the approach to predict the surface structure of other oxyanions from the experimental proton-ion stoichiometry. This is done by applying the Pauling charge distributions of the adsorbed complexes, defined in Fig. 3, in the BS model. The modelling leads to the *predicted* curves shown in Fig. 1 & 2. The correspondence between the data points and the predicted lines is remarkably good. The model satisfactorily predicts the effect of pH (see Fig. 1 & 2). Also the observed effect of ion adsorption loading (a slight bending of the curves) on the macroscopic proton-ion stoichiometry is predicted. The charge distribution that is estimated from the Pauling bond valence principal is in some cases accurate enough to discriminate between surface structures. This is not so surprising because the difference between the calculated charge distribution for a monodentate compared to a bidentate structure is rather large (Fig. 3). Our results lead to a prediction of bidentate complexes for vanadate, chromate, molybdate

and tungstate, and favour the bidentate interpretation of Tejedor-Tejedor and Anderson (21) for phosphate because of its similarity to arsenate. Fine tuning of the charge distribution as predicted by a first order approach using the Pauling concept is probably required if one wants to give a more accurate description of adsorption data. For example, the macroscopic proton-ion stoichiometry for selenate and sulphate is not perfectly predicted in Fig. 2.

In Fig. 4 we have also indicated (small circles) the calculated results if the adsorbing ion is treated as a point charge (as is usually done). The values of $z_0 = -2$ and $z_0 = -3$ correspond to, respectively, bivalent and trivalent point charges located in the surface. The predicted macroscopic proton-ion stoichiometry is slightly less than 2 or 3, respectively. Consequently, placing the full anion charge at the surface leads to an overestimation of the number of co-adsorbed protons. Conversely, placing the full charge at the outermost electrostatic plane results in an underestimation of the macroscopic proton-ion stoichiometry.

Other modelling efforts to rationalise sulphate adsorption on iron hydroxides, using the point charge concept in combination with triple layer or diffuse layer models, require two or three hypothetical surface species (40-42). The model of Bowden et al. (43) allows the point charge to vary position near the surface without considering ligand exchange. These approaches can give a relatively good description of data, but there is no relation to any spectroscopic information.

Our results clearly show that the charge distribution concept is an essential feature of ion adsorption models that aim to use physically realistic surface species. The relation between the charge distribution needed in the model, and the physical structure of the adsorbed complex is the key concept linking spectroscopy to adsorption models. The simple Pauling charge distribution concept is a reasonable first order approach for ions with a relatively large macroscopic proton-ion adsorption stoichiometry. Hiemstra and Van Riemsdijk (25) have shown that the Pauling charge distribution concept leads to a very good description of selenite adsorption behaviour. For ions with a relatively low macroscopic proton-ion adsorption stoichiometry, such as sulphate and selenate, more spectroscopic information is necessary to reach a conclusion about the relation between structure and charge distribution.

Conclusions

1. The macroscopic proton-ion adsorption stoichiometry is determined primarily by the electrostatic interaction of the ion with the surface. The experimental proton-ion adsorption stoichiometry for vanadate, phosphate and arsenate is very similar, as it is for chromate, molybdate and tungstate. The difference between these two groups can be explained by the difference in ionic charge (-2, -3) for these groups of ions at the surface. Within these groups, a similar stoichiometry can only be explained by an identical ion-surface interaction. The macroscopic proton-ion adsorption stoichiometry varies within the group of bivalent ions. Selenite has the highest stoichiometry, sulphate and selenate have the lowest stoichiometry, and chromate, molybdate and

tungstate are intermediate. This variation can be explained by the structure of the adsorbed complexes being different.

2. The macroscopic proton-ion adsorption stoichiometry is independent of the affinity of the adsorbing species and of most other model parameters. It implies that in the model the charge distribution follows directly from the proton-ion adsorption stoichiometry, provided the presence of only one adsorption complex.

3. The simple Pauling bond valence concept can be used as a first order estimate in relating the charge distribution needed in the model to the structure of the adsorbing ion. The approach seems to give the correct prediction for the structure of adsorbed ions with a relatively large macroscopic proton-ion adsorption stoichiometry.

4. The measured proton-ion adsorption stoichiometry can be directly translated to the pH dependency of ion adsorption, using the thermodynamic consistency relationship (11, 12) in combination with the well-known protonation of species in solution. This implies that for a given ion solution chemistry, the pH dependence of adsorption depends primarily on the charge distribution over the interface and therefore on the structure of the adsorbed complex (i.e., independent of the affinity constant, see conclusion #2).

5. The structure of the surface, the structure of the adsorbed species, and the electrostatic potential profile near the surface, are all essential features of an adsorption model if the aim is to model adsorption behaviour using physically realistic surface species.

Acknowledgements

We thank Stephan Hug for determining the sulphate coordination on the goethite used in this study and Anton Korteweg for the BET surface area measurements. We also thank Mike Machesky and the other anonymous reviewers for their valuable comments.

References

1. Stumm W. and Morgan J. J. (1996) *Aquatic Chemistry*. Wiley.
2. Brown G. E., Jr. In *Mineral-Water Interface Geochemistry*, Hochella M. F. and White A. F., Ed. Vol. 23 (MSA, 1990) pp. 309-363.
3. Riemsdijk Van W. H. and Hiemstra. T. (1999) From molecular structure to ion adsorption modeling. In: *Mineral-water interfacial reactions* (Eds. D.L. Sparks, T. J. Grundl) symposium series 715, 68-86.
4. Brown I. D. (1978) Bond valences-Simple structural model for inorganic chemistry. *Chem. Soc. Rev.* 7, 359-376.
5. Hiemstra T., Van Riemsdijk W. H., and Bolt G. H. (1989). Multisite proton adsorption modelling at the solid/solution interface of (hydr)oxides: a new approach. I model description and evaluation of intrinsic reaction constants. *J. Colloid Interface Sci.* 133, 91-104.
6. Hiemstra T., De Wit J. C. M., and Van Riemsdijk W. H. (1989). Multisite proton adsorption modelling at the solid/solution interface of (hydr)oxides: a new approach. II application to various important (hydr)oxides. *J. Colloid Interface Sci.* 133, 105-117.
7. Hiemstra T., Venema P., and Van Riemsdijk W. H. (1996) Intrinsic proton affinity of reactive surface groups of metal (hydr)oxides: The bond valence principle. *J. Colloid Interface Sci.* 184, 680-692.

8. Rustad J. R., Wasserman E., Felmy A. R., and Wilke C. (1998) Molecular dynamics study of proton binding to silica surfaces. *J. Colloid Interface Sci.* **198**, 119-129.
9. Felmy A. R. and Rustad J. R. (1998) Molecular statics calculations of proton binding to goethite surfaces: thermodynamic modeling of surface charging and protonation of goethite in aqueous solution. *Geochim. Cosmochim. Acta* **62**, 25-31.
10. Hiemstra T. and Van Riemsdijk W. H. (1996) A surface structural approach to ion adsorption: the charge distribution (CD) model. *J. Colloid Interface Sci.* **179**, 488-508.
11. Perona M. J. and Leckie J. O. (1985) Proton stoichiometry for the adsorption of cations on oxide surfaces. *J. Colloid Interface Sci.* **106**, 65-69.
12. Černík M., Borkovec M., and Westall J. C. (1996) Affinity distribution description of competitive ion binding to heterogeneous materials *Langmuir* **12**, 6127-6137.
13. Rajan S. S. S. (1978) Sulfate adsorbed on hydrous alumina, ligands displaced, and changes in surface charge. *Soil Sci. Soc. Am. J.* **42**, 39-44.
14. Fokkink L.G. J., de Keizer A. Lyklema J. (1987) Specific ion adsorption on oxides *J. Colloid Inter. Sci.* **118**, 454-462.
15. Machesky M. L., Bischoff B. L., and Anderson M. A. (1989) Calorimetric investigation of anion adsorption onto goethite. *Environ. Sci. Technol.* **23**, 580-587.
16. Robertson A. P. and Leckie J. O. (1998) Acid/base, copper binding, and $\text{Cu}^{2+}/\text{H}^+$ exchange properties of goethite, an experimental and modeling study. *Environ. Sci. Technol.* **32**, 2519-2530.
17. Hug S. J. (1997) In situ Fourier Transform Infrared Measurements of sulfate Adsorption on hematite in aqueous solutions *J. Colloid Interface Sci.* **188**, 415-422.
18. Hayes K. F., Roe A. L., Brown G. E., Hodgens K. O., Leckie J. O., and Parks G. A. (1987) In-situ x-ray absorption study of surface complexes: selenium oxyanions on $\alpha\text{-FeOOH}$. *Science* **238**, 783-786.
19. Waychunas G. A., Rea B. A., Fuller C. C., and Davis J. A. (1993) Surface chemistry of ferrihydrite: part I. EXAFS studies of the geometry of coprecipitated and adsorbed arsenate. *Geochim. Cosmochim. Acta.* **57**, 2251-2269.
20. Manceau A. and Charlet L. (1994) The mechanism of selenate adsorption on goethite and hydrous ferric oxide. *J. Colloid Interface Sci.* **168**, 87-93.
21. Tejedor-Tejedor M. I. and Anderson M. A. (1990) Protonation of phosphate on the surface of goethite as studied by CIR-FTIR and electrophoretic mobility. *Langmuir* **6**, 602-611.
22. Venema P., Hiemstra T., and Van Riemsdijk W. H. (1996) Multi site adsorption of cadmium on goethite. *J. Colloid Interface Sci.* **183**, 515-527.
23. Kinniburgh D. G., Milne C. J., and Venema P. (1995) Design and construction of a personal-computer-based automatic titrator. *Soil Sci. Soc. Am. J.* **59**, (2) 417-422.
24. Pauling L. (1929) The principles determining the structure of complex ionic crystals. *J. Am. Chem. Soc.* **51**, 1010-1026.
25. Hiemstra T. and Van Riemsdijk W. H. (1999) Surface structural ion adsorption modeling of competitive binding of oxyanions by metal (hydr)oxides *J. Colloid Interface Sci.* **210**, 182-193.
26. Westall J. and Hohl H. (1980) A comparison of electrostatic models for the oxide/solution interface. *Adv. Colloid Interface Sci.* **12**, 265-294.
27. Rietra R. P. J. J., Hiemstra. T. and van Riemsdijk W. H. (1999) Sulfate adsorption on goethite. *J. Colloid Interface Sci.* **218**, 511-521.
28. Borkovec M. (1997) Origin of 1-pK and 2-pK models for ionizable water-solid interfaces. *Langmuir* **13**, 2608-2613.
29. Lützenkirchen J. (1998) Comparison of 1-pK and 2-pK versions of surface complexation theory by the goodness of fit in describing surface charge data of (hydr)oxides. *Environ. Sci. Technol.* **32**, 3149-3154.
30. Machesky M. L., Wesolowski D. J., Palmer D. A., and Ichiro-Hayashi K. (1998) Potentiometric titrations of rutile suspensions to 250°C. *J. Colloid Interface Sci.* **200**, 298-309.
31. Schudel M., Behrens S. H., Holthoff H., Kretzschmar R., and Borkovec M. (1997) Absolute aggregation rate constants of hematite particles in aqueous suspensions: a comparison of two different surface morphologies. *J. Colloid Interface Sci.* **196**, 241-253.

32. Venema P., Hiemstra T., and Van Riemsdijk W. H. (1996b) Comparison of different site binding models for cation sorption; description of pH dependency, salt dependency and cation-proton exchange. *J. Colloid Interface Sci.* **181**, 45-59.
33. Waychunas G. A., Fuller C. C., Rea B. A., and Davis J. A. (1996) Wide angle X-ray scattering (WAXS) study of "two-line" ferrihydrite structure: effect of arsenate sorption and counterion variation and comparison with EXAFS results. *Geochim. Cosmochim. Acta.* **60**, 1765-1781.
34. Sun X. and Doner H. E. (1996) An investigation of arsenate and arsenite bonding structures on goethite by FTIR. *Soil Science* **161**, 865-872.
35. Fendorf S., Eick M. J. Grossl P., and Sparks D. L. (1997) Arsenate and Chromate retention mechanism on goethite. I. Surface structure. *Environ. Sci. Technol.* **31**, 315-320.
36. Eggleston C. M., Hug S., Stumm W., Sulzberger B., and Afonso M.dS. (1998) Surface complexation of sulfate by hematite surfaces: FTIR and STM observations. *Geochim. Cosmochim. Acta.* **62** (4) 585-593.
37. Parfitt R. L., Russel J. D., and Farmer V. C. (1976) Confirmation of the surface structure of goethite (αFeOOH) and phosphated goethite by infrared spectroscopy. *J. Chem. Soc. Faraday* **172**, 1082-1087.
38. Persson P., Nilsson N., and Sjöberg S. (1995) Structure and bonding of orthophosphate ions at the iron oxide-aqueous interface. *J. Colloid Interface Sci.* **177**, 263-275.
39. Filius J. D., Hiemstra T., and Van Riemsdijk W. H. (1998) Adsorption of small weak organic acids on goethite: modeling of mechanisms *J. Colloid Interface Sci.* **195**, 368-380.
40. Dzombak D. A. and Morel F. M. M. (1990) Surface complexation modeling: hydrous ferric oxide, Wiley-Interscience, New York.
41. Ali M. A. and Dzombak D. A. (1996). Competitive sorption of simple organic acids and sulphate on goethite. *Environ. Sci. Technol.* **30**, 4, 1061-1071.
42. Hoins U., Charlet L., and Sticher H. (1993) Ligand effect on the adsorption of heavy metals: the sulfate-cadmium-goethite case. *Water, Air, and Soil Pollution* **68**, 241-255.
43. Bowden J. W., Nagarajah S., Barrow N. J., Posner A. M., and Quirk P. J. (1980) Describing the adsorption of phosphate, citrate and selenite on a variable-charge mineral surface. *Aust. J. Soil. Res.* **18**, 49-60.

CHAPTER 3

Sulfate Adsorption on Goethite

Abstract

Recent spectroscopic work has suggested that only one surface species of sulfate is dominant on hematite. Sulfate is therefore a very suitable anion to test and develop adsorption models for variable charge minerals. We have studied sulfate adsorption on goethite covering a large range of sulfate concentrations, surface coverages, pH values and electrolyte concentrations. Four different techniques were used to cover the entire range of conditions. For characterization at low sulfate concentrations, below the detection limit of sulfate with ICP-AES, we used proton-sulfate titrations at constant pH. Adsorption isotherms were studied for the intermediate sulfate concentration range. Acid-base titrations in sodium sulfate and electromobility were used for high sulfate concentrations. All the data can be modeled with one adsorbed species if it is assumed that the charge of adsorbed sulfate is spatially distributed in the interface. The charge distribution of sulfate follows directly from modeling the proton-sulfate adsorption stoichiometry since this stoichiometry is independent of the intrinsic affinity constant of sulfate. The charge distribution can be related to the structure of the surface complex by the use of the Pauling bond valence concept and is in accordance with the microscopic structure found by spectroscopy. The intrinsic affinity constant follows from the other measurements. Modeling of the proton-ion stoichiometry with the commonly used 2-pK models, where adsorbed ions are treated as point charges, is only possible if at least two surface species for sulfate are used.

CHAPTER 4

This chapter has been published:

René P.J.J. Rietra, Tjisse Hiemstra, Willem H. van Riemsdijk
Journal of Colloid and Interface Science 218, 511-521, (1999)

Introduction

The binding of ions on variable charge minerals is generally a function of pH and salt level. It may also be influenced by the simultaneous adsorption of other ions. This may lead to synergism (e.g. calcium and phosphate) or competition (e.g. sulfate and phosphate). As the number of possible interactions in environmental systems is numerous, models are developed to make predictions of the adsorption in these complex systems. Electrostatic surface complexation models (1-3) are in principle able to make predictions in more complex systems. The advantage of these mechanistically oriented binding models according to Cernic et al. (4) is that they can use the same formalism in all systems of interest, and enable in principle the prediction of the characteristics of the individual binding sites and complexes. Today the application of electrostatic surface complexation models is restricted by the uncertainty of the choice of the electrostatic profile at the mineral-water interface and the location of the ions in it. In other words, it is difficult to make an objective separation of the overall free energy of the adsorption reaction into the so-called intrinsic contribution and the electrostatic contribution.

In a mechanistic approach the binding models should at least account for the structure of the surface, the structure of the adsorbate, and the electrostatic profile and location of the ions in it (5). Generally the problem of improving the electrostatic surface complexation models is hindered by the freedom of choice for the number of surface binding sites involved and the number of different adsorbed species. To restrict the number and type of adsorbed species, it is important to know the adsorption mechanisms. With the work of Hayes et al. (6) *in situ* spectroscopy started on variable charge minerals. In the last few years many surface complexes have been identified with spectroscopy (7-15). These studies suggest that most ions form one or more different types of surface complexes. Recent spectroscopic evidence for sulfate reveals that one monodentate surface complex is dominant over a wide range of surface coverages and pH values in case of adsorption on hematite (16, 17) and goethite (Hug pers. comm., 18). Sulfate adsorption on goethite is thus an excellent system to test the capabilities of surface complexation models when they are constrained by the use of a physically realistic adsorbed species.

Our aim is to characterize sulfate adsorption on goethite and to cover a range of conditions that is as broad as possible. With these data surface complexation models can be tested on the basis of the ability to describe and predict the adsorption data. Adsorption of sulfate is therefore characterized as function of ion concentration, pH and ionic strength. To do so we have employed several experimental methods. The concentration range of the classic adsorption isotherm is experimentally restricted. At high sulfate concentrations the amount adsorbed cannot be accurately determined from the difference between the total concentration and the solution concentration, but the system can be characterized under these conditions by acid-base titrations and by measuring the electromobility. At low sulfate concentrations, where it is otherwise difficult to characterize adsorption (below detection limit for ICP-AES), adsorption can be characterized accurately by determining the proton-sulfate adsorption stoichiometry (19). The proton-sulfate adsorption stoichiometry has been determined at constant pH by measuring the

proton consumption as a function of sulfate adsorption. By a thermodynamic relation these data are directly related to the pH dependency of adsorption, as has been shown by Perona and Leckie (20). An important aspect of modeling the proton-ion adsorption stoichiometry with electrostatic surface complexation models is the independence of the stoichiometry from the intrinsic log K. The proton-ion adsorption stoichiometry is only determined by the allocation of the adsorbed charge (19).

Materials and Methods

Synthesis and Characterization

All chemicals (Merck p.a.) were stored in plastic bottles and all experiments have been performed in plastic vessels to avoid silica contamination. The water used throughout the experiments was always ultrapure ($\approx 18 \mu\text{S}/\text{cm}$).

A goethite suspension was prepared according to Hiemstra et al. (21): a freshly prepared 0.5 M $\text{Fe}(\text{NO}_3)_3$ was slowly titrated with 2.5 M NaOH to pH 12, after which the suspension was aged for 3 days at 60°C and subsequently dialyzed in water. The $\text{BET}(\text{N}_2)$ specific surface area of the goethite is $96.4 \text{ m}^2/\text{g}$. Goethite of the same batch was used previously by Geelhoed et al. (22) and Rietra et al. (19).

For acid-base titrations, a stock suspension of goethite at a pH value of 5.5 was continuously purged with N_2 to remove CO_2 . From this salt-free stock suspension, sub-samples of approximately 60 ml were titrated in vessels. In these vessels a N_2 atmosphere was maintained and the suspensions were kept overnight before a titration was performed. The goethite concentration used in the titrations was approximately 12 to 15 g/l goethite. Acid-base titrations have been performed at three NaNO_3 concentrations (0.005-0.02-0.1 M) with NaOH and HNO_3 in an automated set up (23). Venema et al. (24) previously discussed the details about the experimental method used for the titrations.

Acid-base Titrations in Na_2SO_4

Acid-base titrations in Na_2SO_4 have been performed at one concentration (0.033 M Na_2SO_4). Before the addition of Na_2SO_4 , the salt-free suspension was titrated to a pH of approximately 10. The proton adsorption of goethite in equilibrium with Na_2SO_4 could be determined relative to the proton adsorption in equilibrium with NaNO_3 because the goethite was sampled from the same stock suspension as used for the titrations in NaNO_3 . The initial difference in pH between a sample with NaNO_3 and the sample with Na_2SO_4 characterizes the difference in proton adsorption between the samples because the total amount of protons (given as $\text{H}_1\text{-OH}_1$) is identical. As stated previously the acid-base titration of goethite in 0.033 M Na_2SO_4 characterizes the system accurately where it is otherwise difficult to characterize adsorption from the difference between the total concentration and the solution concentration.

Proton-ion Titrations at constant pH

Samples of 60 ml of a stock suspension (electrolyte concentration 0.01 M or 0.1 M NaNO_3) were titrated to $\text{pH} \leq 5.5$ and left overnight in N_2 atmosphere. For the pH-STAT titration a 0.01 M HNO_3 solution and a 0.01 M Na_2SO_4 were used. After each addition of about 0.3 ml Na_2SO_4 the pH was corrected to the initial pH with the acid. A reaction time of at least 20 minutes and a maximum drift criterion of 0.002 pH units per minute was used between each addition of sulfate to signify equilibrium. The total amount of added sulfate was sufficiently small compared with the amount of goethite so that more than 99 % of the sulfate was always adsorbed. The proton balance could be calculated easily from the amount of added acid because the pH was kept constant and no sulfate remains in solution (19).

The relation between the proton co-adsorption and the adsorbed amount of sulfate is not linear. For the benefit of simple data evaluation the proton-ion adsorption data were fit by the following polynomial: $\Gamma_{\text{H}} = a \Gamma_{\text{S}}^2 + b \Gamma_{\text{S}}$ (via linear regression of $\Gamma_{\text{H}}/\Gamma_{\text{S}} = a \Gamma_{\text{S}} + b$). Differentiation of the equation then provides the proton-ion adsorption stoichiometry $\chi = (\partial\Gamma_{\text{H}}/\partial\Gamma_{\text{S}})_{\text{pH}} = 2 a \Gamma_{\text{S}} + b$ (where a and b are conditional constants).

Adsorption Isotherms

Adsorption experiments were performed in individual centrifuge tubes with fixed amounts of electrolyte, goethite, sulfate and differing pH values to give adsorption-edges. Contact with CO_2 was avoided for sulfate adsorption at pH 8 by mixing a CO_2 free goethite suspension in vessels under N_2 atmosphere with different amounts of sulfate. The tubes and vessels were equilibrated and rotated end-over-end for 20 hours. They were centrifuged, and samples of the supernatant were taken for analysis with ICP-AES. The pH was measured in the remaining supernatant.

In most cases, the amount of adsorbed sulfate was calculated from the difference between the total initial sulfate concentration and the sulfate concentration of the supernatant. To prevent using adsorption data with less accuracy than the determined sulfate concentration, only experiments where performed were more than 50% of the added sulfate is adsorbed (a high goethite concentration of 10 g/l is therefore used at pH 8 where adsorption per surface area is low). At fixed pH values the adsorption and equilibrium concentration have been calculated by interpolation of the adsorption edge data.

In systems with a high salt concentration (1 M) we have determined sulfate adsorption via desorption. The advantage of desorption is that hardly any dilution of the sample is necessary because for ICP-AES analyses the NaNO_3 concentration should be below 0.02 M. The supernatant of a suspension with a high salt concentration was decanted after taking a sample for subsequent determination of the equilibrium sulfate concentration and measuring pH (samples were analyzed after 1:50 dilution). A solution of 1 mmol/l K_2HPO_4 with a pH of 11 was added to desorb the sulfate. Again the tubes were equilibrated for 20 hours and subsequently centrifuged. Samples of the supernatant were again analyzed for sulfate. The amount

of sulfate in solution left after decanting the supernatant was taken into account by weighing all the tubes before and after decanting the solution.

Electrophoretic Mobility

Measurements of the electrophoretic mobility have been carried out using a laser Doppler velocimetry setup (ZetaSizer 3, Malvern) according to the method of Minor et al. (25). Electrophoretic mobilities have been measured at pH 4.0 in goethite suspensions of 0.05 g/l in 0.05 M Na₂SO₄, and in 0.1 M NaNO₃ with various sulfate concentrations.

Model calculations

Calculations were carried out with Ecosat, a computer code for the calculation of chemical equilibria (26). The Davies equation (constant is 0.2) is used to calculate the ion activity coefficients at 25°C (the solution equilibria used are in Appendix 1, Table A2). The parameters used in the CD-MUSIC model are optimized by minimizing the difference between the calculated and experimental proton- or ion adsorption data (e.g. $\Sigma(\Gamma_{\text{calc}} - \Gamma_{\text{data}})^2$).

Results and Discussion

Choice of model

An important aspect of ion adsorption is the pH dependency. A correct description of the pH dependency is most critically tested with proton-ion adsorption stoichiometry data. Based on the principle of thermodynamic consistency both are related (4, 20). Recently it has been shown by Rietra et al. (19) that in case of the presence of only one adsorbed species, as is the case for sulfate (16), the modeling of the proton-ion adsorption stoichiometry is independent of the intrinsic affinity. The proton-ion adsorption stoichiometry is only determined by the type of surface species, e.g. inner- or outersphere, protonated or unprotonated (19).

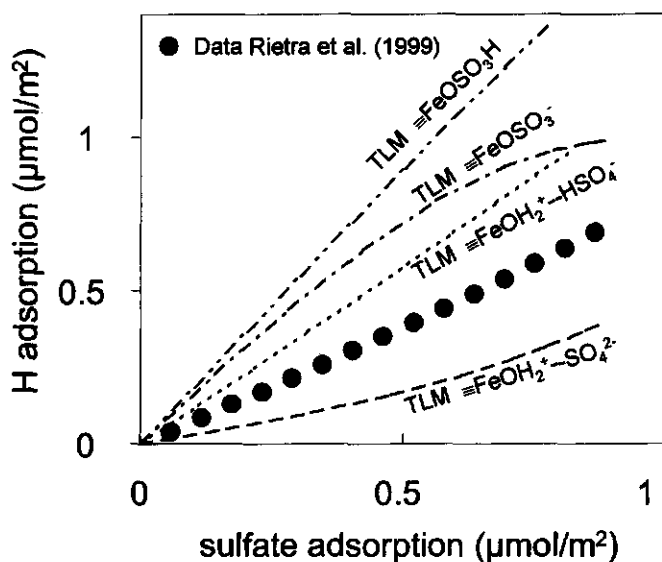


Fig. 1. Data of proton co-adsorption as a function of sulfate adsorption (black circles) and predictions of Triple Layer model (dotted lines) for four different surface species of sulfate (parameters from Hoins et al. (27)). The proton-sulfate adsorption stoichiometry predicted is too low with only an unprotonated outersphere $\equiv\text{FeOH}_2\text{-SO}_4$ complex and is predicted too high with only a protonated outersphere $\equiv\text{FeOH}_2\text{-SO}_4\text{H}$ complex. Both innersphere species ($\equiv\text{FeOSO}_3$ and $\equiv\text{FeOSO}_3\text{H}$) used by Hoins et al. (27) overestimate the proton-sulfate adsorption stoichiometry if adsorbed individually.

We have calculated the expected co-adsorption of protons for four individual surface species, which have been used with the Triple Layer model to describe sulfate adsorption (Fig. 1). The calculated results at pH 4.2 are given in Fig. 1, using the parameter values of Hoins et al. (27). Different values are found but using individual species leads to a too high or a too low stoichiometry. It implies that the use of *one* surface species in the TL model can not describe the pH dependency of sulfate adsorption. We note that the description of the pH dependency with the TL model is possible, but only when more than one surface species is considered. This is in conflict with the spectroscopic data of Hug (16).

Although not shown, use of either the Constant Capacitance (CC) model (14), or the Diffuse Layer (DL) model (28, 29) requires more than one adsorbed sulfate species to describe the correct proton-sulfate adsorption stoichiometry. The main difficulty with predicting the proton-ion adsorption stoichiometry with one species in the TL, CC or the DL model, is the treatment of adsorbed ions as a point charge, located in one of the electrostatic planes. By using a distribution of adsorbed charge, as is done in the CD-MUSIC model approach (30), it is possible to describe the experimental proton-sulfate adsorption stoichiometry by model calculations with only one adsorbed sulfate species (19). Therefore adsorption data of sulfate are analyzed by using the CD-MUSIC model (30). We note that the previously Davis and Leckie (43) have suggested that the use of charge distribution

for adsorbed complexes is possible. In the CD-MUSIC model the charge distribution follows logically from the MUSIC model, upon which it is built, and is related to the structure of adsorbed complexes via the Pauling bond valence concept (19, 30).

Geelhoed et al. (22) was able to describe the pH dependency of sulfate at surface coverages above $1 \mu\text{mol}/\text{m}^2$ with the CD-MUSIC model. However if we use the parameters given by Geelhoed et al. (22) to predict the experimental proton-sulfate adsorption stoichiometry shown in Fig. 1, we find that the data are overestimated by a factor of approximately 1.2. From this we can conclude that a satisfactory description of the adsorption isotherms does not guarantee a good prediction of the pH dependence at low surface coverages and pH 4.2. This aspect will be discussed after the modeling and the assessment of model parameters from experimental data.

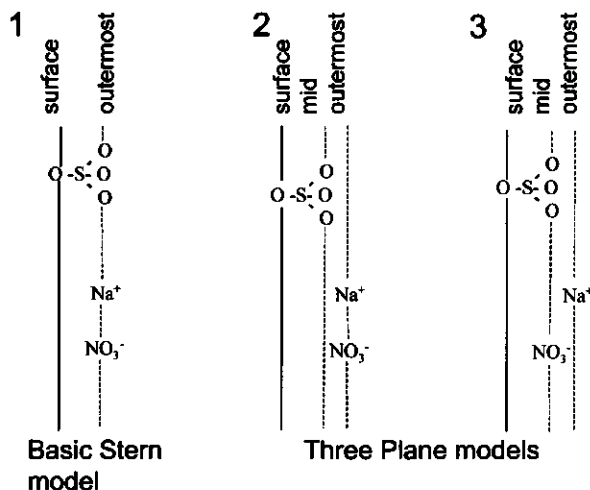


Fig. 2. Schematic representation of the tested models for sulfate adsorption with different locations of the surface ion pairs. The charge of the adsorbed sulfate is distributed across two electrostatic planes.

Charge distribution

The CD-MUSIC model is an extension of the MUSIC (multi site complexation) approach. A central parameter in the model is the distribution of the charge. The innersphere complexes of ions are assumed to have a spatial distribution of charge. One part of the adsorbed species charge is attributed to the surface since not all ligands of the adsorbed complex share oxygens with the solid. The remaining part of the charge is at a certain distance of the surface. The charge attribution (z_i) to the electrostatic planes (i) can be estimated for a known surface structure of an adsorbed ion using the Pauling bond valence concept (19, 30) $z_i = n_i(v-2)$, where n_i is the number of ligands per electrostatic plane i , and v is the Pauling bond valence (valence of central ion divided by coordination number). Application of the Pauling Bond Valence concept, with equal distribution of charge over the ligands, leads to a bond valence (v) of 1.5 valence units (v.u.) per S-O bond, i.e. the charge per oxygen is -0.5 v.u. In case

of a monodentate complex the ligands are unequally distributed in the interface since one ligand is shared with the interface and three are oriented towards the solution ($n_0=1$, $n_1=3$). This leads to an unequal distribution of charge across the electrostatic planes for monodentate sulfate: $z_0 = -0.5$ in the surface plane and $z_1 = -1.5$ in a plane located at some distance from the plane.

It has been suggested that only the singly coordinated surface groups are reactive for innersphere complexation of anions (8, 31, 32). This is plausible for innersphere adsorption of sulfate if we look at predictions of the bond valence contributions for singly, doubly, and triply coordinated oxygens with innersphere sulfate (Fe-O-S, Fe₂-O-S and Fe₃-O-S). Assuming a bond valence for a S-O bond of 1.5 v. u., and 0.5 v. u. for a Fe-O bond, the sum of bond valences on surface oxygen is 0, +0.5, and +1 v.u. respectively for singly, doubly and triply coordinated oxygen. According to Bargar et al. (15) only a neutral or almost neutral sum of bond valences seems plausible, which leads to the prediction that only singly coordinated oxygen will react with sulfate to form an innersphere complex. The site densities of the surface groups are chosen as given in Hiemstra and van Riemsdijk (30).

Assessment of model parameters from data

In the next three sections the assessment of the parameter values for the CD-MUSIC model from experimental data is discussed. Determined first, from the description of the primary charging of variable charge minerals, are the parameter values for: the PZC, the capacitance, and the ion pair formation constants. Secondly, the charge distribution of an adsorbed complex is determined from the proton-ion adsorption stoichiometry. Next, the intrinsic affinity constant of adsorbed sulfate, in combination with the charge distribution, is found from the adsorption isotherms, the acid-base behavior, and the electromobility of goethite in solutions containing sulfate. In the following sections the model predictions will be discussed, the model parameter values will be tested, and the sensitivity of the parameters for different data sets will be examined. In the last section the influence of the choice of the model for the description of the data will be discussed.

Determination of Primary charging parameter values

The Basic Stern model (30) is used, which is the simplest physically realistic electrostatic model for metal hydroxides (33, 34). In this model the sulfate ligands are distributed over the surface-plane and the outermost-plane, and the ion pairs are in the outermost-plane (see Fig. 2 picture 1). The parameter values for the capacitance and equilibrium constants for the surface ion pairs have been optimized for the description of salt dependent acid-base behavior in NaNO₃ (Table 1). In the description of the acid-base behavior the effect of higher or lower equilibrium constant's ($\log K$) for ion pairs can only partially be compensated by lower or higher capacitances. Too low or too high ion pair equilibrium constants (K) do not give very good descriptions. Therefore, the values of the ion pair equilibrium constants are limited to the range $-1.5 < \log K \leq -0.5$. The best description is approximately $\log K = -1$. The corresponding capacitance is 0.91 F/m² (Table 1). This $\log K$ value is in line with the

measurements of Rundberg et al. (35) who determined that sodium adsorption was less than $0.05 \mu\text{mol}/\text{m}^2$ at the PZC (in 0.015 M NaNO_3).

Table 1. Optimized value for the capacity (F/m^2) as function of the ion pair constant in the Basic Stern model from describing the acid-base behavior of goethite in 0.005 - 0.02 - 0.1 M NaNO_3 . The $\log K_H$ was set equal to the PZC. The bold values are used for the calculations in the figures.

$\log K_{\text{Na}} = \log K_{\text{NO}_3}$	capacity	$\Sigma(\Gamma_{\text{H}}^{\text{data}} - \Gamma_{\text{H}}^{\text{calc}})^2$
-1.5	1.02	0.25
-1	0.91	0.18
-0.5	0.79	0.21

Determination of Charge Distribution

We have measured the proton-sulfate adsorption stoichiometry for a range of pH values and for two electrolyte concentrations. An example of the increasing proton co-adsorption as function of sulfate adsorption is given in Fig. 3. With these data we can determine the distribution of charge of sulfate in the interface. The charge distribution is the only adjustable parameter in the calculation of the proton-sulfate adsorption stoichiometry if the capacitance and the ion pair constants are fixed by the description of the acid-base behavior in NaNO_3 .

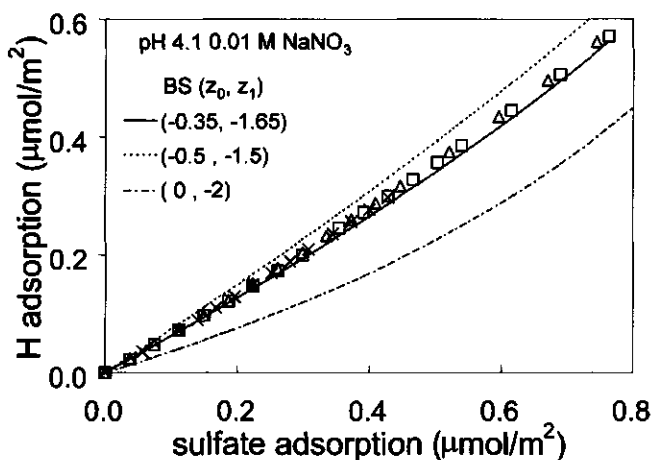


Fig. 3. Experimental and modeled proton co-adsorption as a function of sulfate adsorption at pH 4.1 (0.01 M NaNO_3). Three replicate titrations are shown by difference of symbols (other data in App. 2). Also illustrated is the prediction of the proton-sulfate adsorption stoichiometry for two other charge distributions.

In Fig. 3 the effect of the charge distribution on the calculation of the proton-sulfate adsorption stoichiometry is shown for three possible charge distributions of sulfate across the two electrostatic planes. The charge distribution of $(z_0, z_1) = (-0.5, -1.5)$ corresponds to an ideal Pauling charge distribution for a monodentate coordinated complex, and a charge distribution of $(0, -2)$ corresponds to one of the options for using a point charge. The effect of the charge distribution on the proton co-adsorption

is caused by a different degree of interaction between the adsorbed negative charge and the protons in the surface plane.

The proton-sulfate adsorption stoichiometry, i.e. the slope of the imaginary curve in Fig. 3 ($\chi = \delta\Gamma_H / \delta\Gamma_S$), changes with sulfate loading. We have determined the proton-sulfate adsorption stoichiometry as a function of pH and the ionic strength. The results are described in Appendix 2. Using data sets such as the one shown in Fig. 3, the proton-sulfate adsorption stoichiometry at $0.4 \mu\text{mol/m}^2$ sulfate adsorbed is derived as function of pH and ionic strength (see Fig. 4). The solid lines in Fig. 3 and 4 are calculated assuming a charge distribution of $(-0.35, -1.65)$ for the adsorbed sulfate species.

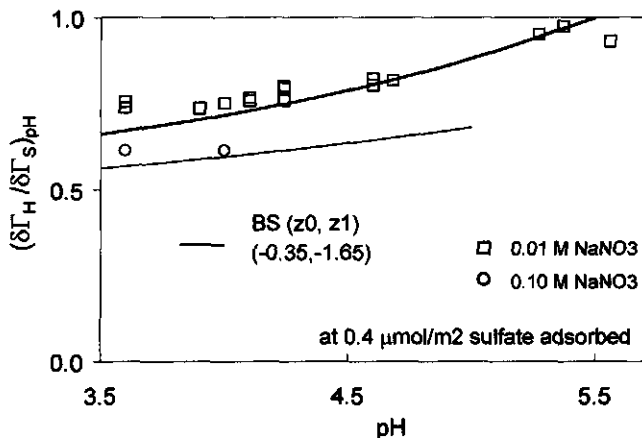


Fig. 4. Experimental and modeled proton-sulfate adsorption stoichiometry ($\chi = \delta\Gamma_H / \delta\Gamma_S$, e.g. the slope of the curve in Fig. 3) as a function of pH at 0.01 M and 0.1 M NaNO_3 . The points show the data while the lines give the predicted results.

Determination of Intrinsic affinity of adsorbed sulphate

With the determined charge distribution it should be possible to describe the pH-dependent sulfate adsorption data for a large range of pH values and sulfate concentrations, if the model and its parameters are correct. The only adjustable parameter left in our evaluation is the intrinsic $\log K_S$ (Appendix 1, Table A1), which can be found using the various adsorption isotherm data. In Fig. 5 the experimental pH and salt dependent adsorption isotherms are shown together with the model calculation. The data show that the adsorption strongly decreases at high ionic strength. The adsorption isotherms show that sulfate is still adsorbed significantly in 1 M NaNO_3 . A larger effect of salt has been found in NaCl (14). Preliminary results have shown that sulfate adsorption in NaNO_3 is higher than adsorption in NaCl (36). The differing effect of chloride and nitrate on sulfate adsorption is also known for sulfate adsorption in soils (37).

As mentioned, spectroscopic results have suggested (16) that sulfate is coordinated at the surface predominantly as a monodentate innersphere species. The calculated charge distribution of adsorbed sulfate should thus correspond with this observation. In case of an ideal charge distribution according to Pauling, a charge distribution of $(-0.5, -1.5)$ is expected. The actual value of $(-0.35, -1.65)$ is slightly

different, which may be due to distortion of the symmetry of adsorbed sulfate (16). It should be noticed that our value only reflects an overall effect. For instance, it is also possible that hydrogen bonds may contribute to the overall value, as has been suggested by Filius et al. (38).

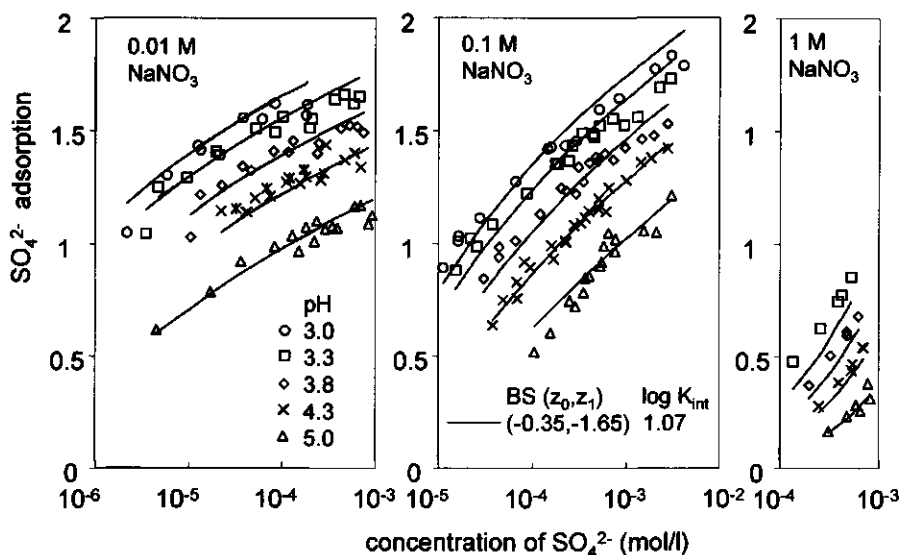


Fig. 5. Experimental and modeled sulfate adsorption isotherms at various pH values in the range 3-5 for three NaNO₃ concentrations (0.01-0.1-1 M). The adsorption strongly decreases as function of the electrolyte concentration.

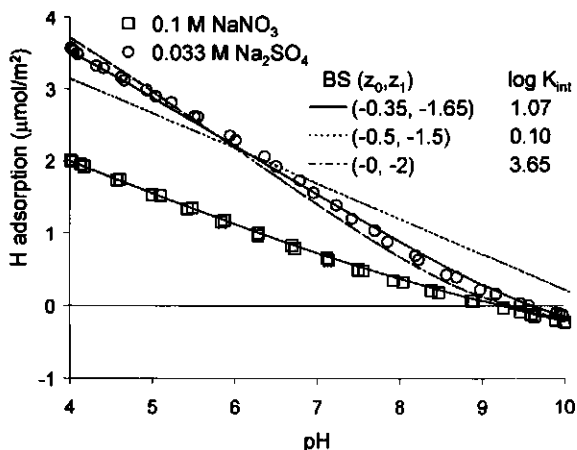


Fig. 6. Experimental and modeled acid-base behavior of goethite in 0.033 M Na₂SO₄. The points show the data while the lines depict the model results. The solid line is predicted and the dotted lines depict the best model descriptions for two other charge distributions. The acid-base titration curve and model description in 0.1 M NaNO₃ is shown for comparison.

Model predictions

Once the model parameter values have been determined for low and intermediate sulfate concentrations, the model can be used for further testing, for instance for data at high sulfate concentrations. We have determined the acid-base behavior (Fig. 6) and electromobility at these conditions (Fig. 7). The proton adsorption is predicted well. The data of the electromobility show that sulfate can change the charge of goethite from positive to negative at pH 4. To our knowledge this has not been reported earlier in literature (39) and it proves that the interaction between sulfate and goethite is not purely electrostatic. Consequently, besides an electrostatic component there is also a significant chemical component to the overall adsorption energy. The goethite is neutral at a sulfate concentration of approximately 6 ± 3 mmol/l sulfate in 0.1 M NaNO_3 , which is predicted reasonably by the given model (3 mmol/l).

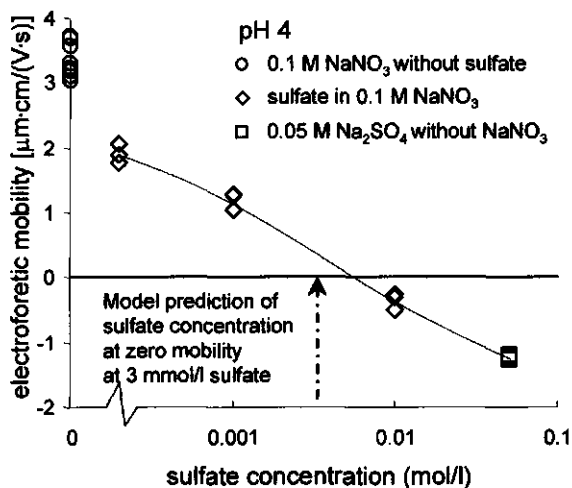


Fig. 7. Electromobility of goethite as a function of sulfate concentration at pH 4. The experimental sulfate concentration at which the mobility is zero is approximately 6 ± 3 mmol/l and the predicted concentration is 3 mmol/l. A dotted line is drawn through the data by hand to interpolate the sulfate concentration at zero mobility.

The charge distribution used in the modeling could be found from the proton-sulfate adsorption stoichiometry measured at a pH value of 4. It may be argued that for other pH ranges the value of the charge distribution may be different due to the contribution of other species, such as the formation of outersphere species. The description of the sulfate adsorption isotherms (Fig. 5) and the proton-adsorption at high sulfate concentration (Fig. 6) is not very sensitive to the choice of more species with different charge distributions because the choice of the intrinsic $\log K_S$ values will influence also the results. The assumption that one adsorbed sulfate species is present can be checked by predicting the adsorption at a very different pH such as pH 8 (Fig. 8). If an outersphere species were to exist along with an innersphere species, the electrostatic part of the total adsorption energy would be smaller for the

outersphere species because it is located at a larger distance from the surface where a lower attractive potential exists. Thus to be present in significant amounts the $\log K_{\text{int}}$ of the outersphere species should be larger than the $\log K_{\text{int}}$ of the innersphere species. An outersphere species will dominate an innersphere species especially at pH values where the electrostatic contribution to the adsorption energy is small, i.e. where the particle charge, and attractive potential, is low. The correct model prediction at pH 8 (Fig. 8) is obtained with the parameter values found at much lower pH values. This implies that the sulfate adsorption can be described over the entire range of pH values and sulfate loadings studied with only one adsorbed sulfate species. The good description of the data supports the spectroscopic results of Hug (16) that one adsorbed sulfate species is dominant across a large range of pH values. An outersphere species can only be incorporated in the model if it has approximately the same $\log K$ as the monodentate adsorbed sulfate species.

Table 2. Optimized charge distribution values for the description of four different sulfate adsorption data sets:

- (1) proton-sulfate adsorption stoichiometry (Appendix 2, example in Fig. 3),
- (2) sulfate adsorption isotherms (from Fig. 5),
- (3) the acid-base titration in 0.033 M Na₂SO₄ (from Fig. 6),
- (4) sulfate adsorption isotherm at pH 8 (Fig. 8).

For each combination of a charge distribution and a $\log K_{\text{int}}$ the best-fit $\log K_{\text{int}}$ is calculated on the basis of goodness-of-fit (Δ^*) (the best-fits for the charge distribution are underlined, the bold values are used for the calculations in the figures). Note that the description of the proton-sulfate adsorption stoichiometry is independent of the choice of $\log K_{\text{int}}$ (Rietra et al., 1999) and that the best-fit $\log K_{\text{int}}$ for pH 8 is rather insensitive for the choice of the charge distribution.

Charge distribution across planes	Goodness-of-fit of data sets							
	1		2		3		4	
	Δ_1	Δ_2	Best-fit $\log K_{\text{int}}$	Δ_3	best-fit $\log K_{\text{int}}$	Δ_4	Best-fit $\log K_{\text{int}}$	
(z_0, z_1)								
(-0.50, -1.50)	2.2	<u>2.01</u>	0.30	<u>0.59</u>	0.10	0.06	0.89	
(-0.45, -1.55)	<u>0.88</u>	<u>1.39</u>	0.55	<u>0.24</u>	0.45	0.06	0.91	
(-0.40, -1.60)	<u>0.53</u>	<u>0.91</u>	0.80	<u>0.09</u>	0.75	0.06	0.93	
(-0.35, -1.65)	<u>1.30</u>	<u>0.62</u>	1.07	<u>0.12</u>	1.10	0.06	0.96	
(-0.30, -1.70)	<u>3.4</u>	<u>0.50</u>	1.35	<u>0.35</u>	1.45	0.06	0.98	
(-0.25, -1.75)	<u>7.0</u>	<u>0.53</u>	1.60	<u>0.77</u>	1.80	0.05	1.00	
(-0.00, -2.00)	<u>59</u>	<u>2.80</u>	3.00	<u>5.10</u>	3.65	0.04	1.11	

$$\Delta_1 = \sum (\Gamma_{\text{H}}^{\text{calc}} - \Gamma_{\text{H}}^{\text{data}}) / \Gamma_{\text{H}}^{\text{avg}})^2 = \sum (2(\Gamma_{\text{H}}^{\text{calc}} - \Gamma_{\text{H}}^{\text{data}}) / (\Gamma_{\text{H}}^{\text{calc}} + \Gamma_{\text{H}}^{\text{data}}))^2$$

$$\Delta_2 = \sum (\Gamma_{\text{S}}^{\text{calc}} - \Gamma_{\text{S}}^{\text{data}})^2$$

$$\Delta_3 = \sum (\Gamma_{\text{H}}^{\text{calc}} - \Gamma_{\text{H}}^{\text{data}})^2$$

$$\Delta_4 = 10^3 \sum (\Gamma_{\text{S}}^{\text{calc}} - \Gamma_{\text{S}}^{\text{data}})^2$$

Sensitivity of model parameters

In the analyses given above the charge distribution could be found directly from the description of the proton-sulfate adsorption stoichiometry and this charge distribution was used to describe the other data sets. The $\log K_{\text{int}}$ was found from

the adsorption isotherms in combination with the charge distribution. The question arises whether these model parameters could also be obtained independently from the other data sets. We therefore studied the effect of choosing different values for the charge distribution, as is shown in Fig. 3, 6 and 8. The figures show the sensitivity of the choice of the charge distribution for the proton-sulfate adsorption stoichiometry, the proton adsorption at high sulfate concentration, and the adsorption isotherms. On basis of the thermodynamic consistency it is logical that when the charge distribution can be found from the proton-ion adsorption stoichiometry that it can also be found from pH dependent adsorption isotherms. In Fig. 8 sulfate adsorption at pH 5 is predicted for different combinations of the charge distribution and the $\log K_{int}$. With the parameter values from the description of the data at pH 5, the adsorption at pH 8 is predicted well. It is clear from Fig. 8 that only a certain value of the charge distribution (-0.35, -1.65), as found earlier, is able to predict the correct pH dependency of the adsorption between pH 5 and 8. The calculated proton-adsorption in 0.033 M Na_2SO_4 for different values of the charge distribution also shows that this kind of data can be used to calculate the charge distribution of adsorbed sulfate.

From the above analysis it can be concluded that all data sets are sensitive to the choice of the charge distribution. It suggests that different types of data can be used to calculate the charge distribution and the intrinsic $\log K_s$. We have tested this by using the proton-sulfate adsorption stoichiometries, the adsorption isotherms, and the proton adsorption in 0.033 M Na_2SO_4 as different data sets. The adsorption isotherm at pH 8 is treated as a separate data set. In the analysis we have systematically fitted the $\log K_{int}$ for different values of the charge distribution. For each set the goodness-of-fit is given in Table 2. The calculations show that approximately the same charge distribution of the adsorbed sulfate species can be found from the acid-base behavior at high sulfate concentrations, or from the adsorption isotherms, as from the proton-sulfate stoichiometry at low sulfate concentrations. The calculations also show that approximately the same $\log K_{int}$ can be found from the adsorption isotherms and the acid-base behavior at high sulfate concentrations. The $\log K_{int}$ determined from the adsorption isotherm at pH 8 is well-constrained since the description of the data is almost independent for the value for the charge distribution. Considering all the data, Table 2 shows that the charge attribution to the surface plane can be estimated to be 0.35 ± 0.05 with a corresponding $\log K_{int} = 1.07 \pm 0.25$.

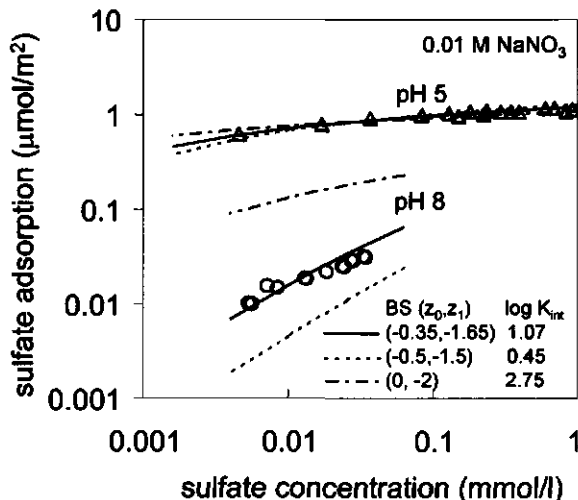


Fig. 8. Experimental and modeled sulfate adsorption isotherms at pH 5 and 8 (0.01 M NaNO_3). The modeled sulfate adsorption at pH 8 is entirely predicted since the parameter values have been fixed on the basis of the proton-sulfate adsorption stoichiometry data in App. 2 and the adsorption isotherms in Fig. 5. The dotted lines demonstrate the prediction for two other charge distributions that adequately describe the adsorption isotherm at pH 5. This demonstrates the sensitivity of the charge distribution value in describing the correct pH dependency.

Detailed modeling of sulfate and ion pairs

In the above analyses we have used the Basic Stern option (see Fig. 2) and we have assumed that the position of the ion pairs is in the same electrostatic plane as the solution oriented ligands of sulfate. In the Three Plane model that was used for sulfate adsorption by Geelhoed et al. (22), the sulfate is distributed across the surface plane and the mid-plane while the ion pairs are located in the outermost plane, as is illustrated by the second picture in Fig. 2. To study the effect of this choice in more detail we have tested possible locations of sulfate and the ion pairs in the Stern layer.

The parameter values for the capacity of the Stern layer, and the ion pair formation constants in the Three Plane model are identical to the Basic Stern model, but the values of the capacitance's for the inner- and outer Stern layers (C_1 and C_2) are not set. However, the charge distribution and the inner- and outer-capacity are directly related, according to, $z_1^{TP} = z_1^{BS} C_2 (C_2 - C)^{-1}$, where z_1 is the charge attributed to the solution-oriented ligands in the Three Plane model (TP) or Basic Stern model (BS). This relation is derived in Appendix 3. With the relation between the charge distribution for sulfate and the capacitance's of the inner- and outer Stern layers, the adsorption isotherms were described by fitting the intrinsic $\log K$ as function of the inner- and outer-capacitance in combination with the charge distribution.

We have found that the quality of the description of the adsorption isotherms decreases if the Three Plane model was used. Increasing the capacitance of the outer Stern layer (C_2) improved the fit. This increase means that the distance between the mid-plane and the outermost-plane decreases and the Three Plane model approaches the Basic Stern model (see picture 1 and 2 in Fig. 2). We found that for the sulfate data

sets only the position of nitrate ion was important in this respect. The location of the sodium ion is insignificant for the description of the sulfate adsorption data. The best fit was found if the position of the nitrate ion coincides with the plane where the solution-oriented ligands of sulfate are located. It is for this reason that the Three Plane model for sulfate by Geelhoed et al. (22) gives a less satisfactory description of all the sulfate data. Placing only the sodium ion at the outermost electrostatic plane (see picture 3 of Fig. 2) hardly affects the description of the sulfate adsorption data. This is interesting because it was found earlier (30) that a separation between the ion pair of sodium and phosphate was necessary to describe the salt dependency of phosphate adsorption. The model represented by picture 3 (Fig. 2) might combine both options. From these findings we conclude that the structure of the Stern layer and the allocation of the adsorbed charge of sulfate and nitrate are important to obtain a consistent description of all the data assuming one surface species of sulfate.

Conclusions

The spectroscopic characterization of the adsorbed sulfate has shown that only one surface species is predominantly present (16), which enables a comparison of how various models can accommodate this information. The Triple Layer model, the Constant Capacitance model and the Diffuse Layer model need at least two adsorbed species for correct description of the pH dependence of sulfate adsorption, which contradicts this spectroscopic information. The basic problem of the commonly used approaches in surface complexation modeling is that the adsorbed ions are treated as point charges. It follows directly from the structure oriented CD-MUSIC model that the charge of specifically bound ions should be distributed over the interface. The charge distribution needed to model the data is in reasonable agreement with the suggestion that sulfate is bound as a monodentate innersphere complex. The CD-MUSIC model describes sulfate adsorption on goethite with one surface species over the complete range of surface coverages ($0-2 \mu\text{mol}/\text{m}^2$), pH range (3 to 8), and salt concentrations (0.01 to 1 mol/l) studied. The calculation of a unique set of parameter values suggests that a separation of the total adsorption energy into an electrostatic and a chemical component can be done in a reasonable way. The description of the sulfate adsorption data is sensitive to the location of the nitrate ion relative to sulfate, and the best description is found when nitrate and the solution-oriented ligands of sulfate are in the same plane.

Acknowledgments

The authors are very grateful for the information of Stephan Hug about the structure of sulfate on goethite. We thank Th. A. Vens for producing the goethite and also thank A. J. Korteweg and A. J. van der Linde from the Department of Biomolecular Sciences (Laboratory of Physical Chemistry and Colloid Science) respectively for the BET analysis and for assistance during use of the Zetasizer.

Appendix 1

Description of CD-MUSIC modeling approach

The proton adsorption behavior of goethite can be represented by the reaction of protons with singly and triply coordinated surface groups (40). In the modeling we have set both $\log K_H$ values equal to the PZC value (24, 30). In NaNO_3 the PZC is pH 9.25 (surface equilibria in Table A). The CD-MUSIC model in the Three Plane version has an electrostatic double layer consisting of two Stern layers and a diffuse layer. Three electrostatic planes are present: the surface plane, the plane at the head end of the diffuse layer (outermost plane) and an intermediate plane (mid-plane).

Surface groups may form ion pairs (41, 42) like many ions in solution. In general the description of the basic charging curves is determined by a combination of three parameters: the capacitance's of the Stern layer, the locations of the ion pairs, and the equilibrium constants of the ion pairs. The charge curves for goethite can be modeled with the CD-MUSIC model of Hiemstra and van Riemsdijk (30) by locating the ion pairs in the outermost plane. The $\log K$ used for ion pairs formation was set to -1 (Table 1: $\log K_{\text{Na}} = \log K_{\text{NO}_3}$).

In Pauling's bond valence concept ions distribute their charge over the coordinating ligands. This concept is applied to adsorbed surface species by distributing the charge of the central ion of a complex. The charge of the surface ligands is attributed to the surface plane while the charge of the solution-directed ligands is placed in the mid-plane or the outermost plane. The adsorption equilibrium of sulfate with singly coordinated surface groups can be written as equation 7 (Table A1), if adsorbed sulfate is coordinated with one surface group.

The modeled changes of charge as formulated in Table A1 (z_0 and z_1) can be interpreted as a charge distribution of the central ion S over the surface-plane and another plane if it is assumed that the surface oxygen's and protons are in the surface-plane. For sulfate an equal distribution of the valence of S over its four ligands gives a bond valence of $v = 6(S)/4 = 1.5$ v. u.. The charge attribution to the electrostatic planes is related to the bond valence (v) with $z_i = n_i(v-2)$, where n_i is the number of ligands per electrostatic plane.

Table A1. Surface equilibrium equations as used in the Basic Stern model. The adsorbed -2 charge of sulfate ($z_0+z_1 = -2$) is distributed across the surface plane (with potential ψ_0) and the outermost electrostatic plane (with potential ψ_1).

	equilibrium	$\ln K_i$
1	$(\text{FeOH}_2^{+0.5}) = K_i(\text{FeOH}^{0.5})(\text{H}^+)$	$\ln K_H - \psi_0 F / (RT)$
2	$(\text{Fe}_3\text{OH}^{+0.5}) = K_i(\text{Fe}_3\text{O}^{0.5})(\text{H}^+)$	$\ln K_H - \psi_0 F / (RT)$
3	$(\text{FeOH}^{0.5} \cdot \text{Na}^+) = K_i(\text{FeOH}^{0.5})(\text{Na}^+)$	$\ln K_{\text{Na}} - \psi_1 F / (RT)$
4	$(\text{Fe}_3\text{O}^{0.5} \cdot \text{Na}^+) = K_i(\text{Fe}_3\text{O}^{0.5})(\text{Na}^+)$	$\ln K_{\text{Na}} - \psi_1 F / (RT)$
5	$(\text{FeOH}_2^{+0.5} \cdot \text{NO}_3^-) = K_i(\text{FeOH}_2^{+0.5})(\text{NO}_3^-)$	$\ln K_{\text{NO}_3} + \psi_1 F / (RT)$
6	$(\text{Fe}_3\text{OH}^{+0.5} \cdot \text{NO}_3^-) = K_i(\text{Fe}_3\text{OH}^{+0.5})(\text{NO}_3^-)$	$\ln K_{\text{NO}_3} + \psi_1 F / (RT)$
7	$(\text{FeO}^{+0.5+z_0}\text{SO}_3^{z_1}) = K_i(\text{FeOH}_2^{+0.5})(\text{SO}_4^{2-})$	$\ln K_S - (z_0\psi_0 + z_1\psi_1)F / (RT)$

Table A2. Formation constants of species in solution.

	equilibrium	Log K^0
1	$(H^+)(SO_4^{2-}) \rightleftharpoons (HSO_4^-)$	1.98
2	$(Na^+)(SO_4^{2-}) \rightleftharpoons (NaSO_4^-)$	0.7
3	$(H^+)(OH^-) \rightleftharpoons (H_2O)$	-14.0

Appendix 2

Data of proton-sulfate titrations at different pH values and salt concentrations. Each curve that gives the proton co-adsorption as a function of sulfate adsorption is fitted by a polynomial and the values for the coefficients are listed. The coefficients of this polynomial, $\Gamma_H^* = a_{pH,salt}\Gamma_S^2 + b_{pH,salt}\Gamma_S$, can also be used to express the proton-sulfate stoichiometry by $\chi = (\partial\Gamma_H/\partial\Gamma_{SO_4})_{pH} = 2a_{pH,salt}\Gamma_S + b_{pH,salt}$ (with $\Gamma_H^* = 0$ if $\Gamma_S = 0$). The quality of the data description by the Basic Stern model with a charge distribution of adsorbed sulfate as given in the figures (-0.35, -1.65) is given as $\Delta = \Sigma(\Gamma_H^{calc}/\Gamma_H^{data})$.

pH	[NaNO ₃]	a	b	number of data	Γ_S range ($\mu\text{mol}/\text{m}^2$)	Δ data description by model
3.6	0.01	0.05	0.72	9	0.95	0.86
3.6	0.01	0.07	0.68	11	0.86	0.89
3.9	0.01	0.15	0.62	19	0.78	0.96
4	0.01	0.1	0.67	10	0.77	0.93
4.1	0.01	0.17	0.63	13	0.43	0.96
4.1	0.01	0.18	0.63	16	0.74	0.96
4.1	0.01	0.17	0.62	19	0.84	0.97
4.24	0.01	0.07	0.7	13	0.77	0.94
4.24	0.01	0.16	0.68	13	0.77	0.92
4.24	0.01	0.2	0.64	13	0.77	0.95
4.6	0.01	0.17	0.69	11	0.76	0.94
4.6	0.01	0.15	0.69	12	0.79	0.96
4.68	0.01	0.17	0.68	11	0.77	0.97
5.27	0.01	0.31	0.71	12	0.53	0.99
5.37	0.01	0.33	0.71	11	0.49	1.00
5.56	0.01	0.28	0.71	10	0.37	1.06
6.2	0.01	0.52	0.77	3	0.19	1.09
3.6	0.10		0.61	9	0.48	0.86
4	0.10		0.61	7	0.27	0.87

Appendix 3

Here we make a comparison between the Three Plane model and the Basic Stern model (see picture 1 and 2 of Fig. 2). Calculated is the relation between the position of the mid-plane and the charge distribution necessary to give identical electrostatic potentials at the surface plane and the outer-most plane, and identical surface charge. The consequence of this relation is that different values of the inner- and

outer-capacitance, in combination with different values of the charge distribution can give equal proton co-adsorption levels. The relation is calculated as example for a bivalent anion with a charge distribution across the surface plane (z_0) and to the mid-plane (z_1), where

$$z_0 + z_1 = -2 \quad [1]$$

For simplicity the ion pairs are not included. The charge in the surface plane (σ_0) and the mid-plane (σ_1) are written as:

$$\sigma_0 = F ([SH] + [S-A](1+z_0) - 0.5N_s) \quad [2]$$

$$\sigma_1 = F [S-A] z_1 \quad [3]$$

and as,

$$\sigma_0 = C_1 (\psi_0 - \psi_1) \quad [4]$$

$$\sigma_0 + \sigma_1 = C_2 (\psi_1 - \psi_2) \quad [5]$$

The parameter [SH] is the sum of the concentration of $[FeOH^{+0.5}]$ and $[Fe_3OH^{+0.5}]$, while [S-A] and N_s are respectively the concentration of sites reacted with the bivalent anion and the total site density (singly and triply coordinated sites). The relation between the total, inner- and outer capacitance is given by $C^{-1} = C_1^{-1} + C_2^{-1}$, which can be rewritten as:

$$C = C_1 C_2 (C_1 + C_2)^{-1} \quad [6]$$

The conditions are that the electrostatic potential of the Basic Stern model and the Triple Layer model are alike at the surface plane and the outermost plane: ψ_0 and ψ_2 , and that the total H consumption is constant. Simplifying the equations [1]-[6] to a function of C with z_1 solves the problem. Substituting [6] in [4,5], and rewriting gives:

$$\sigma_0 C_2 C^{-1} + \sigma_1 = C_2 (\psi_0 - \psi_2) \quad [7]$$

Substituting the equations of [1] and [2, 3] in [7] gives after rewriting:

$$z_1 = C_2 (C - C_2)^{-1} \{ (C/F(\psi_0 - \psi_2) - [SH] + 0.5N_s)[S-A]^{-1} + 1 \} \quad [8]$$

In the Basic Stern model $C_2 \rightarrow \infty$, thus the charge attribution of the bivalent anion to the outermost plane (z_1^{BS}) can be compared to the charge attribution to the mid-plane in the Three Plane model (z_1^{TP}) with equation [8]:

$$z_1^{BS} = - \{ (C/F(\psi_0 - \psi_2) - [SH] + 0.5N_s)[S-A]^{-1} + 1 \} \quad [9]$$

therefore:

$$z_1^{TP} = - z_1^{BS} C_2 (C_2 - C)^{-1} \quad [10]$$

Example: if in a Basic Stern model $z_1^{BS} = -1.65$ gives a good description of the proton-ion adsorption stoichiometry of a bivalent anion, then $z_1^{TP} = -2.02$ gives an equally good description in a Three Plane model with $C_2 = 5 \text{ F/m}^2$ (assuming a total capacitance of $C = 0.91 \text{ F/m}^2$). The calculated adsorption isotherms are however different and are steepest in the BS option. In principle the pH dependent adsorption isotherms therefore enable the determination of the charge distribution and the capacitances. Including the ion pairs in the derivation gives an identical result.

References

1. Sposito, G., "The surface chemistry of soils." Oxford University Press, NY, 1984.
2. Dzombak, D. A., and Morel, F. M. M., "Surface complexation modeling: hydrous ferric oxide." Wiley, NY, 1990.
3. Stumm, W., and Morgan J. J., "Aquatic Chemistry: chemical equilibria and rates in natural waters." Wiley, NY, 1996.
4. Cernik, M., Borkovec, M., and Westall, J. C., (1996) Affinity distribution description of competitive ion binding to heterogeneous materials *Langmuir* **12**, 6127-6137.
5. Hiemstra T. and Van Riemsdijk W. H. (1999) Surface structural ion adsorption modeling of competitive binding of oxyanions by metal (hydr)oxides *J. Colloid Interface Sci.* **210**, 182-193.
6. Hayes K. F., Roe A. L., Brown G. E., Hodgens K. O., Leckie J. O., and Parks G. A. (1987) In-situ x-ray absorption study of surface complexes: selenium oxyanions on α -FeOOH. *Science* **238**, 783-786).
7. Tejedor-Tejedor M. I. and Anderson M. A. (1990) Protonation of phosphate on the surface of goethite as studied by CIR-FTIR and electrophoretic mobility. *Langmuir* **6**, 602-611.
8. Waychunas G. A., Rea B. A., Fuller C. C., and Davis J. A. (1993) Surface chemistry of ferrihydrite: part I. EXAFS studies of the geometry of coprecipitated and adsorbed arsenate. *Geochim. Cosmochim. Acta.* **57**, 2251-2269.
9. Manceau A. and Charlet L. (1994) The mechanism of selenate adsorption on goethite and hydrous ferric oxide. *J. Colloid Interface Sci.* **168**, 87-93.
10. Spadini, L. Manceau, A., Schindler, P.W., and Charlet, L. (1994) Structure and stability of Cd^{2+} surface complexes on ferric oxides. *J. Colloid Interface Sci.* **168**, 73-86.
11. Manning, B. A., Fendorf, S. E., and Goldberg, S. (1998) Surface structures and stability of arsenic(III) on goethite: spectroscopic evidence for inner-sphere complexes. *Env. Sci. Tech.* **32**, 2383-2388.
12. Sun X. and Doner H. E. (1996) An investigation of arsenate and arsenite bonding structures on goethite by FTIR. *Soil Science* **161**, 865-872.
13. Fendorf S., Eick M. J. Grossl P., and Sparks D. L. (1997) Arsenate and Chromate retention mechanism on goethite. I. Surface structure. *Environ. Sci. Technol.* **31**, 315-320.
14. Persson, P., and Lövgren, L. (1996) Potentiometric and spectroscopic studies of sulfate complexation at the goethite-water interface. *Geochim. Cosmochim. Acta.* **60**, 2789-2799.
15. Bargar, J.R., Brown, G.E. Jr. and Parks, G.A. (1997) Surface complexation of Pb(II) at the oxide-water interfaces: II. XAFS and bond-valence determination of mononuclear and polynuclear Pb(II) sorption products on iron oxides. *Geochim. Cosmochim. Acta* **61**, 2639-2652.
16. Hug, S. J., (1997) In Situ Fourier Transform Infrared Measurements of sulfate Adsorption on hematite in aqueous solutions *J. Colloid Interface Sci.* **188**, 415-422.
17. Eggleston, C. M., Hug, S. J., Stumm, W., Sulzberger, B., and Afonso, M.dS. (1998) Surface complexation of sulfate by hematite surfaces: FTIR and STM observations *Geochim. Cosmochim. Acta.* **62**, 585-593.
18. Sugimoto, T., and Wang, Y., (1998) Mechanism of the shape and structure control of monodispersed α -Fe₂O₃ particles by sulfate ions *J. Colloid Interface Sci.* **207**, 137-149.
19. Rietra, R. P. J. J., Hiemstra, T., and van Riemsdijk, W. H., (1999) The relation between molecular structure and ion adsorption behavior on variable charged minerals *Geochim. Cosmochim. Acta.* **63**, 3009-3015.
20. Perona M. J. and Leckie J. O. (1985) Proton stoichiometry for the adsorption of cations on oxide surfaces. *J. Colloid Interface Sci.* **106**, 65-69.
21. Hiemstra T., De Wit J. C. M., and Van Riemsdijk W. H. (1989). Multisite proton adsorption modelling at the solid/solution interface of (hydr)oxides: a new approach. II application to various important (hydr)oxides. *J. Colloid Interface Sci.* **133**, 105-117.
22. Geelhoed, J. S., Hiemstra, T., and van Riemsdijk, W. H., (1997) Phosphate and sulfate adsorption on goethite: Single anion and competitive adsorption *Geochim. Cosmochim. Acta* **61**, 2389-2396.

CHAPTER 4

23. Kinniburgh D. G., Milne C. J., and Venema P. (1995) Design and construction of a personal-computer-based automatic titrator. *Soil Sci. Soc. Am. J.* **59**, (2) 417-422.
24. Venema P., Hiemstra T., and Van Riemsdijk W. H. (1996) Multi site adsorption of cadmium on goethite. *J. Colloid Interface Sci.* **183**, 515-527.
25. Minor, M., van der Linde A. J., van Leeuwen, H. P., and Lyklema, J. (1997) Dynamic aspects of electrophoresis and electroosmosis: A new fast method for measuring particle mobilities *J. Colloid Interface Sci.* **189**, 370-375.
26. Keizer, M. G., and van Riemsdijk, W. H. "ECOSAT: technical report of the department soil science and plant nutrition" Wageningen Agricultural University, Wageningen, 1998.
27. Hoins, U., Charlet, L., and Sticher, H., (1993) Ligand effect on the adsorption of heavy metals: the sulfate-cadmium-goethite case *Water, Air, and Soil Pollution* **68**, 241-255.
28. Ali, M. A., and Dzombak, D. A., (1996) Interactions of copper, organic acids, and sulfate in goethite suspensions. *Geochim. Cosmochim. Acta* **60** 5045-5053.
29. Ali, M. A., and Dzombak, D. A., (1996) Competitive sorption of simple organic acids and sulfate on goethite. *Environ. Sci. Tech.* **30**, 1061-1071.
30. Hiemstra T. and Van Riemsdijk W. H. (1996) A surface structural approach to ion adsorption: the charge distribution (CD) model. *J. Colloid Interface Sci.* **179**, 488-508.
31. Russell, J. D., Parfitt, R. L., Fraser, A. R., and Farmer, V. C., (1974) Surface structures of gibbsite, goethite, and phosphated goethite. *Nature* **248**, 220-221.
32. Torrent, J., Barron, V., and Schwertmann, U., 1990 Phosphate adsorption and desorption by goethites *Soil Sci. Soc. Am. J.* **54**, 1007-1012.
33. Borkovec M. (1997) Origin of 1-pK and 2-pK models for ionizable water-solid interfaces. *Langmuir* **13**, 2608-2613.
34. Lützenkirchen J. (1998) Comparison of 1-pK and 2-pK versions of surface complexation theory by the goodness of fit in describing surface charge data of (hydr)oxides. *Environ. Sci. Technol.* **32**, 3149-3154.
35. Rundberg, R. S., Albinsson, Y., and Vannerberg, K., (1994) Sodium adsorption onto goethite. *Radiochimica Acta* **66/67**, 333-339.
36. Rieta, R. P. J. J., Hiemstra, T., and van Riemsdijk, W. H., (1998) Characterization of ion adsorption with proton-ion titrations. *Mineralogical Magazine.* **62A**, 1269-1270.
37. Zhang, G. Y., Brümmer, G. M., and Zhang, Z. N., (1996) Effect of perchlorate, nitrate, chloride and pH on sulfate adsorption by variable-charge soils *Geoderma* **73**, 217-229.
38. Filius J. D., Hiemstra T., and Van Riemsdijk W. H. (1998) Adsorption of small weak organic acids on goethite: modeling of mechanisms *J. Colloid Interface Sci.* **195**, 368-380.
39. Hansmann, D. D., and Andersson, M. A. (1985) Using electrophoresis in modeling sulfate, selenite, and phosphate adsorption onto goethite *Environ. Sci. Tech.* **19**, 544-551.
40. Hiemstra T., Venema P., and Van Riemsdijk W. H. (1996) Intrinsic proton affinity of reactive surface groups of metal (hydr)oxides: The bond valence principle. *J. Colloid Interface Sci.* **184**, 680-692.
41. Smit, W., and Holten, C. L. M., (1980) Zeta-potential and radiotracer adsorption measurements on EFG Al₂O₃ single crystals in NaBr solutions *J. Colloid Interface. Sci.* **78**, 1-14.
42. Sprycha, R., (1984) Surface charge and adsorption of background electrolyte ions at anatase/electrolyte interface *J. Colloid Interface Sci.* **102**, 173-185.
43. Davis, J. A., and Leckie, J. O., in: Chemical modeling-speciation, sorption, solubility, and kinetics in aqueous systems, E. A. Jenné, ed., ACS symposium series, vol. 93, chap. 15, 1979.

Comparison of selenate and sulfate adsorption on goethite

Abstract

The adsorption behavior of selenate (SeO_4) on goethite has been studied over a wide range of conditions. The SeO_4 adsorption has been compared with the binding of SO_4 . The experimental results are interpreted in the view of very recent spectroscopic work on the speciation and coordination of adsorbed selenate and sulfate on goethite. The spectroscopic results suggest that at pH values above 6 outersphere complexes are dominant while in the main adsorption range at lower pH values monodentate innersphere complexes are dominant. The qualitative results from spectroscopy can suit very well with the CD-MUSIC modeling of the large set of SeO_4 adsorption data. The charge distributions obtained for the innersphere complexes are in line with the spectroscopically determined coordinations of the adsorbed anions. The formation of outersphere complexes cannot be established from the macroscopic adsorption data without the spectroscopic knowledge. However description of the adsorption data including and differentiating between both species can be done very satisfactory with the CD-MUSIC approach.

Materials and Methods

Synthesis and Characterization

All chemicals (Merck p.a.) were stored in plastic bottles and all experiments have been performed in plastic vessels to avoid silica contamination. The water used throughout the experiment was always ultrapure water ($\approx 18 \mu\text{S}/\text{cm}$). The goethite suspension has been prepared according to Hiemstra et al. (17): a freshly prepared 0.5 M $\text{Fe}(\text{NO}_3)_3$ was slowly titrated with 2.5 M NaOH to pH 12, after which the suspension was aged for 3 days at 60°C and subsequently dialyzed in water. The BET(N_2) specific surface area of the goethite is $96.4 \text{ m}^2/\text{g}$. Goethite of the same batch was used previously (4,5,16,18). Acid-base titrations have been described and discussed earlier (4, 16) and the details of the experimental methods have been discussed by Venema et al. (27).

Acid-base Titrations in Na_2SeO_4 and Na_2SO_4

Acid-base titrations of goethite suspensions (10g/l) in Na_2SeO_4 and Na_2SO_4 (4) have been performed at one concentration (0.033 M Na_2SeO_4 or Na_2SO_4). Before the addition of the anion solution the salt-free suspension was titrated to a pH 5.5 and kept in N_2 atmosphere during one night to remove CO_2 . After titrating the suspension to a pH of approximately 10 a volume of Na_2SeO_4 or Na_2SO_4 (0.9 M) was added, leading to the appropriate initial anion concentration (0.033 M). The proton adsorption in 0.033 M Na_2SeO_4 or Na_2SO_4 (without NaNO_3) could be determined relative to the proton adsorption in 0.1 M NaNO_3 because the goethite was sampled from the same stock suspension as used for the titrations in NaNO_3 . The initial difference in pH between the goethite suspension with 0.1 M NaNO_3 and the sample with the anions (0.033 M SeO_4 or SO_4), leads to a difference in the $\text{H}_1\text{-OH}_1$ mass balance, resulting in a different proton adsorption of both suspensions. The balance $\text{H}_1\text{-OH}_1$ is calculated from the experimental proton activity using the appropriate activity coefficient for $I=0.1 \text{ M}$ in combination with the water equilibrium.

Adsorption Isotherms

Adsorption experiments were performed in individual centrifuge tubes with fixed amounts of salt, goethite, selenate or sulfate, and different pH values (pH 3-5) to give adsorption-edges. In case of higher pH values (pH 5.8 and 8.0) contact with CO_2 was explicitly avoided by mixing a CO_2 free goethite suspension in vessels with different amounts of anion solution. The final goethite concentration in the vessels and tubes varied to get in all cases more than 50 % adsorption of the total amount of anion added: 3.1 g/l for the pH range 3-5, 9.7 g/l for pH 5.8, and 20.6 g/l for pH 8. The tubes and vessels were equilibrated for 20 hours by end-over-end rotation. They were centrifuged, and samples of the supernatant were taken for analysis with ICP-MS or hydride-AAS in case of selenate and ICP-AES in case of sulfate. The pH was measured in the remaining supernatant. The amount of adsorbed selenate or sulfate was calculated from the difference between the total initial anion concentration and

the anion concentration of the suspension. These data have been used to construct adsorption isotherms. At fixed pH values, the adsorption and equilibrium concentration have been calculated by interpolation of the data of the adsorption edges. In all cases the percentage adsorbed is higher than 50% of the total ion concentration thus preventing the use of adsorption data with less accuracy than the determined ion concentration.

Adsorption of selenate as a function of pH and salt concentration has been determined in our laboratory for another goethite preparation. In this experiment the surface loading was very low ($<0.1 \mu\text{mol}/\text{m}^2$). The goethite used was from another batch with very similar acid-base characteristics (27). No special precautions were made for to avoid contact with CO_2 . The procedures are as given for the other experiments, except the Se analysis that was done with furnace AAS.

Modeling adsorption data

The data have been evaluated with the CD-MUSIC approach. We will use here Basic Stern option as electrostatic model (14), as has been used recently to describe the sulfate adsorption on goethite (4). In Table 1 the model parameter values (Table 1) have been given. A description of the relevant model characteristics is given here.

CD-MUSIC is an extension of the MUSIC (multi site complexation) approach. A central parameter in the model is the distribution of the charge. The innersphere complexes of ions are assumed to have a spatial distribution of charge. One part of the charge of the adsorbed species is attributed to the surface since not all ligands of the adsorbed complex share oxygens with the solid. The remaining part of the charge is at a certain distance of the surface. The charge attribution (z_i) to the electrostatic planes (i) can be estimated for a known surface structure of an adsorbed non-protonated oxyanion using the Pauling bond valence concept (5, 14) $z_i = n_i(v-2)$, where n_i is the number of oxygen ligands per electrostatic plane i, and v is the Pauling bond valence (valence of central ion divided by coordination number). Application of the Pauling Bond Valence concept, with equal distribution of charge over the ligands, leads to a bond valence (v) of 1.5 valence units (v.u.) per Se-O or S-O bond, i.e. the charge per oxygen is -0.5 v.u.. In case of a monodentate complex the ligands are unequally distributed in the interface since one ligand is shared with the interface and three are oriented towards the solution ($n_0=1$, $n_1=3$). This leads to an unequal distribution of charge across the electrostatic planes for monodentate sulfate: $z_0 = -0.5$ in the surface plane and $z_1 = -1.5$ in a plane located at some distance from the plane. In case of bidentate formation, the charge distribution will be quite different. On this basis, the CD-MUSIC model can distinguish between formation of bidentate and monodentate complexes, as has been shown by Rietra et al. (5).

It is plausible that only the singly coordinated surface groups are reactive for innersphere complexation of selenate and sulfate if we focus on the charge of the common ligand in surface complexes built from interaction of SeO_4 ions and singly, doubly, and triply coordinated oxygens (Fe-O-Se, $\text{Fe}_2\text{-O-Se}$ and $\text{Fe}_3\text{-O-Se}$). Assuming a bond valence for a Se-O bond of 1.5 v. u., and 0.5 v. u. for a Fe-O bond, the sum of bond valences on surface oxygen is 0, +0.5, and +1 v.u. respectively for singly, doubly and triply coordinated oxygen. According to Bargar et al. (19) only a neutral or almost

neutral sum of bond valences seems plausible, which leads to the prediction that only singly coordinated oxygen will react with sulfate to form an innersphere complex.

The site densities of the surface groups are chosen as given in Hiemstra and van Riemsdijk (14). The protonation of the singly (3.45 sites/nm^2) and triply coordinated surface groups (2.70 sites/nm^2) is described by the surface equilibria as given in Appendix A1. The $\log K_H$ values are assumed to be equal to the PZC of goethite in NaNO_3 (PZC is pH 9.25). The electrolyte ions are assumed to form ion pairs with the surface groups ($\log K_{\text{Na}} = \log K_{\text{NO}_3} = -1$).

Model calculations

Calculations were carried out with Ecosat, a computer code for the calculation of chemical equilibria (20) in which the fitting program FIT (24) has been incorporated. The Davies equation (constant is 0.2) is used to calculate the ion activity coefficients at 25°C (the solution equilibria used are in Appendix 1, Table A2). The adjustable model parameters in the CD-MUSIC model, i.e. the intrinsic anion adsorption constants and the corresponding charge distribution, are calculated by minimizing the difference between the calculated and experimental ion adsorption according to the Residual Sum of Squares: $\text{RSS} = \sum (\Gamma^{\text{calc}} - \Gamma^{\text{data}})^2$. In this paper we calculate the best-fitting intrinsic affinity constants in combination with the charge distribution on the basis of the description of the adsorption data with or without taking spectroscopic information of the surface speciation into account.

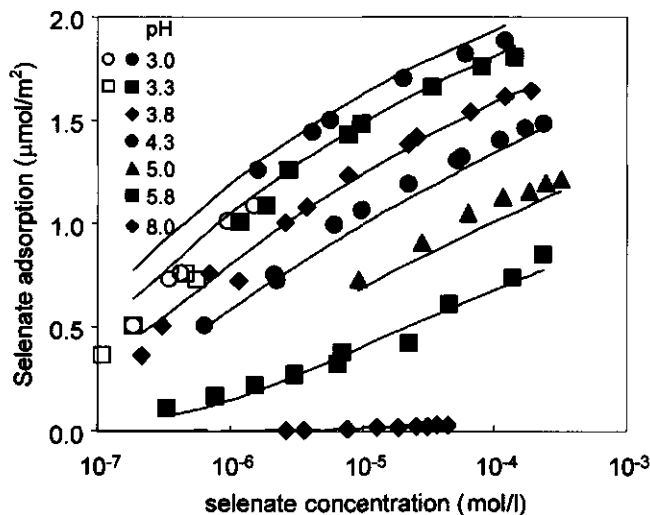


Fig. 1. Experimental and modeled adsorption isotherms of selenate on goethite in 0.01 M NaNO_3 . The open symbols at low pH are excluded in the modeling. The model lines are calculated assuming an inner- and outersphere species (Table 1, nr. 2), but are indistinguishable from the lines calculated with one species (see text).

Results and Discussion

Comparison of selenate and sulphate

Previously the proton co-adsorption as a function of selenate and sulfate adsorption has been determined and compared with other anions (5). The slope of the proton co-adsorption is the proton-ion adsorption stoichiometry if protonation of the solution species is negligible as is the case for selenate and sulfate at $\text{pH} > 4$. The proton-ion adsorption stoichiometry is related directly to the pH dependency of adsorption as follows from a thermodynamic relation derived by Perona and Leckie (21). It follows from the proton co-adsorption data (5) that the pH dependency of selenate adsorption is slightly larger as compared to sulfate. The proton stoichiometry is mainly determined by the electrostatic interaction of the adsorbed anions with protons present at the surface (5). The fitted stoichiometry is not sensitive with respect to the number of protons defined in the intrinsic adsorption reaction of SO_4 and SeO_4 (5). It implies that the contribution of the intrinsic reaction can not be elucidated from the data analysis.

In Fig. 1 the adsorption isotherms of selenate are shown. In Fig 2 the adsorption is compared with the adsorption of sulfate. In Fig. 2a selenate and sulfate adsorption are compared on a linear-logarithmic scale while in Fig. 2b they are compared on a double logarithmic scale. The drawn lines are model curves and will be discussed later. The adsorption of selenate is higher than the adsorption of sulfate at low pH and high anion concentrations. The differences become smaller at pH 5 and are negligible at pH 8. It can be concluded from the proton co-adsorption data (5), and from the adsorption isotherms, that selenate has a slightly larger pH dependency than sulfate.

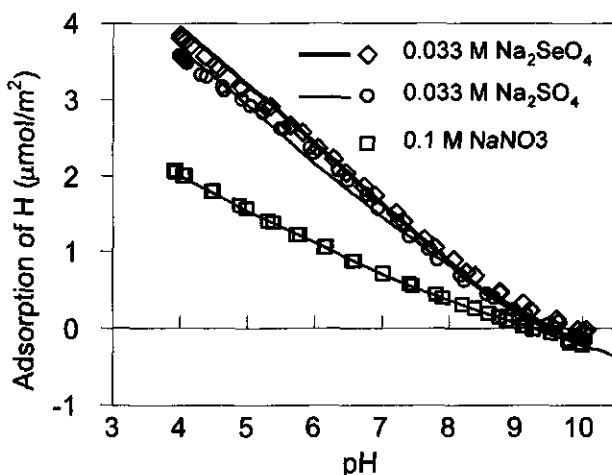


Fig. 3. Experimental and modeled acid-base behavior of goethite (Table 1, nr. 2) in 0.033 M Na_2SeO_4 and Na_2SO_4 .

In Fig. 3 the proton adsorption is shown in 0.033 M Na_2SeO_4 and compared with the proton adsorption in 0.033 M Na_2SO_4 from Rietra et al. (4). Also from

these data it follows that the adsorption of selenate and sulfate is slightly different, as follows from the different slope, which was not only observed in this experiment but also in a previous work (5) The steeper slope for SeO_4 is linked to the slightly higher pH dependency of the SeO_4 adsorption. It is noted that, in contrast to the data, no significant higher proton adsorption is expected for selenate compared to sulfate at pH values above 9.

Modeling the adsorption data

The adsorption isotherms of selenate (Fig.1) can be modeled by assuming one adsorbed species as has been done previously (4) for sulfate. Only two parameters, the intrinsic log K and the charge distribution, are needed to model the selenate adsorption since the other model parameters (capacity and ion pairs) are found from the modeling of the primary charging behavior as given previously (4,5,16). In case of one type of surface species, the charge distribution is found independently from the log $K_{\text{Se}}^{\text{intr}}$ (defined in Appendix 1) by modeling the proton co-adsorption as a function of selenate adsorption. The proton co-adsorption as a function of selenate adsorption (5) was determined at a pH 4.2 (0.01 M NaNO_3) and can be described with a charge distribution of $z_0 = -0.6$ and $z_1 = -1.4$ for the adsorbed species. The corresponding intrinsic adsorption constant follows from modeling the adsorption data in Fig. 1, yielding a log $K_{\text{Se}}^{\text{intr}} = 0.08$.

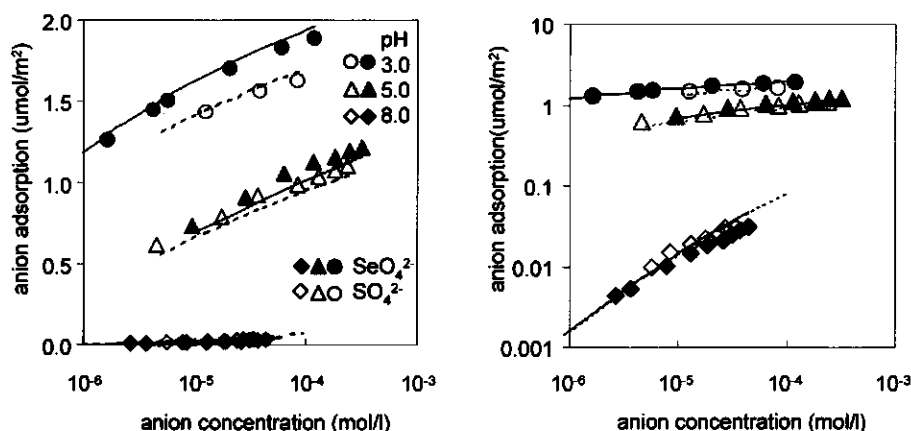


Fig. 2. Experimental and modeled adsorption isotherms of selenate and sulphate (Table 1, setnr. 2 and 4) on goethite in 0.01 M NaNO_3 : (a) on lin-log scale, (b) on log-log scale. The adsorption of selenate is slightly more pH dependent than sulfate. Selenate has a higher adsorption at low pH while at high pH the adsorption of selenate and sulfate are almost equal. At pH 8 the adsorption of selenate and sulfate is almost alike.

The model gives an excellent description of all the adsorption data of selenate and is able to quantify the differences found between selenate and sulfate. However at low surface coverage the selenate adsorption isotherms at pH 3 and pH 3.3 show anomalous behavior (open symbols). This is not caused by incomplete separation of goethite and the supernatant because the Fe concentration was low ($[Fe] < 6 \mu\text{g/l}$) compared to the selenate concentration (Fe was determined in the same sample as Se with ICP-MS). From the thermodynamic consistency between adsorption isotherms and proton co-adsorption data it follows that the correct model description of the proton co-adsorption as function of selenate adsorption at pH 4.2 (0.01 M) also gives a correct pH dependency of selenate adsorption. The correct pH dependency, except at low surface coverage around pH 3 and pH 3.3, demonstrates this. Competition of anions with adsorbed carbonate can cause the anomalous behavior as was shown by Van Geen et al. (22) but this effect is only expected at higher pH values (experiments at pH 5 and pH 8 were however performed in CO_2 -free N_2 atmosphere). In principle contamination of the goethite with an ion that only binds strong at pH values below 3.8 can cause the anomalous behavior. However, no evidence could be found for this from the acid-base behavior or proton co-adsorption data that have been determined at pH values above 4. Since also another goethite batch showed the same anomalous behavior, contamination is not very likely.

Table 1. For selenate and sulfate, the optimized Charge Distribution and affinity constants for a single complex, and for a combination of an innersphere complex and an outersphere complex. The optimization for the combinations was performed for selenate using the adsorption isotherms of Fig. 4 and for sulfate using the adsorption isotherms of Fig 5 and 8 in Rietra et al. (4). The optimized Residual Sum of Squares (RSS) is shown in Fig. 5. The parameters for the outersphere species were set on the basis of the pH 8 data.

setnr.	anion			$\log K_i$	z_0	z_1
1.	Selenate	single complex		0.08	-0.60 ^{*b}	-1.40
2.	Selenate	two complexes	outersphere	1.1 ^{*a}	-0.2	-1.8
			innersphere	-0.14	-0.64	-1.36
3.	Sulfate	single complex ^{*a}		1.07	-0.35	-1.65
4.	Sulfate	two complexes	outersphere	1.1 ^{*a}	-0.2	-1.8
			innersphere	0.26	-0.48	-1.52

^{*a} model parameters from Rietra et al. (4).

^{*b} The value of z_0 and z_1 based on proton ion titration of Rietra et al. (5) is -0.60 and -1.40 respectively for selenate and -0.40 and -1.60 for sulfate.

Modeling the speciation and coordination according to spectroscopy

Recent spectroscopic work (2,3) points to a dominant monodentate innersphere complex below pH 6 for sulfate and selenate, whereas above pH 6 the outer sphere complexes for both ions are dominant. This is qualitatively in agreement with the analysis made earlier for sulfate using the CD-MUSIC model (4): the outersphere complex will attribute less negative charge to the surface, which leads to less coadsorption of protons and to a smaller pH dependency than the innersphere complex. Spectroscopy shows that at high pH the outersphere complex is the dominant one. The innersphere species will also be present, but at a lower

The choice of the charge distribution for the innersphere complex influences the calculated distribution between inner- and outersphere complexes at a given pH and loading. This phenomenon can be used in our analysis. The data of Wijnja and Schulthess (2) show an estimated percentage of 50 % outersphere complex, at pH=6 and a concentration of 1 mmol/l Se or S. It should be noticed that this estimation is uncertain since quantification of the spectroscopic results in terms of relative amount of outer- and innersphere complexes as function of pH and loading is still problematic (personal note of Wijnja). The value of the charge distribution that explains the spectroscopic observations is given in Fig.4b where we show the predicted amount of outersphere complexes as function of the charge distribution of the innersphere complex. The charge distributions resulting in 50% outersphere complexes are plotted in Fig 4b as black spheres. These spheres are also given in Fig.4a, showing for the given charge distribution the corresponding RSS when fitting the adsorption data. A remark should be made on the choice of the charge attribution of the outersphere complex to the outermost electrostatic plane. For the results shown in Fig.4, a charge distribution of $z_0 = -0.2$ and $z_1 = -1.8$ for the outersphere complex of selenate and sulfate was used because a charge distribution of $z_0=0$ and $z_1=-2$ gives a less good description of the sulfate adsorption data in combination with the condition of 50% outersphere complexes at pH 6 (not shown).

We may conclude that the description of the adsorption data for selenate and sulfate does not significantly improve with the incorporation of the outersphere complex, but on the other hand, a good description can be given using the spectroscopic information. The results of our analysis (Fig. 4) shows that the incorporation of the spectroscopic knowledge leads to approximately the same charge distribution for the innersphere selenate complex as the value that is determined from the adsorption isotherms (minimum RSS, black triangles) or the proton-ion titration at low pH (open squares). The charge distribution for sulfate is slightly different using the adsorption isotherms in combination with spectroscopic knowledge, or the value from the proton-ion titrations. The results also show that the charge distributions of the innersphere complexes of SeO_4 and SO_4 are slightly different. The charge distributions found for the innersphere complexes of selenate ($z_0=-0.64$, $z_1=-1.36$) and sulfate ($z_0 = -0.48$, $z_1 = -1.52$) correspond approximately to an equal charge distribution over the ligands in combination with the assumption of one common ligand with the surface, i.e. a monodentate complex. This is fully in line the spectroscopic finding, suggesting a dominant monodentate innersphere complex at low pH values (1, 2, 26). Recently bidentate surface complexation for SeO_4 has been suggested (29). The data, obtained with ex-situ IR spectroscopy in KBr tablets, may be relevant for dry conditions. However, for aqueous conditions bidentates of SeO_4 can be definitely excluded based on the CD-MUSIC model interpretation (5) and in-situ spectroscopy (1-3). For selenate the model with and without incorporation of the outersphere complex can also be used to predict the selenate adsorption as function of the ionic strength. The calculations can be compared with the experimental data (Fig. 5), which represent low SeO_4 loading. The experimental data on the effect of ionic strength at low Se loading are very

comparable with the results found by Hayes et al. (25). The model is able to describe the change of the ionic strength very satisfactorily.

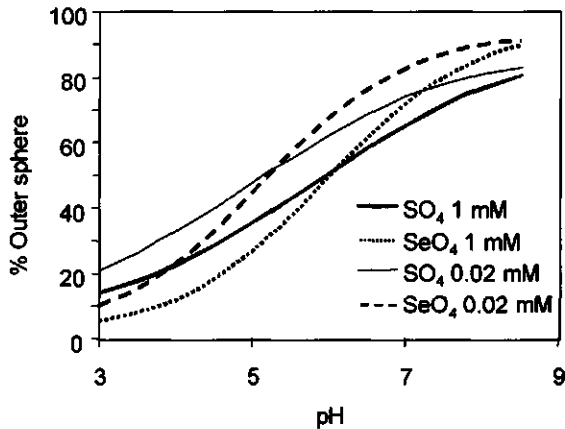


Fig. 5. Experimental and modeled adsorption edges of selenate on goethite at very low surface coverages (adsorption below $0.1 \mu\text{mol}/\text{m}^2$) at different concentrations of NaNO_3 (Table 1, nr. 2). It is interesting to note that the system is approximately, with the same range of pH and loading, as Hayes et al.(25).

Based on the modeling results, we have calculated the expected contribution of outersphere complexes as function of pH for 0.02 mM and 1 mM SeO_4 and SO_4 (Fig.6). The concentration of 0.02 mM corresponds to the experimental conditions in Hug (1) and Peak et al.(3) and the concentration of 1 mM corresponds to Wijnja and Schultess (2). The distribution for selenate is different from sulfate, due to a slight difference in the charge distribution of the innersphere complexes for both anions. The more significant appearance of outersphere complexes for sulfate at relatively low concentrations is in line with the measurements of Peak et al. (3). The effect that the relative amount of the outersphere sulfate increases with decreasing ionic strength as found by spectroscopy (3), is however not supported by the model using the determined model parameters. A quantification of the spectroscopic results on selenate and sulfate may therefore be valuable to improve the relation between the model parameters and the surface speciation.

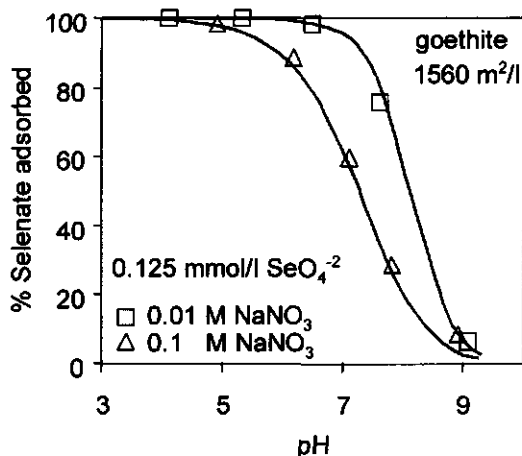


Fig. 6. Calculated distribution of outersphere complex (Table 1, nr. 2 and 4) across pH range at an equilibrium concentration of 0.02 mM and 1 mM selenate or sulfate (Hug (1) and Peak et al. (3) used 0.02 mM SO_4 while Wijnja and Schulthess used 1 mM) in 0.01 M NaNO_3 .

Conclusions

The adsorption behavior of selenate and of sulfate on goethite is very similar. Spectroscopy suggests the presence of outersphere complexes at high pH and innersphere monodentate complexation at low pH. This behavior results from a different charge distribution of both complexes in the interface. The various aspects of adsorption can be modeled using the surface speciation and coordination that is in line with spectroscopic results. The quality of the description of the data is not sensitive for the introduction of an outersphere species. The charge distribution calculated on the basis of macroscopic adsorption data (adsorption isotherms and proton-ion titrations) for the monodentate innersphere complex is for selenate approximately identical, and for sulfate in the same range, as the charge distribution calculated using an equal distribution of inner- and outersphere complexes at pH 6, as found by spectroscopy, as a criterion.

Acknowledgements

The authors thank Th. A. Vens for producing the goethite and for his contribution to the experiments. We also thank A. J. Korteweg from the Department of Biomolecular Sciences (Laboratory of Physical Chemistry and Colloid Science) for the BET analysis. Dr. H. Wijnja is acknowledged for sharing his spectroscopy information.

INNER- AND OUTERSPHERE ADSORPTION

References

- Hug, S. J. (1997) In Situ Fourier Transform Infrared Measurements of sulfate Adsorption on hematite in aqueous solutions. *J. Colloid Interface Sci.* **188**, 415-422.
- Wijnja, H. and Schulthess, C. P. (2000) Vibrational spectroscopy study of selenate and sulfate adsorption mechanisms on Fe and Al(hydr)oxide surfaces. *J. Colloid Interface Sci.* **229**, 289-297.
- Peak, D., Ford, R. G., and Sparks, D. L. (1999) An in situ ATR-FTIR investigation of sulfate bonding mechanisms on goethite. *J. Colloid Interface Sci.* **218**, 289-299.
- Rietra, R. P. J. J., Hiemstra, T., and van Riemsdijk, W. H. (1999) Sulfate adsorption on goethite. *J. Colloid Interface Sci.* **218**, 511-521.
- Rietra, R. P. J. J., Hiemstra, T., and van Riemsdijk, W. H., (1999) The relation between molecular structure and ion adsorption behavior on variable charged minerals *Geochim. Cosmochim. Acta.* **63**, 3009-3015.
- Davis, J. A., and Leckie, J. O. (1980) Surface ionization and complexation at the oxide/water interface. 3 adsorption of anions. *J. Colloid Interface Sci.* **74**, 32-43.
- Ryden, J. C., Syers, J. K., and Tillman, R. W. (1987) Inorganic anion sorption and interactions with phosphate sorption by hydrous ferric oxide gel. *J. Soil Sci.* **38**, 211-217.
- Yamaguchi, N. U., Okazaki, M., and Hashitani, T. (1999) Volume changes due to SO_4^{2-} , SeO_4^{2-} , and H_2PO_4^- adsorption on amorphous iron(III) hydroxide in an aqueous suspension. *J. Colloid Interface Sci.* **209**, 386-391.
- Zhang, P. C., and Sparks, D. L. (1990) Kinetics and mechanisms of sulfate adsorption/desorption on goethite using pressure-jump relaxation *Soil Sci. Soc. Am. J.* **54**, 1266-1273.
- Zhang, P. C., and Sparks, D. L. (1990) Kinetics of selenate and selenite adsorption/desorption at the goethite/water interface *Environ. Sci. Technol.* **24**(12) 1848-1856.
- Wu C., Lin C., and Lo S. (1999) Kinetics of sulfate and selenate adsorption/desorption onto $\gamma\text{-Al}_2\text{O}_3$ by pressure-jump technique. *J. Environ. Sci. Health A34*(3), 605-624.
- Hayes K. F., Roe A. L., Brown G. E., Hodgens K. O., Leckie J. O., and Parks G. A. (1987) In-situ x-ray absorption study of surface complexes: selenium oxyanions on $\alpha\text{-FeOOH}$. *Science* **238**, 783-786.
- Manceau, A. and Charlet, L. (1994) The mechanism of selenate adsorption on goethite and hydrous ferric oxide. *J. Colloid Interface Sci.* **168**, 87-93.
- Hiemstra, T., and van Riemsdijk, W. H. (1996) A surface structural approach to ion adsorption: the charge distribution (CD) model. *J. Colloid Interface Sci.* **179**, 488-508.
- Hiemstra, T., and van Riemsdijk, W. H. (1999) Surface structural ion adsorption modeling of competitive binding of oxyanions by metal (hydr)oxides *J. Colloid Interface Sci.* **210**, 182-193.
- Davis, J. A., James, R., Leckie, J. O. (1978) Surface ionization and complexation at the oxide/water interface. I Computation of electrical double layer properties in simple electrolytes. *J. Colloid Interface Sci.* **63**, 480-499 (1978).
- Rietra, P. J. J. J., Hiemstra, T. and van Riemsdijk, W. H. (2000) Electrolyte anion affinity and its effect on oxyanion adsorption on goethite. *J. Colloid Interface Sci.* **229**, 199-206.
- Hiemstra, T., de Wit, J. C. M., van Riemsdijk, W. H. (1989) Multisite proton adsorption modeling at the solid/solution interface of (hydr)oxides: a new approach. II Application to various important (hydr)oxides *J. Colloid Interface Sci.* **133**, 105-117.
- Geelhoed, J. S., Hiemstra, T., and van Riemsdijk, W. H., (1997) Phosphate and sulfate adsorption on goethite: Single anion and competitive adsorption *Geochim. Cosmochim. Acta* **61**, 2389-2396.
- Bargar, J.R., Brown, G.E. Jr. and Parks, G.A. (1997) Surface complexation of Pb(II) at the oxide-water interfaces: II. XAFS and bond-valence determination of mononuclear and polynuclear Pb(II) sorption products on iron oxides. *Geochim. Cosmochim. Acta* **61**, 2639-2652.
- Keizer, M. G. and van Riemsdijk, W. H. "ECOSAT: technical report of the department soil science and plant nutrition" Wageningen Agricultural University, Wageningen, 1998.

21. Perona, M. J. and Leckie, J. O. (1985) Proton stoichiometry for the adsorption of cations on oxide surfaces *J. Colloid Interface Sci.* **106**, 65-69.
22. Van Geen, A., Robertson, A. P., Leckie, J. O. (1994) Complexation of carbonate species at the goethite surface: implications for adsorption of metal ions in natural waters. *Geochim. Cosmochim. Acta* **58**, 2073-2086.
23. Filius J. D., Hiemstra T., and Van Riemsdijk W. H. (1998) Adsorption of small weak organic acids on goethite: modeling of mechanisms *J. Colloid Interface Sci.* **195**, 368-380.
24. Kinniburgh, D. G. "Fit: technical Report WD/93/23", British Geological Survey, Keyworth, 1993.
25. Hayes, K. F., Papelis, C., and Leckie, J. O. (1988) Modeling ionic strength on anion adsorption at hydrous oxide/solution interfaces. *J. Colloid Interface. Sci.* **125**, 717-726.
26. Sugimoto, T., and Wang, Y., (1998) Mechanism of the shape and structure control of monodispersed α -Fe₂O₃ particles by sulfate ions *J. Colloid Interface Sci.* **207**, 137-149.
27. Venema P., Hiemstra T., and Van Riemsdijk W. H. (1996) Multi site adsorption of cadmium on goethite. *J. Colloid Interface Sci.* **183**, 515-527.
28. Dzombak D. A. and Morel F. M. M. "Surface complexation modeling: hydrous ferric oxide", Wiley, NY, 1990.
29. Su, C. and Suarez, D.L., *Soil Sci. Soc. Am. J.* **64**, 101 (2000).

Appendix

Table A1. Surface equilibrium equations as used in the Basic Stern model. The adsorbed -2 charge of selenate and sulfate ($z_0+z_1 = -2$) is distributed across the surface plane (with potential ψ_0) and the outermost electrostatic plane (with potential ψ_1). Note that the adsorption equilibria of the anions are written with the protonated surface groups FeOH^{+0.5} and Fe₃OH^{+0.5}.

Equilibrium	ln K _i
1 (FeOH ₂ ^{+0.5})=K _i (FeOH ^{-0.5})(H ⁺)	ln K _H - $\psi_0 F / (RT)$
2 (Fe ₃ OH ^{+0.5})=K _i (Fe ₃ O ^{-0.5})(H ⁺)	ln K _H - $\psi_0 F / (RT)$
3 (FeOH ^{-0.5} -Na ⁺)=K _i (FeOH ^{-0.5})(Na ⁺)	ln K _{Na} - $\psi_1 F / (RT)$
4 (Fe ₃ O ^{-0.5} -Na ⁺)=K _i (Fe ₃ O ^{-0.5})(Na ⁺)	ln K _{Na} - $\psi_1 F / (RT)$
5 (FeOH ₂ ^{+0.5} --NO ₃ ⁻)=K _i (FeOH ₂ ^{+0.5})(NO ₃ ⁻)	ln K _{NO3} + $\psi_1 F / (RT)$
6 (Fe ₃ OH ^{+0.5} --NO ₃ ⁻)=K _i (Fe ₃ OH ^{+0.5})(NO ₃ ⁻)	ln K _{NO3} + $\psi_1 F / (RT)$
7 (FeOH ₂ ^{+0.5+z0} --SeO ₄ ^{z1})=K _i (FeOH ₂ ^{+0.5})(SeO ₄ ^{z2})	ln K _{Se} ^{outer} - ($z_0\psi_0 + z_1\psi_1$)F/(RT)
8 (FeO ^{+0.5+z0} SeO ₃ ^{z1})=K _i (FeOH ₂ ^{+0.5})(SeO ₄ ^{z2})	ln K _{Se} ^{inner} - ($z_0\psi_0 + z_1\psi_1$)F/(RT)
9 (FeOH ₂ ^{+0.5+z0} --SO ₄ ^{z1})=K _i (FeOH ₂ ^{+0.5})(SO ₄ ^{z2})	ln K _S ^{outer} - ($z_0\psi_0 + z_1\psi_1$)F/(RT)
10 (FeO ^{+0.5+z0} SO ₃ ^{z1})=K _i (FeOH ₂ ^{+0.5})(SO ₄ ^{z2})	ln K _S ^{inner} - ($z_0\psi_0 + z_1\psi_1$)F/(RT)

Table A2. Formation constants of species in solution (I=0).

equilibrium	Log K ⁰
1 (H ⁺)(SeO ₄ ^{z2}) <=> (HSeO ₄)	1.906
2 (H ⁺)(SO ₄ ^{z2}) <=> (HSO ₄ ⁻)	1.98
3 (Na ⁺)(SO ₄ ^{z2}) <=> (NaSO ₄ ⁻)	0.7
4 (H ⁺)(OH ⁻) <=> (H ₂ O)	-14.0

Interaction between calcium and phosphate adsorption on goethite

Abstract

Quantitatively, little is known about the ion interaction processes that are responsible for the binding of phosphate in soil, water and sediment, which determine the bioavailability and mobility of phosphate. Studies have shown that metal hydroxides are often responsible for the binding of PO_4 in soils and sediments but the binding behavior of PO_4 in these systems often differs significantly from adsorption studies on metal hydroxides in laboratory. The interaction between PO_4 and Ca adsorption was studied on goethite because Ca can influence the PO_4 adsorption equilibria. Since adsorption interactions are very difficult to discriminate from precipitation reactions, conditions were chosen to prevent precipitation of Ca- PO_4 solids. Adsorption experiments of PO_4 and Ca, individually and in combination, show a strong interaction between adsorbed Ca and PO_4 on goethite for conditions below the saturation index of apatite. It is shown that it is possible to predict the adsorption and interaction of PO_4 and Ca on electrostatic arguments using the model parameter values derived from the single-ion systems, and without invoking ternary complex formation or precipitation. The model enables the prediction of the Ca- PO_4 interaction for environmentally relevant calcium and phosphate concentrations.

This chapter has been accepted.

**René P. J. J. Rietra, Tjisse Hiemstra, Willem H. van Riemsdijk
Environmental Science and Technology**

Introduction

It is well known that cations can affect the behavior of anions in environmental systems vice versa (1). The most important cation in environmental systems from a quantitative point of view is often Ca. Calcium influences the behavior of important anions, such as phosphate, in a complex manner since both precipitation and adsorption equilibria are potentially important. Interactions between calcium and phosphate have been studied in soil and aquatic systems (2-10), for minerals such as calcite, goethite, aluminum oxide, and MnO_2 (11-16), which all serve as model compounds for environmental systems. Models for ion adsorption on variable charge minerals have been developed in the last twenty years but are seldom used to fully describe the adsorption equilibria of environmentally important systems, although the binding in the environment of an important oxyanion like phosphate is strongly related to these metal hydroxides. The use of variable charge models is hampered because some environmentally important equilibria are quantitatively less well known, such as the interaction of organic matter with oxides and the interaction of common environmental ions such as calcium, magnesium, carbonate and silicic acid with environmentally relevant oxyanions and heavy metals.

In the present study, we will describe the adsorption and interaction of phosphate and calcium with goethite. Previous studies were not fully successful due to the problematic distinction between adsorption and precipitation reactions. In some model systems involving goethite, the high concentration of Ca (0.01 M) presumably caused precipitation of octa-calcium-phosphate (11, 15). In the present study the total concentrations of PO_4 , Ca and goethite were chosen to give equilibrium concentrations below the solubility equilibrium of octa-calcium-phosphate, and even below apatite, which is the most stable form of calcium-phosphates. Since apatite will only be formed in solutions that are supersaturated for a considerable time with respect to octa-calcium-phosphate (17), we believe that in the systems used in this study no precipitation of phosphate and Ca occurred in solution. We do not rule out that unknown surface-precipitation mechanisms can exist or occur, but we believe that surface-precipitation is less probable if the interaction on goethite between PO_4 and Ca in a binary system can be modeled on the basis of adsorption equilibria from single-sorbate systems containing PO_4 and Ca alone.

In this study we will quantify and model the Ca and PO_4 adsorption on goethite, and the interaction between both adsorbed ions. We will use the model parameters derived from the single-ion systems of Ca and PO_4 to predict the adsorption in the mixed calcium-phosphate systems. Specifically, we have studied PO_4 adsorption as a function of pH, from pH 4 to pH 11, with and without Ca, at a total PO_4 concentration of 0.5 mmol/l, and at three goethite concentrations. The Ca adsorption without PO_4 was also studied as a function of pH at two Ca concentrations. The corresponding proton release was also measured. In addition, we have studied the Ca-goethite interaction by acid-base titrations in $Ca(NO_3)_2$.

Many surface complexation models (11,15,18-20) have been used for the description of PO_4 adsorption using surface species that are not observed by

spectroscopy (21,22). An important advantage of using models that do account for structural information with regard to surface complexes derived from spectroscopy, is the possibility to validate the adsorption models using spectroscopically derived surface speciation and coordination rather than simply by a satisfactory description of macroscopic data. The CD-MUSIC model has been developed as a framework to describe ion adsorption by combining available information on structure and the type of surface complexes with the macroscopic adsorption behavior (22-25). The challenge in this study is to measure and model the effects of co-adsorbing Ca on the PO₄ adsorption by goethite. We will use the CD-MUSIC model as it has been used previously to model PO₄ adsorption (22) and will compare it with spectroscopically determined PO₄ speciation on goethite (21). Spectroscopic data on the coordination of adsorbed Ca are not available. However, the coordination of adsorbed strontium (Sr) (26-28), which has a rather similar adsorption behavior to Ca on iron hydroxides (18, 29, 30), has spectroscopically been determined. Analysis of adsorbed Sr with EXAFS suggests formation of outersphere surface complexes across a range of pH values (26-28) with some innersphere Sr present at very high pH (10.2) values (27).

Materials and Methods

Synthesis and characterisation

All chemicals (Merck p.a.) were stored in polyethylene bottles and all experiments were performed in plastic vessels to avoid silica contamination. The water used throughout the experiments was always ultrapure ($\approx 18 \mu\text{S}/\text{cm}$). A goethite suspension was prepared according to Hiemstra et al. (31). The goethite used here was from the same batch that was characterized earlier (32-34). The BET(N₂) specific surface area of the goethite was 96.4 m²/g. The pristine point of zero charge (PPZC) of 9.25 has been determined from acid-base titrations in NaNO₃ (34).

Adsorption edges

As will be explained further below, adsorption experiments were performed to study Ca and PO₄ adsorption individually, and Ca and PO₄ in combination, under conditions in which the formation of calcium phosphate minerals, PO₄ desorption, and CO₂ contamination are minimized.

At high pH values, CO₂ might influence the adsorption behavior and therefore CO₂ was excluded explicitly. To do so, adsorption was studied in small 20-ml low-density polyethylene vessels, often used as scintillation vessels. These vessels have proved to be gas tight, since solutions could be held at pH 8 for a period of two months without losing the purple color of added phenolphthalein as an indicator. After opening these vessels to the air, the solutions lost their purple color quickly showing that they were not significantly contaminated by CO₂ during storage.

In a large vessel, CO₂ free stock suspensions of goethite were prepared by purging at pH 6 moist N₂(g) through the suspension for several hours using a CO₂-

gas trap. Depending on the type of experiment, base (0.1 M NaOH), PO₄ solution (0.01 M NaH₂PO₄) or Ca solution (0.01 M Ca(NO₃)₂) was added to stock suspensions. Prior to the addition of a certain stock suspension to the small vessels, nanopure water and different volumes (0-0.2 ml) of 0.1 M HNO₃ were added to the small vessels in order to obtain final pH values within the range of pH 4 to 11. Also Ca was added to the small vessels, in case of experiments with both Ca and PO₄, as will be explained below. Aliquots from specific stock goethite suspensions were taken with a 5-ml syringe and pumped into the small 20-ml vessels under N₂(g) to prevent CO₂ contamination. The stock suspensions were prepared in such manner that after mixing of the suspension with PO₄, the pH had only to be adjusted with acid in the 20 ml vessels. This was done to prevent hysteresis, which could arise from slow desorption of PO₄, since lowering of the pH leads to more adsorption, as will be shown in this study. Precipitation of calcium phosphate was prevented in experiments with both Ca and PO₄, by adding a stock suspension that had been pre-equilibrated with PO₄ for at least two hours, to the small vessels, containing Ca solution and acid, as described earlier.

After a reaction time of 24 hours in an end-over-end shaker, the small vessels were centrifuged at 2000 rpm. The samples with only PO₄ had to be centrifuged at 20,000 rpm. All supernatants were acidified after collection. PO₄ concentrations were determined using the molybdate blue method and Ca concentrations were determined using AAS (Varian). The pH was determined in the clear solution above the centrifuged goethite, while under N₂(g).

Acid-base titrations in Ca(NO₃)₂

For the acid-base titrations in calcium nitrate solutions, a salt-free stock suspension of goethite at pH 5.5 was prepared as described earlier (35). Details of the apparatus and preparation of the CO₂-free base have been discussed previously (24, 36). The suspension was continuously purged with N₂ to remove CO₂. From this salt- and CO₂-free stock suspension, sub-samples of approximately 60 ml were titrated into vessels, in which a N₂ atmosphere was maintained. Acid-base titrations of goethite suspensions (11g/l) in Ca(NO₃)₂ were performed at three Ca(NO₃)₂ concentrations, i.e. 1.7, 6.7, and 33 mmol/l. The same salt-free goethite stock suspension was used for acid-base titrations in NaNO₃ to characterize the titration behavior and the PZC of the goethite (35). This procedure allows the determination of the proton adsorption of goethite in equilibrium with Ca(NO₃)₂ relative to the proton adsorption in NaNO₃, because the goethite was taken from the same stock suspension as used for the titrations in NaNO₃.

Model calculations

The adsorption of Ca and PO₄ is modeled with the Charge Distribution and Multi-Site Complexation (CD-MUSIC) model (23,38). This model has previously been applied to describe the adsorption of PO₄ (22). The Basic Stern Model (22, 37) is used for the compact part of the electrostatic double layer. An important feature of

the CD-MUSIC model is the notion that innersphere surface complexes should not be treated as point charges at the scale of the interface. Innersphere complexes of ions are assumed to have a spatial distribution of charge. A fraction of the charge is attributed to the surface since only a fraction of the ligands of the adsorbing polyvalent ions are involved in ligand exchange with the surface. The remaining part of the charge is located at a certain distance of the surface.

As a first approach, the charge attribution to the electrostatic planes can be estimated for known surface structures of adsorbed ions by using the Pauling bond valence concept (23, 25). The charge distribution across the electrostatic planes can be expressed in the charge distribution value, i.e. the fraction f of the central ion (P^{5+} , in case of phosphate; Ca^{2+} , in case of calcium) that is attributed to the surface plane. As identified by spectroscopy (21), PO_4 predominantly forms a bidentate surface complex, which protonates at low pH and high surface loading. At high pH monodentate complexes are formed. Phosphate adsorption modeling is based on the spectroscopically identified coordination and speciation (22). In case of a monodentate PO_4 complex, the charge distribution value (f) is estimated to be 0.25 since only one of the four ligands is located at the surface. In case of a bidentate PO_4 complex, f is estimated to be 0.5.

Calcium adsorption modeling is based on the outersphere coordination of strontium (26-28), with possibly an innersphere complex at $pH > 10$ (28). In the simplest approach, all charge of the Ca^{2+} outersphere complex is assumed to be located at the outermost part of the Stern layer, similar to electrolyte ion complexes (35). However, a small charge attribution of the outersphere complex to the surface plane of approximately 0.1 or 0.2 valence unit (v.u.) is possible if strong hydrogen bonds form between the surface groups and the outersphere complex (39). For the innersphere bidentate complex of Ca, f is predicted to be 0.33 if adsorbed (hexa-coordinated) Ca^{2+} has two ligands in common with the surface plane.

The model parameters to describe the basic charging behavior of goethite, i.e. site densities, capacitance of the Stern layer and affinity constants of ion pairs, have been reported previously (34,35), as has a complete description of the CD-MUSIC model (22). Calculations were carried out with Ecosat, a computer code for the calculation of chemical equilibria (40). The relevant affinity constants describing the solution equilibria were taken from Lindsay (9), and are identical to the constants in MINTEQA2 (51), except the constant for $NaHPO_4^-$ which is taken from (51), as used previously (22). The Davies equation (constant is 0.2) has been used to calculate the ion activity coefficients at 25°C. The adsorption reactions for PO_4 are as defined in (22). The parameter values have been optimized for our adsorption data using the computer code FIT from Kinniburgh (41), which has recently been incorporated in Ecosat.

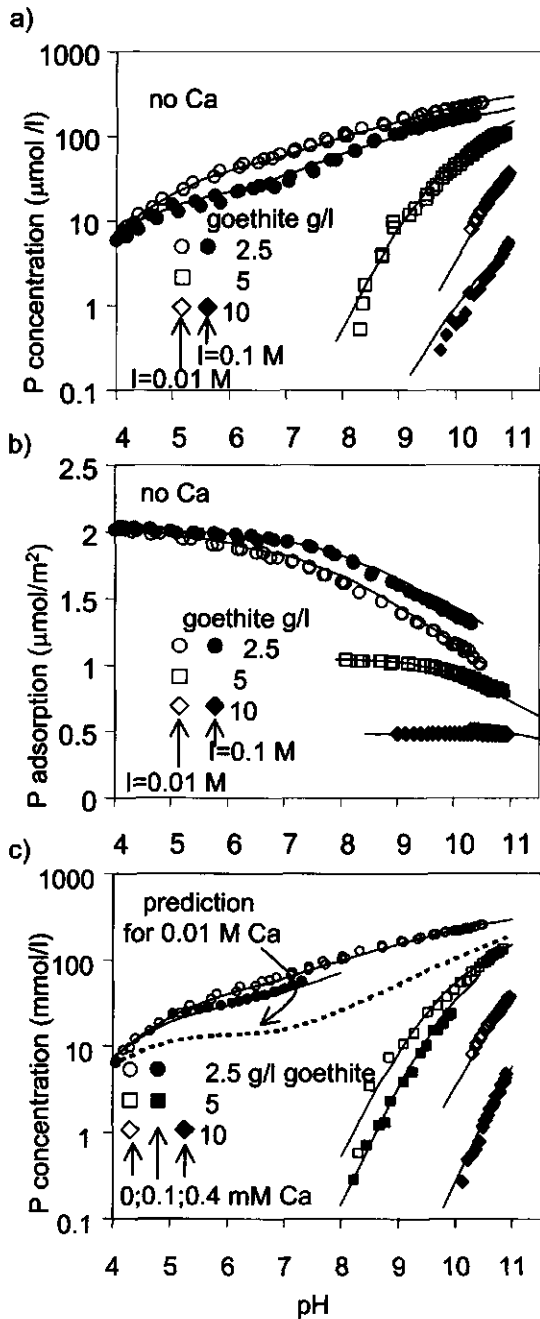


Fig 1. Experimental and modeled effect of pH, Ca, goethite- or salt concentration (NaNO₃) on: PO₄ concentration (Fig. 1a,c) and corresponding PO₄ adsorption (Fig. 1b) at a total PO₄ concentration for all systems of 0.5 mmol/l. For the model calculations options 1 of Table 1 was used. The dashed line in Fig. 1c gives the predicted PO₄ concentration in the presence of 0.01 M Ca solution (2.5 g/l goethite).

Results and Discussion

Before discussing the Ca-PO₄ interaction, we first focus on the individually measured binding of PO₄ and of Ca in single-ion systems.

Adsorption in the PO₄ monocomponent system

In Fig. 1 the adsorption of PO₄ is shown as a function of pH and ionic strength level for various solid/solution ratios, leading to a variable degree of PO₄ loading. The PO₄ adsorption data can be described very accurately using two innersphere PO₄ complexes, i.e. a bidentate and a protonated bidentate (Table 1, option I). The calculated bidentate surface speciation corresponds to the results found by CIR-FTIR spectroscopy (21).

At high pH, some monodentate PO₄ surface complex formation (10% ± 5% at pH=8) has been detected with CIR-FTIR (21). In our model, this minor complex is not necessary for a correct description of our PO₄ adsorption data. It shows that the adsorption characteristic of this species (pH dependency) is not different enough from the bidentate complex to be noticed by fitting the data, in particular as the species is present in a minor amount. However, it is possible to incorporate the monodentate species in the description, fitting the adsorption data under the restriction of a quantitatively correct prediction of the IR spectroscopy results (Table 1, PO₄ option II). Modeling the data with or without monodentate hardly affects the derived values for the model parameters of the dominant bidentate complexes and the quality of the data description is approximately identical for both options. A point of concern is the low CD value for the monodentate complex, obtained by objective fitting. A Pauling Bond valence analysis shows that the low CD value is much better explained assuming monodentate formation with doubly coordinated groups than with singly coordinated groups. In case of the formation of Fe₂O-PO₃, we will get a zero charge at the common ligand, which is considered as a stable situation (53). We can not rule out the formation of such a monodentate surface complex, since this complex has been observed with EXAFS at very small Fe hydroxide clusters at the lowest levels of PO₄ and the highest degree of neutralization of the Fe clusters (52).

Table 1. Surface complexes of phosphate^a and calcium on goethite and the charge distribution of the surface complexes across the two electrostatic planes in the Basic Stern model: the surface- (0-plane), and the outermost plane (1-plane) at the head end of the diffuse double layer. For the model curves in Fig. 1-3 option I is used

	Surface complex	Log K	FeOH ^{0.5}	H	PO ₄	Ca	f	z ₀	z ₁	
P	I	Fe ₂ O ₂ PO ₂	29.42	2	2	1	0	0.48	0.39	-1.39
		Fe ₂ O ₂ PO ₂	35.65	2	3	1	0	0.58	0.90	-0.90
	II	Fe ₂ O ₂ PO ₂	29.42	2	2	1	0	0.46	0.31	-1.31
		Fe ₂ O ₂ PO ₂ H	35.75	2	3	1	0	0.58	0.91	-0.91
		FeOPO ₃	19.68	1	1	1	0	0.20	0 ¹	-2 ¹
Ca	I	FeOHCa	3.55	1	0	0	1	0.1	0.2	1.8
		(FeOH) ₂ Ca	2.50	2	0	0	1	0.33	0.66 ^b	1.33 ^b
	II	FeOH-Ca	3.70	1	0	0	1	0	0 ^b	2 ^b

^a The charge attributions for phosphate are related to the charge distribution of phosphate, protonation (H) of the phosphate, and the to surface component FeOH^{0.5} according to Hiemstra and van Riemsdijk (22), where $z_0 = -2(H) + 5f$, f is the fraction of charge from the central P directed to the surface plane, $z_1 = -4(O) + 5(1-f)$ in case of Fe₂O₂PO₂, and $z_1 = -4(O) + 5(1-f) + 1(H)$ in case of Fe₂O₂PO₂H. In the case of FeOPO₃: $z_0 = -1(H) + 5f$, and $z_1 = -6(O) + 5(1-f)$.

^b charge distribution of complexes that have been set, all other charge distributions and log K's have been calculated on the basis of residual square of sums (RSS) where $RSS = \sum (c^{data} - c^{calc})^2$, and c is the concentration in mol/l.

Adsorption in the Ca monocomponent system

The Ca adsorption of single-ion systems is presented in Fig.2a,b. It is important to note that the figure contains, in addition to the Ca adsorption data measured in the single-Ca systems (spheres), also data referring to the mixed Ca-PO₄ systems (squares and diamonds), to be discussed later. Lets focus on the single-Ca systems (spheres). The adsorption of Ca increases with pH and is relatively weak compared to many heavy metal cations. The adsorption is limited to pH values near or above the PZC of goethite. The influence of the change of the ionic strength is small (open vs. solid spheres). The effect of NaNO₃ changes at pH values of near the PZC. Similar results have been published earlier for a differently produced goethite (43).

If Ca adsorbs, protons are released. The proton exchange, corresponding to the Ca data of Fig. 2a&b (spheres), is presented in Fig.3b. The proton release is usually not published together with ion adsorption data, but can be equally valuable as ion adsorption data (44) for the determination of the modeling parameters.

Figure 3a characterizes the proton-calcium interaction at low Ca concentrations. This interaction can also be studied in the higher concentration range using acid-based titrations of goethite in Ca(NO₃)₂ solutions (Fig.3b). The results in Fig. 3b are given relative to the acid-base behavior of goethite in NaNO₃ (dashed lines). The data show a significant effect of Ca on the acid-base behavior of goethite over the whole experimental pH range, but it is most strongly above pH 7. This demonstrates that although the interaction between Ca and goethite is weak, the overall interaction can be significant under conditions relevant for the environment. Similar data have been determined earlier for other preparations of goethite and other oxides and recently also as a function of temperature (42).

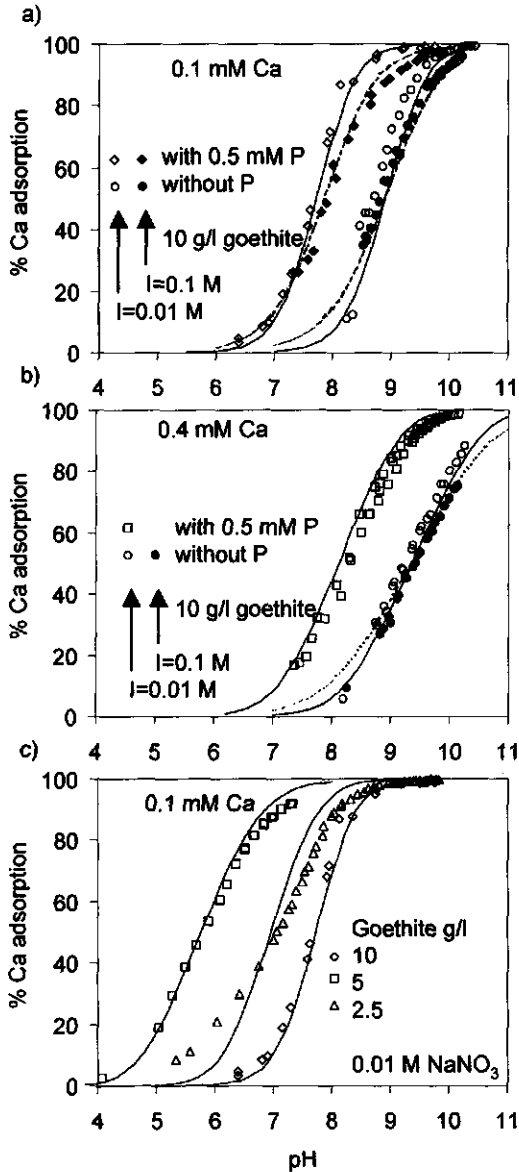


Fig. 2. Calcium adsorption onto goethite as a function of pH for systems with and without PO_4 . The influence of the ionic strength (open symbols 0.01 M, closed symbols 0.1 M NaNO_3) is illustrated for systems with 0.1 mM Ca (Fig.2a) and 0.4 mM Ca (Fig.2b) in the absence or presence (0.5 mM) of PO_4 . The increase in Ca adsorption with a decreasing goethite concentration is given in Fig. 2c (0.5 mM P). The solid lines denote the model calculations for 0.01 M NaNO_3 , the dotted lines for 0.1 M NaNO_3 . For the model calculations option I from Table 1 was used.

Table 2. Optimised affinity constants for a series of chosen Charge Distribution coefficients of adsorbed calcium for the description of the proton titration in $\text{Ca}(\text{NO}_3)_2$ (Fig.2), the calcium adsorption (Fig.3) and corresponding H consumption (Fig.4), assuming one surface species for calcium*. The best-fit residual sum of squares are italicised for individual data sets and are found for charge distributions where $z_0 = 0.2$ or 0.3 and $z_1 = 1.8$ or 1.7 (indicated as bold numbers). The combination of $\log K^m = 3.55$ and charge distribution coefficients $z_0 = 0.2$ and $z_1 = 1.8$ is given as option I for calcium in Table 1.

z_0	z_1	Titration		Adsorption edge		Δ H adsorption	
		H-adsorption		Ca concentration		Δ H adsorption	
		(Fig. 2)		(Fig. 3)		(Fig. 4)	
		Log K	RSS	log K	RSS	Log K	RSS
0.5	1.5	2.5	0.296	3.36	0.0138	3.15	0.172
0.4	1.6	2.75	0.141	3.43	0.0093	3.25	0.155
0.3	1.7	3.0	<i>0.103</i>	3.50	<i>0.0073</i>	3.35	0.146
0.2	1.8	3.3	0.168	3.58	0.0084	3.45	<i>0.143</i>
0.1	1.9	3.65	0.375	3.66	0.0124	3.60	0.152
0.0	2.0	3.9	0.722	3.74	0.0197	3.80	0.169

* data have been fitted on the basis of residual sum of squares (RSS). In case of the H adsorption (Figure 2) and (Figure 4): $\text{RSS} = \sum (\Gamma^{\text{data}} - \Gamma^{\text{calc}})^2$, where Γ is the proton consumption in $\mu\text{mol}/\text{m}^2$, and in case of the calcium adsorption (Figure 3): $\text{RSS} = \sum (c^{\text{data}} - c^{\text{calc}})^2$, where c is the calcium concentration in mmol/l .

Adsorption in the PO_4 -Ca system

The Ca adsorption in the mixed systems is given in Fig.2. The adsorption of Ca in the presence of PO_4 is much higher compared to the same systems without PO_4 . In Fig. 1c the PO_4 behavior is given which corresponds to the Ca- PO_4 systems of Fig. 2. The open spheres in Fig.2c refer to an additional Ca- PO_4 system. For reference, we present also the behavior of the same systems without the presence of Ca. The addition of Ca has its strongest influence on the PO_4 binding at high pH and this is due to the relatively strong binding of Ca at these high pH values. The PO_4 concentration at pH 10 decreases more than a factor ten by adding only 0.4 mM Ca.

The effect of the particle density in the Ca- PO_4 system has been studied separately (Fig. 1c&2c) and illustrates a remarkable point. One observes that more Ca is adsorbed when less goethite is present in the system. The stronger adsorption of Ca at lower goethite concentrations can be explained by the higher surface coverage of goethite with negatively charged PO_4 . The higher PO_4 loading results in a decrease of the repulsive potential. Even charge reversal may occur. This effect is much stronger than the decrease in reactive surface area. It clearly illustrates the dominance of electrostatics in regulating the cation and anion adsorption behavior. No effect of altering the order of addition of acid, Ca and PO_4 were found (not shown) which emphasizes that reversible processes control the sorption behavior. The calculated logarithmic saturation index for apatite, the most stable calcium-phosphate mineral, is at its maximum (-0.88) in the system with the highest pH, Ca and PO_4 amounts, i.e. no precipitation is expected.

As shown in Fig.2c, the Ca adsorption in Ca- PO_4 systems does not remain restricted to high pH values. It can also be found under acid conditions at a relatively high PO_4 loading created by adding the low amount of 2.5 g goethite/l

(Fig.2c). The effect is due to the reduction of the positive potential near the surface upon binding of negatively charged PO_4 ions. The induced reduction of the electrostatic repulsion allows more adsorption of Ca^{2+} .

Modelling Ca adsorption

The adsorption behavior of Ca was modeled for the various data sets. In a first approach, we have assumed the presence of only one type of surface complex. The difference in ionic strength (open versus solid symbols) leads to a common intersection point (CIP) at each Ca level for the Ca data in Fig. 2a&b and Fig. 3b. The effect of NaNO_3 is different on either side of the CIP, but both effects are explained by the decrease of electrostatics at high ionic strength, being either repulsive (low pH) or attractive (high pH).

For each data set we have optimized the affinity constant ($\log K$) for different charge distributions (see Table 2). For each chosen CD value, we have given the residual sum of squares (RSS). The results in Table 2 show that approximately the same charge distribution for adsorbed Ca is obtained using the three different kinds of data sets (Fig 2a&b, Fig. 3a and Fig 3b). The lowest RSS values were found with the charge attribution to the surface (z_0) of 0.2 or 0.3 v.u. The majority of the Ca^{2+} charge remains in the 1-plane ($z_1=1.7$ or 1.8 v.u.). No systematic difference in parameters was found between the modeling of the monocomponent and the multicomponent systems. This indicates that the behavior of Ca can be described well based on the combination of the affinity constants and charge distributions as obtained for the pure Ca or PO_4 systems. All model lines are calculated using the presence of only one surface species for Ca (Option I of Table 1).

The fitted value of z_0 and z_1 can be interpreted as a compromise between a charge distribution of an outersphere complex with all charge in the 1-plane ($z_1=+2$) and a bidentate innersphere complex of hexa-coordinated Ca ($z_1=1.33$). Such complexes have been suggested for Sr (26-28). The data of Figs. 1-3 can also be modeled assuming the presence of these two types of complexes. Using the above suggested charge distribution, the corresponding affinity constants for Ca have been determined by fitting. The results are given in Table 1 as option II. We found that introduction of two Ca complexes (option II) did not improve the quality of the fit significantly. In this case (option II in Table 1) the fraction of Ca innersphere complexes will increase with increasing pH but the outersphere complex is calculated to be dominant for all data. This effect can be understood based on electrostatics and thermodynamic consistency. The complex with the largest attribution to the surface (innersphere) will have the largest proton exchange (25, 45, 46), which will lead to the largest pH dependency for this species (25, 47). This implies that the innersphere species will ultimately become the predominant surface species at sufficiently high pH. This may be realistic since for Sr innersphere complex formation has been suggested for Sr at high pH (28), with outersphere complexes predominating at lower pH (26, 27). The opposite trend occurs for anions (48, 49). As follows from Fig. 1c and Fig. 2, the interaction between Ca and PO_4 is predicted satisfactorily with a set of constants that also describe the single-sorbate systems. It shows that the CD-MUSIC model gives adequate predictions for

adsorption behavior in the binary sorbate systems. Consequently, it is not necessary to assume the existence of ternary complexes of Ca and PO_4 or certain precipitation reactions to explain the interaction between Ca and PO_4 for the conditions of these experiments.

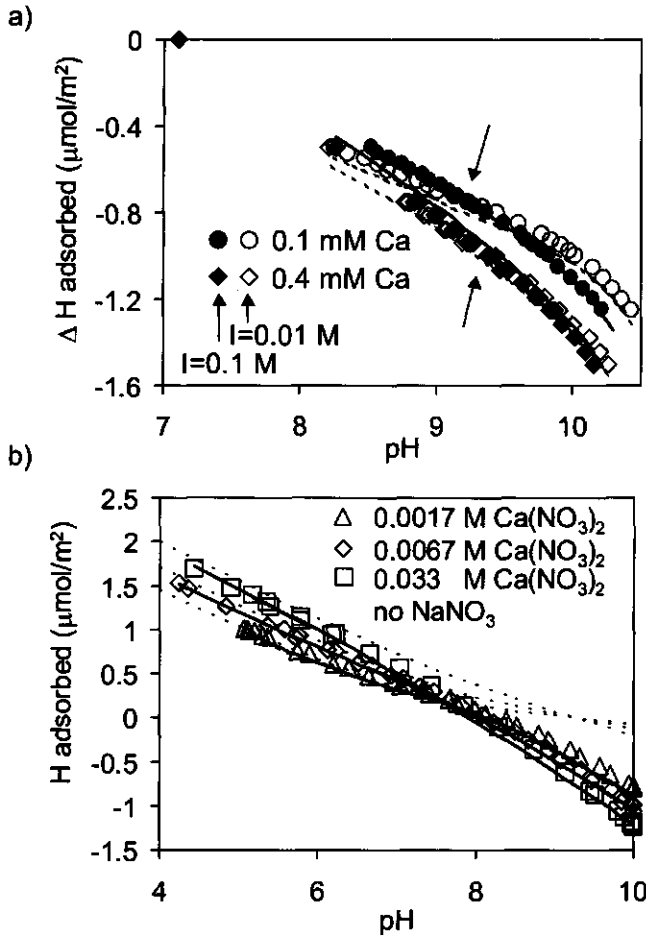


Fig 3. The proton consumption in the single-Ca goethite systems. In Fig 3a the proton adsorption in the Ca-goethite systems of Fig. 2a&b are given. The proton consumption has been determined relative to a data point at pH 7.1 where the experimental Ca adsorption is almost negligible. The data or curves in 0.01 M NaNO_3 and 0.1 M NaNO_3 are denoted respectively by open and solid symbols, or dotted and straight lines. The arrows point to the experimental CIP. In Fig 3b the proton adsorption is given at three concentrations of $\text{Ca}(\text{NO}_3)_2$. The proton adsorption is determined relative to the charge in NaNO_3 measured by the acid-base behavior of goethite in 0.005-0.02-0.1 M NaNO_3 from ref. 34 and represented here as dotted lines. For the model calculations option I from Table 1 was used.

Environmental Implications

In natural waters the Ca concentration ranges often from approximately less than 0.1 (fresh surface water) to above 10 mmol/l (sea water). The lower values correspond to the experimental conditions of our Ca-PO₄ experiments. We have shown that the Ca effect on PO₄ adsorption is very significant at high pH. In eutrophic surface waters these high pH values can be reached temporarily due to the photosynthesis process which removes the CO₂ component of HCO₃⁻, releasing OH⁻. If calcite is present, additional Ca²⁺ may be released, e.g. CaCO₃ → Ca²⁺ + 2 OH⁻ + CO₂. Both conditions (high pH and increased Ca concentrations) influence the binding of PO₄ to colloidal particles (Fig. 1c), which now can be quantified.

In soil systems, the Ca concentrations are often higher than the concentrations used in our Ca-PO₄ experiments. One may try to measure effects of Ca on PO₄ adsorption, as was done in the work of Barrow et al. (11) and Hawke et al. (15). It is however difficult to distinguish between adsorption and precipitation in such systems. The prediction of PO₄ adsorption by goethite in 0.01 M Ca(NO₃)₂ shows that adsorption is already effected above pH 4 (dashed line Fig. 1c).

The interaction of Ca and PO₄ may also influence the bioavailability of PO₄ in the rhizosphere of roots. Based on the mean Ca concentration in plants (mmol/kg) and corresponding transpiration coefficients (mm water/kg), one can calculate the mean required Ca concentration of the soil solution. This turns out to be approximately 0.1 mM. In general, the mean actual concentration is a factor 10-50 higher, leading to a supply of Ca with the influx of water in the root system which is higher than what can be taken up by the plant roots (50). This phenomenon results in an elevated Ca concentration in the rhizosphere (50). Based on the present study, we predict a strong suppression of the local PO₄ concentration of the soil solution in the rhizosphere and the corresponding flux towards the root surface due to increased PO₄ adsorption at elevated Ca concentrations. The bioavailability of phosphorous will be reduced, and most strongly at high pH.

Acknowledgements

The authors thank Mr. Th. A. Vens for producing the goethite and also thank Mr. A. J. Korteweg from the department of Biomolecular Sciences (Laboratory of Physical Chemistry and Colloid Science) for the BET analysis. We acknowledge the efforts of the reviewers to improve the paper.

References

1. Stumm, W. *Chemistry of the Solid-water interface*; Wiley: New York, 1992; 426 p.
2. Clark, J. S.; Peech, M. Influence of neutral salts on the phosphate ion concentration in soil solutions (1960) *Proc. Soil Sci. Soc. Am.*, 24, 7-17.
3. Barrow, N. J. (1972) Influence of solution concentration of calcium on the adsorption of phosphate, sulphate and molybdate. *Soil Sci* 113, 175-1980.
4. Smillie, G. W.; Curtin, D.; Syers, J. K. (1987) Influence of exchangeable calcium on phosphate retention by weakly acid soils. *Soil Sci. Soc. Am. J.* 51, 1169-1172.
5. Pierzynski, G. M.; Logan, T. J.; Traina, S. J. (1990) Phosphorus chemistry and mineralogy in excessively fertilized soils: solubility equilibria. *Soil Sci. Am. J.* 54, 1589-1595.

6. Lookman, R.; Geerts, H.; Grobet, P.; Merckx, R.; Vlassak, K. (1996). Phosphate speciation in excessively fertilized soil: a ^{31}P and ^{27}Al MAS NMR spectroscopy study. *Eur. J. Soil Sci.*, **47**, 125-130.
7. Castro, B.; Torrent, J. (1998) Phosphate sorption by calcareous vertisols and inceptisols as evaluated from extended P-sorption curves. *Eur. J. Soil Sci.* **49**, 661-667.
8. Tunesi, S.; Poggi, V.; Gessa, C. (1999) Phosphate adsorption and precipitation in calcareous soils: the role of calcium ions in solution and carbonate minerals. *Nutrient Cycling in Agrosystems*, **53**, 219-227.
9. Lindsay, W. L. *Chemical Equilibria in Soils*; Wiley-Interscience: New York, 1979; 347 p.
10. Stumm, W.; Morgan, J. J., *Aquatic Chemistry*, John Wiley & Sons: New York, 1996; 1022 p.
11. Barrow, N. J.; Bowden, J. W.; Posner, A. M.; Quirck, J. P. (1980) Describing the effects of electrolyte on adsorption of phosphate by a variable charge surface. *Aust. J. Soil Sci.*, **18**, 395-404.
12. Helyar, K. R.; Munns, D. N.; Burau, R. G. (1976) Adsorption of phosphate by gibbsite I effects of neutral chloride salts of calcium, magnesium, sodium, and potassium. *J. Soil Sci* **27**, 307-314.
13. Parfitt, R. L. (1979) The nature of the phosphate-goethite ($\alpha\text{-FeOOH}$) complex formed with $\text{Ca}(\text{H}_2\text{PO}_4)_2$ at different surface coverage. *Soil Sci. Soc. Am. J.*, **43**, 623-625.
14. House, W.A.; Donaldson, L. (1986) Adsorption and coprecipitation of phosphate on calcite. *J. Colloid Interface Sci.* **112**, 309-324.
15. Hawke, D.; Carpenter, P.D.; Hunter, K.A. (1989) Competitive adsorption of phosphate on goethite in marine electrolytes. *Environ. Sci. Tech.* **23**, 187-191.
16. Yao, W.; Millero, F. J. (1996) Adsorption of phosphate on manganese dioxide in seawater. *Environ. Sci. Technol.* **30**, 536-541.
17. Kemenade, van, M. J. J. M.; Bruyn, P. L. (1987) A kinetic study of precipitation from supersaturated calcium phosphate solutions. *J. Colloid Interface Sci.* **118**, 564-585.
18. Dzombak, D. A.; Morel, F. M. M. *Surface complexation modelling: hydrous ferric oxide*; John Wiley & Sons: New York, 1990; 393 p.
19. Sigg, L. and Stumm, W. (1981) The interaction of anions and weak acids with the hydrous goethite ($\alpha\text{-FeOOH}$) surface. *Colloid Surf*, **2**, 101-117.
20. Goldberg, S. and Sposito, G. (1984) A chemical model of phosphate adsorption by soils: I reference oxide minerals. *Soil Sci. Soc. Am. J.* **48**, 772-778.
21. Tejedor-Tejedor M. I. and Anderson M. A. (1990) Protonation of phosphate on the surface of goethite as studied by CIR-FTIR and electrophoretic mobility. *Langmuir* **6**, 602-611.
22. Hiemstra, T., and van Riemsdijk, W. H. (1996) A surface structural approach to ion adsorption: the charge distribution (CD) model. *J. Colloid Interface Sci.* **179**, 488-508.
23. Hiemstra, T., and van Riemsdijk, W. H. (1999) Surface structural ion adsorption modeling of competitive binding of oxyanions by metal (hydr)oxides. *J. Colloid Interface Sci.* **210**, 182-193.
24. Venema, P.; Hiemstra, T.; van Riemsdijk, W.H. (1996) Multisite adsorption of cadmium on goethite. *J. Colloid Interface Sci.* **183**, 515-527.
25. Rietra, R. P. J. J., Hiemstra, T., and van Riemsdijk, W. H., (1999) The relation between molecular structure and ion adsorption behavior on variable charged minerals. *Geochim. Cosmochim. Acta.* **63**, 3009-3015.
26. Sahai, N.; Carrol, S.A.; Roberts, S.; O'Day, P.A. (2000) X-ray Absorption spectroscopy of strontium(II) coordination. *J. Colloid Interface Sci.* **222**, 198-212.
27. Collins, C. R.; Sherman, D. M.; Ragnarsdóttir, K. V. (1998) The adsorption mechanism of Sr^{2+} on the surface of goethite. *Radiochim. Acta* **81**, 201-206.
28. Axe, L.; Bunker, G. B.; Anderson, P.R.; Tyson, T. A. (1998) An XAFS analysis of strontium at the hydrous ferric oxide surface. *J. Colloid Interface Sci.*, **199**, 44-52.
29. Kinniburgh, D. G.; Syers, J. K.; Jackson, M. L. (1975) Specific adsorption of trace amounts of calcium and strontium by hydrous oxides of iron and aluminium. *Soil Sci. Soc. Am. J.*, **39**, 464-470.
30. Breeuwsma, A.; Lyklema, J. (1971) Interfacial electrochemistry of haematite ($\alpha\text{-Fe}_2\text{O}_3$). *Discuss. Faraday Soc.* **52**, 324-333.

31. Hiemstra, T., de Wit, J. C. M., van Riemsdijk, W. H. (1989) Multisite proton adsorption modeling at the solid/solution interface of (hydr)oxides: a new approach. II Application to various important (hydr)oxides *J. Colloid Interface Sci.* **133**, 105-117.
32. Geelhoed, J. S., Hiemstra, T., and van Riemsdijk, W. H., (1997) Phosphate and sulfate adsorption on goethite: Single anion and competitive adsorption *Geochim. Cosmochim. Acta* **61**, 2389-2396.
33. Geelhoed, J. S.; Hiemstra, T.; van Riemsdijk, W. H. (1998) Competitive interaction between phosphate and citrate on goethite. *Environ. Sci. Tech.* **32**, 2119-2123.
34. Rietra, R. P. J. J., Hiemstra, T., and van Riemsdijk, W. H. (1999) Sulfate adsorption on goethite. *J. Colloid Interface Sci.* **218**, 511-521.
35. Rietra, P. J. J. J., Hiemstra, T. and van Riemsdijk, W. H. (2000) Electrolyte anion affinity and its effect on oxyanion adsorption on goethite. *J. Colloid Interface Sci.* **229**, 199-206.
36. Kinniburgh D. G., Milne C. J., and Venema P. (1995) Design and construction of a personal-computer-based automatic titrator. *Soil Sci. Soc. Am. J.* **59**, (2) 417-422.
37. Westall J. and Hohl H. (1980) A comparison of electrostatic models for the oxide/solution interface. *Adv. Colloid Interface Sci.* **12**, 265-294.
38. Hiemstra T., Van Riemsdijk W. H., and Bolt G. H. (1989). Multisite proton adsorption modelling at the solid/solution interface of (hydr)oxides: a new approach. I model description and evaluation of intrinsic reaction constants. *J. Colloid Interface Sci.* **133**, 91-104.
39. Filius J. D., Hiemstra T., and Van Riemsdijk W. H. (1998) Adsorption of small weak organic acids on goethite: modeling of mechanisms *J. Colloid Interface Sci.* **195**, 368-380.
40. Keizer, M. G.; van Riemsdijk, W. H. "ECOSAT: technical report of the department soil science and plant nutrition" Wageningen Agricultural University, Wageningen, 1998.
41. Kinniburgh, D. G. "Fit: technical report WD/93/23", British Geological Survey, Keyworth, 1993.
42. Ridley, M. K.; Machesky, M.K.; Wesolowski, D.J.; Palmer, D.A. (1999) Calcium adsorption at the rutile-water interface: apotentiometric study in NaCl media to 250°C. *Geochim. Cosmochim. Acta*, **63**, 3087-3096.
43. Ali, M. A.; Dzombak, D. A. (1996) Effects of simple organic acids on sorption of Cu^{2+} and Ca^{2+} on goethite. *Geochim. Cosmochim. Acta.* **60**, 291-304.
44. Černik M., Borkovec M., and Westall J. C. (1996) Affinity distribution description of competitive ion binding to heterogeneous materials *Langmuir* **12**, 6127-6137.
45. Fokkink L.G. J., de Keizer A. Lyklema J. (1987) Specific ion adsorption on oxides *J. Colloid Inter. Sci.* **118**, 454-462.
46. Venema P., Hiemstra T., and Van Riemsdijk W. H. (1996) Comparison of different site binding models for cation sorption; description of pH dependency, salt dependency and cation-proton exchange. *J. Colloid Interface Sci.* **181**, 45-59.
47. Perona, M. J. and Leckie, J. O. (1985) Proton stoichiometry for the adsorption of cations on oxide surfaces *J. Colloid Interface Sci.* **106**, 65-69.
48. Peak, D., Ford, R. G., and Sparks, D. L. (1999) An in situ ATR-FTIR investigation of sulfate bonding mechanisms on goethite. *J. Colloid Interface Sci.* **218**, 289-299.
49. Wijnja, H. and Schulthess, C. P. (2000) Vibrational spectroscopy study of selenate and sulfate adsorption mechanisms on Fe and Al(hydr)oxide surfaces. *J. Colloid Interface Sci.* **229**, 289-297.
50. Marschner, H., *Mineral Nutrients of higher Plants*. Chapter 8 and 15. Second ed. Academic Press, 1995.
51. Allison, J. D.; Brown, D. S; Novo-Gradac, K. J. *MINTEQA2/PRODEFA2 A Geochemical Assesment model for environmental systems: version 3.11 databases and version 3.0 user's manual*. Environmental Research Laboratory, U.S., EPA, Athens, G.A.
52. Rose, J.; Flank, A.; Mason, A.; Bottero, J.; Elmerich, P. (1997) Nucleation and growth mechanisms of Fe oxyhydroxide in the presence of PO_4 ions. 2. P K-edge EXAFS study. *Langmuir*, **13**, 1827-1834.
53. Bargar, J.R., Brown, G.E. Jr. and Parks, G.A. (1997) Surface complexation of Pb(II) at the oxide-water interfaces: II. XAFS and bond-valence determination of mononuclear and polynuclear Pb(II) sorption products on iron oxides. *Geochim. Cosmochim. Acta* **61**, 2639-2652.

Miscellaneous & Future Challenges

Miscellaneous data

In this thesis the model parameters have been tested by modeling extensive data sets and by using charge distributions values that can represent surface complexes, based on spectroscopy. On the basis of rather scarce data (given in the Appendix) model parameters for chromate, molybdate, vanadate, silicic acid, arsenate and arsenite are given in Table 1 together with the parameters from the previous chapters. For vanadate and arsenate the same charge distributions are used here as found for phosphate (Chapter 6, Table 1, option 1) because these ions have the same proton-ion stoichiometries for the experimental circumstances used in Chapter 3. For chromate, molybdate and tungstate the charge distributions on the basis of the Pauling bond valence concept gives a perfect description of the proton-ion stoichiometries (see Chapter 3) and are therefore used for the modeling the adsorption. In all cases it is found that the adsorption data can be modeled using charge distribution values that are in line with the charge distribution based on microscopic knowledge (Table 1).

Not shown in this thesis are data of the adsorption of aluminum on goethite and the interactions of adsorbed aluminum with sulphate and phosphate. It has been determined that the effect of the adsorption of aluminium on the adsorption of sulphate and vice versa is negligible. Aluminium adsorption has an effect on the phosphate adsorption but this effect depends on the order of addition of Al and P to goethite. The data have not been modeled, as the system is not in equilibrium.

Table 1 Affinity constants and charge distributions for ions used in this thesis. The equilibria are given in Table A1 of the Appendix. The charge distribution based on the modelling (macro) is compared to the charge distribution based on a structural configuration using the Pauling bond valence concept (micro)*.

Component		log K	$(z_0, z_1)_{macro}$	$(z_0, z_1)_{micro}$
H	log K_H	9.25	(1,0)	(1,0)
Na	log K_{Na}	-1	(0,1)	(0,1)
Cl	log K_{Cl}	-0.5	(0,1)	(0,1)
NO ₃	log K_{NO_3}	-1	(0,1)	(0,1)
ClO ₄	log K_{ClO_4}	-1.7	(0,1)	(0,1)
SO ₄	log $K_{SO_4}^{mono}$	9.51	(-0.35, -1.65)	(-0.5, -1.5)
SO ₄	log $K_{SO_4}^{out}$	10.35	(-0.2, -1.8)	(0, -2) à (-0.2, -1.8)
SeO ₄	log $K_{SeO_4}^{mono}$	9.11	(-0.35, -1.65)	(-0.5, -1.5)
SeO ₄	log $K_{SeO_4}^{out}$	10.35	(-0.2, -1.8)	(0, -2) à (-0.2, -1.8)
SeO ₃	log $K_{SeO_3}^{bi}$		(-1.35, -0.65)	(-1.33, -0.67)
CrO ₄	log $K_{CrO_4}^{bi}$	21.3	(-1, -1)	(-1, -1)
MoO ₄	log $K_{MoO_4}^{bi}$	21.3	(-1, -1)	(-1, -1)
WO ₄	log $K_{WO_4}^{bi}$	23.0	(-1, -1)	(-1, -1)
PO ₄	log $K_{PO_4}^{bi}$	29.42	(-1.61, -1.39)	(-1.5, -1.5)
PO ₄	log $K_{PO_4}^{biH}$	35.75	(-1.09, -1.91)	(-1.5, -1.5)
PO ₄	log $K_{PO_4}^{mono}$	19.68	(-0.35, -1.65)	(-0.75, -2.25)
AsO ₄	log $K_{AsO_4}^{bi}$	28.9	(-1.69, -1.31)	(-1.5, -1.5)
VO ₄	log $K_{VO_4}^{bi}$	32.5	(-1.69, -1.31)	(-1.5, -1.5)
SiO ₄	log $K_{SiO_4}^{biH2}$	51.45	(-1.8, -2.2)	(-2, -2)
AsO ₃	log $K_{AsO_3}^{biH}$	41.8	(-1.8, -1.2)	(-2, -1)
Ca	log K_{Ca}^{bi}	2.2	(0.67, 1.33)	(0.67, 1.33)
Ca	log K_{Ca}^{out}	3.7	(0, 2)	(0, 2) à (0.2, 1.8)

*The charge distribution value can be given in various ways, here is presented as the distribution of the charge of the *unprotonated* anion or unhydrolysed cation, for example the -2 charge of the adsorbed monodentate complex of SO_4^{2-} across both electrostatic planes is $z_0 = -0.5$, $z_1 = -1.5$. The charge (z_i) can be estimated using the Pauling bond valence concept $z_i = n_i (v-2)$, where n_i is the number of ligands per electrostatic plane and v is the Pauling bond valence (valence of the central ion divided by the coordination number).

Future Challenges

To obtain knowledge of the significance of a multisite approach versus the simplified approach used in this thesis (2site-1pK approach) adsorption data and spectroscopic knowledge for other ions and other minerals is necessary. The challenge is therefore to test the current model and to get consistent model parameters sets for ions on one or more variable charge minerals. The pH stat titrations can be used very well for this purpose.

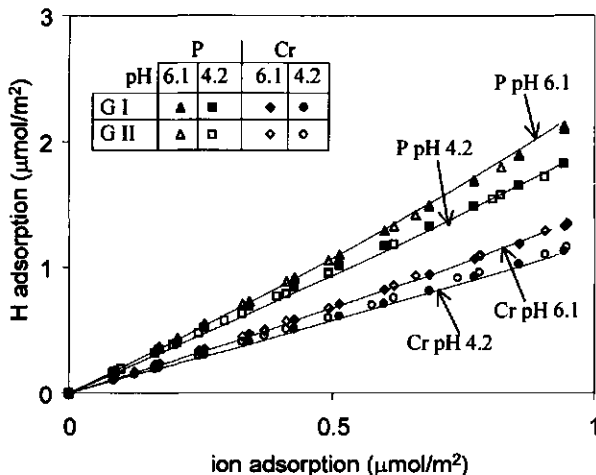


Fig. 1. Proton consumption as a function of chromate and phosphate adsorption at constant pH: pH 4.2 or pH 6.1 (0.01 M NaNO₃). The curves show the CD-MUSIC predictions as in Chapter 3. Goethite I (GI) was used in this thesis. In contrast to GI, goethite II (GII) is made by quickly neutralising FeCl₃ with NaOH and has a lower specific surface area (for preparation see ref. 1).

It is encouraging to see in Fig. 1 that two different types of goethite, GI and GII, give proton-ion adsorption stoichiometries for chromate and phosphate that are indistinguishable. GI is a high surface area goethite while GII is a low surface area goethite (in this case BET(N₂)=40.6 m²/g). The goethite used in this thesis is a high surface area goethite. This type of goethite is produced by slow hydrolysis of Fe(NO₃)₃, which results in a well-crystallized goethite, and has a specific surface area of 96.4 m²/g (GI). Low surface area goethites have often been used in research and are produced by fast hydrolysis of a Fe salt with NaOH. The phosphate adsorption is higher on GII compared to GI in terms of phosphate per surface area (1). The differences between both goethites cannot be explained solely by a difference of the Stern capacity or the site density. As discussed in Chapter 3, the modeling of the proton-ion adsorption stoichiometry is not very sensitive for these model parameters. This means that the charge distribution for the adsorbed complexes of chromate and phosphate on both goethites are very similar. It is therefore probable that adsorption data for different goethites from literature can be used to get consistent model parameters sets by using identical charge distributions for each ion for different types of goethite.

In Chapter 5 it is concluded that it is not possible to infer an outersphere complex from modeling the available macroscopic adsorption data without the information from spectroscopy. In case of sulphate and selenate it might be possible to study the competition between both ions on goethite to further test the model parameters from Chapter 5. A prediction of the competition of both ions with the different model parameter sets gives different results (not shown). This might imply that macroscopic data are sensitive enough to characterize the different adsorbed complexes of sulphate and selenate provided that enough relevant data are available.

References

1. Hiemstra T. and Van Riemsdijk W. H. (1996) A surface structural approach to ion adsorption: the charge distribution (CD) model. *J. Colloid Interface Sci.* **179**, 488-508.
2. Venema P., Hiemstra T., and Van Riemsdijk W. H. (1996) Multi site adsorption of cadmium on goethite. *J. Colloid Interface Sci.* **183**, 515-527.
3. Lindsay, W. L. *Chemical Equilibria in Soils*; Wiley-Interscience: New York, 1979; 347 p.
4. Allison, J. D.; Brown, D. S; Novo-Gradac, K. J. *MINTEQA2/PRODEFA2 A Geochemical Assessment model for environmental systems: version 3.11 databases and version 3.0 user's manual*. Environmental Research Laboratory, U.S., EPA, Athens, G.A.
5. Smith, R. M.; Martell, A. E. *Critical Stability Constants* Vol. 4. Plenum, New York, 1981.

Appendix .

The adsorption of a range of ions has been determined using the goethite suspension and the ion solution as mentioned in Chapter 3 except for Fig. A2a for which the goethite suspension as characterized by Venema et al. (2) was used. The adsorption experiments were performed according to the method used in Chapter 4 and 5.

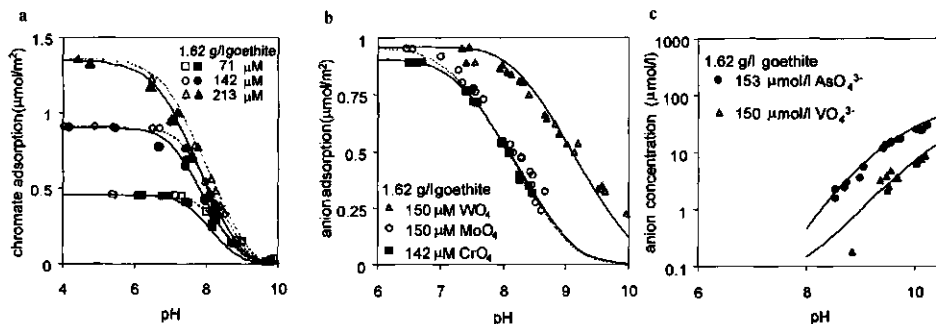


Fig. A1. Adsorption of anions at a goethite concentration of 1.62 g/l, (a) adsorption of CrO_4 in 0.01 M and 0.1 M NaNO_3 , resp. open and bold symbols (b) adsorption of CrO_4 , MoO_4 , WO_4 in 0.01 M NaNO_3 , (c) concentration of AsO_4 and VO_4 in 0.01 M NaNO_3 .

The model parameters from this thesis have been summarised in Table 1 of this Chapter. The formation reactions are given in Table A1 of this appendix. The surface species are defined in mol/l and therefore the log K values for the bidentate equilibria are corrected with the term $\rho \text{AN}_{\text{SI}}$ (where ρ is the solid-solution ratio in

kg/l, A is the specific surface area in m^2/l , and N_{s1} is the site density of the reference group FeOH). The equilibrium expression can be read across the table: The general expression for the surface species concentration (S) is: $S = \Pi[C_k]^{n_k} 10^{\log K}$, in which the term $\Pi[C_k]^{n_k}$ is the product of the component concentrations, including the electrostatic contributions, surface and solution components. The coefficients n_k are found in the rows. The electrostatic coefficients z_0 and z_1 can be derived from the charge distributions of the adsorbed complexes (see Table 1). The electrostatics of the Basic Stern model and site densities used have been described in detail in reference 1. The capacity used in this thesis is 0.905 F/m^2 (Chapter 3).

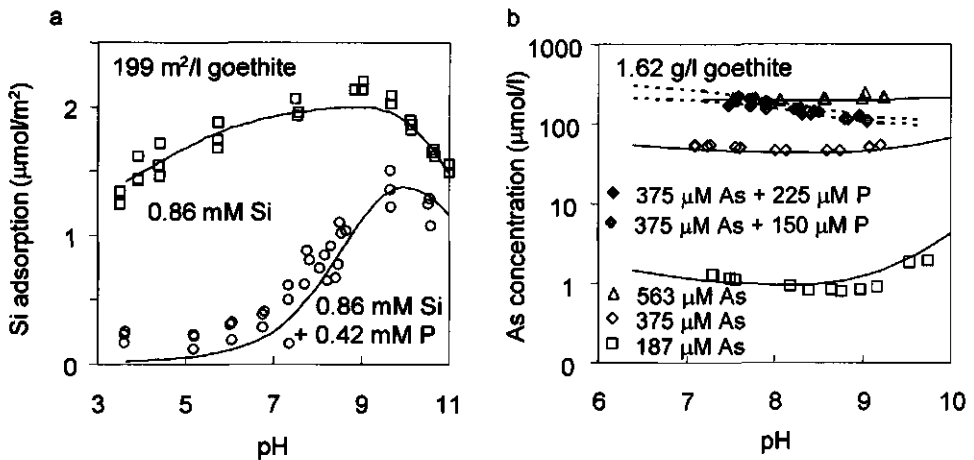


Fig. A2. Adsorption on goethite in 0.01 M NaNO_3 showing the effect of phosphate on (a) silicic acid adsorption (in this case the goethite as described by Venema was used) (b) arsenite adsorption (concentration is shown) at a total AsO_2 concentrations of 375 $\mu\text{mol/l}$, in comparison to arsenite adsorption without P at 187, 375 and 562 $\mu\text{mol/l}$ AsO_2 .

Table A1 Surface species for goethite. Speciation in solution is as given in previous chapters and is from Lindsay (3), and if not available there from MINTEQA2 (4), or Smith and Martell (5).

Surface species (mol/l)	Components					Log K
	$\frac{-F\psi_0}{e RT}$	$\frac{-F\psi_1}{e RT}$	FeOH	Fe ₃ O	H	
FeOH ^{-0.5}			1			0
FeOH ₂ ^{+0.5}	1		1			log K _H
FeOH ^{-0.5} - Na ⁺		1	1		log [Na ⁺]	log K _{Na}
FeOH ₂ ^{+0.5} - Cl ⁻	1	-1	1		log [Cl ⁻]	log K _{Cl} + log K _H
FeOH ₂ ^{+0.5} - NO ₃ ⁻	1	-1	1		log [NO ₃ ⁻]	log K _{NO3} + log K _H
FeOH ₂ ^{+0.5} - ClO ₄ ⁻	1	-1	1		log [ClO ₄ ⁻]	log K _{ClO4} + log K _H
Fe ₃ O ^{-0.5}				1		0
Fe ₃ OH ^{+0.5}	1		1	1		log K _H
Fe ₃ O ^{-0.5} - Na ⁺		1	1		log [Na ⁺]	log K _{Na}
Fe ₃ OH ^{+0.5} - Cl ⁻	1	-1	1	1	log [Cl ⁻]	log K _{Cl} + log K _H
Fe ₃ OH ^{+0.5} - NO ₃ ⁻	1	-1	1	1	log [NO ₃ ⁻]	log K _{NO3} + log K _H
Fe ₃ OH ^{+0.5} - ClO ₄ ⁻	1	-1	1	1	log [ClO ₄ ⁻]	log K _{ClO4} + log K _H
FeO ^p SO ₃ ^q	1+z ₀	z ₁	1	1	log [SO ₄ ²⁻]	log K _{SO4} ^{mono}
FeOH ₂ ^p - SO ₄ ^q	1+z ₀	z ₁	1	1	log [SO ₄ ²⁻]	log K _{SO4} ^{out}
FeO ^p SeO ₃ ^q	1+z ₀	z ₁	1	1	log [SeO ₄ ²⁻]	log K _{SeO4} ^{mono}
FeOH ₂ ^p - SeO ₄ ^q	2+z ₀	z ₁	1	1	log [SeO ₄ ²⁻]	log K _{SeO4} ^{out}
Fe ₂ O ₂ ^p SeO ^q	2+z ₀	z ₁	2	2	log [SeO ₃ ²⁻]	log K _{SeO3} ^{bi} - log(ρAN _{s1})
Fe ₂ O ₂ ^p CrO ₂ ^q	2+z ₀	z ₁	2	2	log [CrO ₄ ²⁻]	log K _{CrO4} ^{bi} - log(ρAN _{s1})
Fe ₂ O ₂ ^p MoO ₂ ^q	2+z ₀	z ₁	2	2	log [MoO ₄ ²⁻]	log K _{MoO4} ^{bi} - log(ρAN _{s1})
Fe ₂ O ₂ ^p WO ₂ ^q	2+z ₀	z ₁	2	2	log [WO ₄ ²⁻]	log K _{WO4} ^{bi} - log(ρAN _{s1})
Fe ₂ O ₂ ^p PO ₂ ^q	2+z ₀	z ₁	2	2	log [PO ₄ ³⁻]	log K _{PO4} ^{bi} - log(ρAN _{s1})
Fe ₂ O ₂ ^p POOH ^q	2+z ₀	z ₁ +1	2	3	log [PO ₄ ³⁻]	log K _{PO4} ^{bih} - log(ρAN _{s1})
FeO ^p PO ₃ ^q	1+z ₀	z ₁	1	1	log [PO ₄ ³⁻]	log K _{PO4} ^{mono}
Fe ₂ O ₂ ^p AsO ₂ ^q	2+z ₀	z ₁	2	2	log [AsO ₄ ³⁻]	log K _{AsO4} ^{bi} - log(ρAN _{s1})
Fe ₂ O ₂ ^p VO ₂ ^q	2+z ₀	z ₁	2	2	log [VO ₄ ³⁻]	log K _{VO4} ^{bi} - log(ρAN _{s1})
Fe ₂ O ₂ ^p SiO ₂ H ₂ ^q	2+z ₀	z ₁ +2	2	4	log [SiO ₄ ⁴⁻]	log K _{SiO4} ^{bih2} - log(ρAN _{s1})
Fe ₂ O ₂ ^p AsOH ^q	2+z ₀	z ₁ +1	2	3	log [AsO ₃ ³⁻]	log K _{AsO3} ^{bih} - log(ρAN _{s1})
(FeOH) ₂ ^p - Ca ^q	z ₀	z ₁	2		log [Ca ²⁺]	log K _{Ca} ^{out} - log(ρAN _{s1})
(FeOH) ₂ ^p Ca ^q	z ₀	z ₁	2		log [Ca ²⁺]	log K _{Ca} ^{bi} - log(ρAN _{s1})
sum	Σ ₁	Σ ₂	Σ ₃	Σ ₄	Σ ₅	

Summary

Transport and bioavailability of a large range of components in the environment is influenced by the interaction with variable charged minerals. Examples of these components are nutrients for plants such as phosphate and molybdate, and toxic components such as arsenite and cadmium. Examples of variable charged minerals that are present in most soils are goethite and gibbsite. There is a relatively large amount of information with respect to the binding of ions to these minerals in simple electrolyte solutions. However, in environmental systems, such as soils and sediments, the composition of the solution is much more complex. Ions from the solution influence the binding of each other, some ions enhance each others binding while other ions show competitive effects. Due to the combination of different processes, and due to changes of the solution composition, the prediction of the behavior of many components in environmental systems is difficult and often not possible. In principle surface complexation models can deal with adsorption equilibria in multicomponent systems but these models lack unification, cannot describe surface species as found in spectroscopy, or lack reliable model parameters.

The goal of this thesis is to improve the surface complexation model for ion adsorption on variable charge minerals and to determine model parameter values for ions that are relevant in environmental systems. The main tool to further develop the model for variable charge minerals is the incorporation of the spectroscopic knowledge about the structure and coordination of adsorbed ions. The CD-MUSIC model is used, as it is the only surface complexation model that enables the incorporation of this structural information.

In this thesis it is tested if model parameters for adsorbed ions can be related to the spectroscopically determined structure and coordination of the adsorbed ions. Adsorption on goethite is used because a relatively large amount of knowledge is available for ion adsorption and the structure of adsorbed species on goethite. Moreover, goethite is one of the most important iron(hydr)oxides in soils. For simplicity mainly ions are studied for which it is appropriate to assume that these are only reactive to one type of surface group on goethite: e.g. sulphate, phosphate. This enables the use of a simplification of the model for goethite and minimizes the amount of model variables. In this approach only the singly and the triply coordinated groups are used for modeling adsorption: both surface groups are reactive for protons and for outersphere adsorption of electrolyte ions, and have the same binding affinities, while only the singly coordinated group is reactive for innersphere complexation for these ions. The doubly coordinated oxygen's are supposed to be inert, both with respect to proton and oxyanion adsorption. The Basic Stern model is used to describe the electrostatics because it is the simplest physically realistic model to incorporate the CD-MUSIC model.

Usually ion adsorption is characterized as a function of ion concentration and pH. A thermodynamic relation is available which relates the pH dependency of

ion adsorption to the proton-ion adsorption stoichiometry. In Chapter 2 this thermodynamic relation for unhydrolyzed/unprotonated ions is extended for ions that do hydrolyze/protonate in solution by incorporation of the degree of protonation in solution. In Chapter 3 an experimental method is presented to accurately determine the proton-ion adsorption stoichiometry at equilibrium concentrations that are below the detection limit for the adsorbing species in solution. Calculations with the general electrostatic Basic Stern model show that the proton-ion adsorption stoichiometry is independent of the magnitude of the chemical component of the standard adsorption Gibbs free energy of adsorption (i.e. the intrinsic $\log K$ for the surface coordination reaction). It is found that the intrinsic $\log K$ value is important for determining the relation between the concentration in solution and the adsorbed amount, but not for the resulting proton-ion stoichiometry for the conditions of our experiments. The proton-ion stoichiometry is only governed by the electrostatic interactions and therefore reflects the allocation of adsorbed charge at the interface.

In the CD-MUSIC model it has been postulated that allocation of adsorbed charge at an interface can be estimated on the basis of the structure and coordination of the adsorbed complexes. The charge of an adsorbing ion such as sulphate is not treated as a point charge at the surface plane but instead its -2 charge is distributed, as a function of its adsorbed structure, across the surface plane and the outer-electrostatic plane. In case of a monodentate complex of sulphate one of the four oxygen groups ("ligands") is directed to the surface and three ligands are oriented to the solution. An equal distribution of the charge across the ligands is expected on the basis of the bond valence theory of Pauling. The attribution of adsorbed charge for adsorbed sulphate can thus be estimated to be -0.5 to the surface plane and -1.5 to the outer-electrostatic plane.

This concept is in principle valid for all ions and is demonstrated for three different ion complexes on goethite for which the structure is well known: monodentate sulphate, bidentate arsenate, and the bidentate complex of selenite. Also proton-ion adsorption data for selenate, tungstate, chromate, arsenate, phosphate and vanadate are obtained. Using the charge distributions on the basis of the Pauling bond valence concept, and the known microscopic structures, we have predicted the proton-ion adsorption stoichiometry for the ions mentioned. The excellent agreement between the model predictions and the experimental data points demonstrates that the experimental proton-ion stoichiometry can indeed be used to predict the surface coordination of an ion complex, and vice versa. The findings demonstrate for the first time the relationship between molecular surface structure and macroscopic ion adsorption phenomena.

Monovalent electrolyte ions are normally assumed to be adsorbed as outersphere complexes. These ions are therefore used to test if a model can describe the effect of outersphere complexation because many other ions are adsorbed as innersphere complexes or as a combination of inner- and outersphere complexes. Reported in Chapter 2 of this thesis, is the influence of various types of background electrolytes (NaCl , NaNO_3 , and NaClO_4) on the proton adsorption, and on the adsorption of sulphate and phosphate on goethite. The formation constants of monovalent electrolyte anions on the goethite surface are derived from proton

adsorption data. It is shown that the derived formation constants enable the prediction of the effect of different electrolyte anions on adsorption of polyvalent anions.

In Chapter 4 sulphate adsorption on goethite is characterised covering a large range of sulphate concentrations, surface coverage's, pH values and electrolyte concentrations using four different techniques. All the data can be modeled by assuming only one type of complex of adsorbed sulphate. The modeled charge distribution suggests that this is a monodentate complex. Very recent spectroscopic work has confirmed that in the main adsorption range at lower pH values monodentate innersphere complexes are indeed dominant for sulphate and selenate but at pH values above 6 outersphere complexes for both ions are dominant. In Chapter 5 the adsorption behavior of sulphate are compared with the binding of selenate. The sulphate results from Chapter 4 have been re-interpreted, together with the data for selenate, in the view of latest spectroscopic work on the speciation and coordination of adsorbed selenate and sulphate on goethite. The description of the adsorption data including the differentiation between both species can be done very satisfactory with the CD-MUSIC approach. The modeled charge distributions obtained for the innersphere complexes are in line with charge distributions as derived from the spectroscopically determined structure and coordination for both ions. It is found that the formation of outersphere complexes sulphate and selenate cannot be established solely from the macroscopic adsorption data without the spectroscopic knowledge. This is rather similar to results of monodentate and bidentate complexes of phosphate. These complexes exist at high pH values, according to spectroscopic work, but the phosphate data in Chapter 6 can be modeled by assuming both surface complexes but also by assuming only the bidentate complex.

In Chapter 6 the interaction between phosphate and calcium adsorption has been studied on goethite because calcium can influence the phosphate adsorption equilibria and these are very difficult to discriminate from precipitation equilibria in soils and sediments. The model parameter values for calcium and phosphate from single-sorbate experiments have been verified in experiments with both ions for conditions below the saturation index of apatite. Using the derived model parameter values it is possible to predict the adsorption and interaction of phosphate and calcium for environmental conditions.

In Chapter 7 adsorption data are given for the ions for which the proton-ion adsorption stoichiometry has been determined in Chapter 3, and data for the adsorption of silicic acid and arsenite are given. The modeling parameter values are summarized for all ions that have been studied in this thesis.

Samenvatting

Transport en beschikbaarheid van een groot aantal stoffen voor planten en dieren worden beïnvloed door de binding van deze stoffen aan mineralen in bodems. Voorbeelden van dergelijke stoffen zijn nutriënten voor planten zoals fosfaat en molybdaat, maar ook toxische stoffen zoals arseen en cadmium. Voorbeelden van mineralen die ruimschoots voorkomen in bodems zijn goethiet en gibbsiet. Er is al relatief veel kennis van de binding van specifieke stoffen aan mineralen vanuit eenvoudige oplossingen, zoals bijvoorbeeld een oplossing van NaCl. In bodems en sedimenten is de oplossing echter samengesteld uit meerdere ionen. Deze ionen beïnvloeden de binding van elkaar op een complexe wijze: sommige soorten ionen zijn in competitie met elkaar en andere bevorderen de binding van elkaar. Door wijzigingen van de samenstelling van de bodemoplossing en door de veelheid aan processen is een voorspelling van de binding aan bodemmineralen vaak moeilijk of niet mogelijk. Er zijn modellen die in principe dit soort ingewikkelde interacties kunnen berekenen maar de modellen beschikken niet over gevalideerde model gegevens of geven maar een beperkte beschrijving van de beschikbare data. Het doel van dit proefschrift is om in de toekomst het complexe bindingsgedrag aan bodemmineralen beter te voorspellen.

Electrostatistische en chemische interacties bepalen de ion binding aan minerale oppervlakken. Experimenteel is het moeilijk om deze interacties te onderscheiden en daardoor zijn verschillende modellen ontstaan. Het is mogelijk om op basis van nieuwe gegevens over de microscopische structuur van de gebonden ionen tot een betere toetsing van modellen te komen. De oppervlakken waaraan binding kan plaatsvinden kunnen negatief of positief geladen worden indien geladen ionen door een specifieke chemische affiniteit binden. Zo'n geladen oppervlak wordt altijd geneutraliseerd door ionen met een tegengestelde lading. Als deze tegengesteld geladen ionen zich in de oplossing bevinden dan ontstaat er een ophoping van deze ionen aan het oppervlak, enerzijds als gevolg van de aantrekking door het oppervlak, en anderzijds door het tegenovergestelde effect van de Brownse beweging (diffusie) in oplossing. Dit beeld van een lading aan een oppervlak en een diffuse tegenlading heet een elektrische dubbellaag. Vanuit de oplossing gezien ondervindt een ion dat zich naar een geladen oppervlak beweegt een potentiaal. In dit proefschrift wordt het zogenaamde Stern-Gouy-Chapman model gebruikt als beschrijving van de elektrische dubbellaag. Dit model beschrijft de electrostatistische potentiaal, onder andere als functie van de afstand tot een oppervlak.

Er zijn zoals gezegd meerdere modellen voor de binding van ionen. De modellen gebruiken meestal het Stern-Gouy-Chapman model, of een vereenvoudiging daarvan, als basis, maar de modellen maken verschillende aannames over de locatie van de lading van geadsorbeerde ionen. In bijna alle modellen worden ionladingen beschouwd als puntladingen die oftewel in het vlak adsorberen waar ook protonen adsorberen of in een vlak op enige afstand van het oppervlak. In het CD-MUSIC model wordt de lading van geadsorbeerde ionladingen verdeeld over het oppervlak en een electrostatisch vlak op enige afstand van het oppervlak als functie van de structuur van een geadsorbeerd ion. In dit model wordt de ruimte die een ion inneemt, en de verdeling van de lading over deze

ruimte dus niet verwaarloosd ten opzichte van de grootte van het compacte deel van de elektrische dubbellaag. Deze verdeling van lading kan zoals blijkt uit mijn onderzoek vaak worden afgeleid uit een van de zogenaamde Pauling principes. Dit Pauling principe definieert een bindingsvalentie die gelijk is aan een deel van de lading van het centrale "kation" (P, S) door de lading evenredig te verdelen over de (negatieve) liganden die het centrale ("kat")ion omringen. In dit proefschrift is bijvoorbeeld de adsorptie van sulfaat uitgebreid bestudeerd. Uit het Pauling principe volgt dat de twee min lading van het sulfaat ion in gelijke mate kan worden toegekend aan de vier omringende zuurstofgroepen van het sulfaat ion. Elk zuursof 'ligand' krijgt dus een lading van -0.5 toegekend. Bij een monodentaat complex van sulfaat aan een mineraal vormt een ligand de binding met het oppervlak, en zijn de drie overige liganden naar de oplossing gericht, wat resulteert in een lading van -0.5 in het oppervlak en -1.5 in het electrostatische vlak op enige afstand van het oppervlak. De negatieve lading die aan het oppervlak wordt toegekend wordt in de structuur verder geneutraliseerd door de aanwezige kationen van het mineraal waaraan het ion bindt. De electrostatische bijdrage aan de totale bindingsaffiniteit is in het CD-MUSIC model is direct gerelateerd aan de structuur van de gebonden ionen. Omdat er in de laatste jaren via spectroscopisch onderzoek meer bekend geworden is van de structuur en de coördinatie van gebonden ionen aan mineralen is het mogelijk om het CD-MUSIC model te toetsen. In dit proefschrift is specifieke chemische binding van een reeks ionen aan het mineraal goethiet onderzocht omdat relatief veel bekend is over de binding van ionen aan goethiet en over de structuur van de gebonden ionen.

Gewoonlijk wordt ion adsorptie gekarakteriseerd als functie van de ion concentratie en de pH. Via een thermodynamische vergelijking is te zien dat de pH afhankelijkheid van de binding van ionen direct gerelateerd is aan de zuur of base consumptie per geadsorbeerd ion. Deze informatie, de proton-ion adsorptie stoichiometrie kan bijvoorbeeld experimenteel worden verkregen door middel van een pH-stat titratie. In Hoofdstuk 2 wordt afgeleid hoe deze thermodynamische vergelijking eruit ziet voor ionen die in de oplossing hydrolyzeren/protoneren als functie van de pH. In Hoofdstuk 3 wordt op basis van deze kennis een methode gepresenteerd om de pH afhankelijkheid van ion binding nauwkeurig te bepalen. De experimentele methode karakteriseert de zuur/base consumptie tijdens een pH stat ion titratie. De totale ion toevoeging wordt zodanig afgestemd dat de evenwichtsconcentratie in oplossing verwaarloosbaar blijft waardoor de geadsorbeerde hoeveelheid vrijwel identiek is aan de toegediende hoeveelheid van het betreffende ion.

In Hoofdstuk 3 tonen berekeningen met een algemeen bindingsmodel dat de proton-ion adsorptie stoichiometrie onafhankelijk is van de grootte van het chemische deel van de bindingsaffiniteit (oftewel de intrinsieke log K van de reactie). Dit heeft belangrijke consequenties voor het karakteriseren van de ion binding aan mineralen met een variabele lading. De intrinsieke log K is belangrijk voor de relatie tussen de concentratie in oplossing en de geadsorbeerde hoeveelheid, maar niet voor de proton-ion adsorptie stoichiometrie. De proton-ion adsorptie stoichiometrie wordt bepaald door de geadsorbeerde lading, en de verdeling daarvan aan het oppervlak. De structuur van de geadsorbeerde complexen kan zoals

eerder gezegd bepaald worden via spectroscopie, en zodoende kan de distributie van geadsorbeerde lading worden geschat volgens het Pauling principe. Het concept is in principe geldig voor alle ionen en wordt allereerst gedemonstreerd voor drie ionen waarvan de structuur van de geadsorbeerde species goed bekend is via spectroscopie, namelijk de complexen van sulfaat, arsenaat en seleniet op goethiet. Ook is de proton-ion adsorptie stoichiometrie bepaald voor de adsorptie van selsenaat, wolframaat, chromaat, arsenaat, fosfaat en vanadaat. Gebruik makend van de ladingsdistributies volgens de definitie van Pauling voor de bekende geadsorbeerde structuren, is de proton-ion adsorptie stoichiometrie voorspelt voor de ionen. De goede overeenkomst tussen de voorspelling en de data geeft aan dat de experimentele proton-ion adsorptie stoichiometrie inderdaad gebruikt kan worden voor de voorspelling van de structuur van geadsorbeerde complexen, en omgekeerd. Deze bevindingen demonstreren de relatie tussen de moleculaire structuur van geadsorbeerde complexen en het macroscopische adsorptiegedrag.

In hoofdstuk 2 van dit proefschrift worden de binding en modellering onderzocht van electrolyt anionen omdat algemeen aangenomen wordt dat deze anionen niet via ligand-uitwisseling binden en alleen als outersphere complexen binden aan goethiet. Getoond wordt het effect van verschillende typen oplossingen (NaCl , NaNO_3 , en NaClO_4) op het zuur-base gedrag van goethiet, en op de binding van sulfaat en fosfaat aan goethiet. Beneden het ladingsnulpunt bij pH 9.25 neemt de binding van zuur af in de volgorde van $\text{Cl} > \text{NO}_3 > \text{ClO}_4$. De afname van de binding van zuur beïnvloedt de binding van oxyanionen aan goethiet. Anion adsorptie van relatief sterk bindende polyvalente anionen (sulfaat en fosfaat) neemt in oplossingen toe in de volgorde van $\text{Cl} < \text{NO}_3 < \text{ClO}_4$. De bindingsconstanten van de monovalente elektrolyt anionen aan goethiet (bindingen zonder liganduitwisseling) worden gekwantificeerd op basis van het zuur-base gedrag. Deze bindingsconstanten blijken een goede voorspelling te geven van het effect dat de verschillende elektrolyten hebben op de binding van sulfaat en fosfaat.

In Hoofdstuk 4 is de binding van sulfaat aan goethite uitgebreid gekarakteriseerd over een groot bereik van sulfaatconcentraties, bezetting, pH niveaus en electrolyt concentraties. Alle data kunnen gemodelleerd worden met één type adsorptiecomplex. In recente spectroscopische studies is bevestigd dat bij lage pH waarden monodentate complexen dominant zijn maar dat bij $\text{pH} > 6$ de outersphere complexen van sulfaat en selsenaat dominant zijn. In Hoofdstuk 5 is het bindingsgedrag van sulfaat vergeleken met die van selsenaat. De resultaten van sulfaat uit het vorige hoofdstuk, en die van selsenaat, zijn geanalyseerd in het licht van de recente studies. De incorporatie van de inner- en outersphere complexen verloopt in het CD-MUSIC model zeer goed en de data kunnen beschreven worden met het CD-MUSIC model waarbij de gebruikte ladingsdistributies overeenkomen met de complexen zoals ze zijn vastgesteld via spectroscopie. De vorming van de outersphere complexen kan echter niet worden vastgesteld op basis van de macroscopische adsorptie data. Dit komt overeen met de modellering van het bindingsgedrag van fosfaat (Hoofdstuk 6) in relatie tot de via spectroscopie vastgestelde complexen. Bij hoge pH zijn monodentate en bidentate complexen vastgesteld. Het bindingsgedrag kan echter zowel gemodelleerd worden met de

aanname van aanwezigheid van beide complexen maar ook met enkel bidentaats complexen.

In Hoofdstuk 6 is de interactie tussen fosfaat en calcium bestudeerd. Dit is interessant omdat de aanwezigheid van calcium een sterke invloed heeft op fosfaat adsorptie en omdat het vaak zeer moeilijk is om onderscheid te maken tussen adsorptie en precipitatie reacties in dergelijke systemen. De model parameters voor calcium en fosfaat zoals verkregen uit de experimenten met alleen fosfaat of calcium, zijn gebruikt om de binding te voorspellen van experimenten waarin zowel fosfaat en calcium zijn gebruikt. De experimenten zijn zodanig uitgevoerd dat er geen calciumfosfaat mineralen ontstaan. Gebruik makend van de model parameters is het mogelijk om de interactie tussen fosfaten en calcium te voorspellen onder condities waarbij wel mineralen van fosfaat en calcium kunnen ontstaan, condities zoals die in het milieu voorkomen. Het toont een sterke interactie tussen calcium en fosfaat bij het adsorptieproces, en een te verwaarlozen pH afhankelijkheid van de fosfaat binding bij neutrale pH waarden.

Tenslotte worden in Hoofdstuk 7 de resultaten samengevat in de vorm van een tabel met de evenwichtsreacties van de onderzochte ionen aan goethiet. Om te komen tot een volledige beschrijving van de bindingsreacties aan goethiet in bodems dienen ook de evenwichten met andere ionen beschreven te worden. Hierbij kan gebruik gemaakt worden van de resultaten uit de literatuur maar dan dient er wel rekening mee gehouden te worden met het feit dat veel onderzoekers andere typen goethiet, of andere mineralen hebben gebruikt. Consistente datasets en sets van model parameters per mineraaltype zijn daarom nodig. De methodiek die in dit proefschrift is gebruikt is van belang bij het ontwikkelen van een optimale meetstrategie om de modelparameters nauwkeurig te bepalen met een relatief geringe experimentele inspanning.

Levensloop

René Peter Jan José Rietra werd geboren op 7 april 1967 te Weert en is getogen te Valkenswaard. In Valkenswaard ging hij naar de St Willibrordes MAVO, en naar het Hertog Jan College voor de HAVO en VWO. In 1987 ging hij naar de Landbouwniversiteit Wageningen en volgde de studie Bodemkunde (L-15) met afstudeervakken in Bodemscheikunde, Bodemvruchtbaarheid en Fysische Chemie. In 1994-1995 deed hij vervangende dienst bij het toenmalige Instituut voor Bos- en Natuuronderzoek (Alterra), afdeling Ecotoxicologie. Van 1985 tot 1998 deed hij promotieonderzoek bij het Departement voor Omgevingswetenschappen, sectie Bodemkunde en Plantenvoeding van de Universiteit Wageningen, thans sectie Bodemkwaliteit. Sinds 1 juni 1999 werkt hij bij het Energieonderzoek Centrum Nederland (ECN) te Petten bij de werkgroep Emissie-Karakterisering en Reductie.